Anonymous Referee #3

Dear Authors,
many thanks for your revisions.

In the replies to all four reviewers you mention the requirements of the PalMod Project. Apparently all reviewers consider these requirements difficult, and suggest other and scientifically more useful data selection. This should make you think how useful these constraints are, and if you can really derive robust aridity for all regions with these constraints. These constraints are clearly impacting on the robustness of your results (negatively, according to four reviewers), and I do think that this needs to be openly stated in the manuscript.
Dear reviewer,
Thanks again for your comments. We have revised the manuscript according to the suggestions. Our replies are marked in red as follows.

I do see the synthesis as an important contribution, and I do see that you carefully thought about how to combine information from different geoarchives.
I do see that you are trying to improve your manuscript, but when you are unable to make your data basis wider and follow reviewers' suggestions, please discuss how the PalMod requirements impact on the robustness of your result – this is yet missing in the discussing part. Generally, I have the impression that you neglect reviewers' well-meant suggestions in some cases without need.
→ We do not neglect your suggestions or those of other reviewers. We have tried to implement as much of it as possible - but we are also bound by the requirements of PalMod.
→ A section on the PalMod requirements impacting the synthesis is added to the discussion.

Before publication I expect that the discussion needs to be more self-critical and needs to include statements for all regions how the PalMod requirements impact on/bias your overall result and the aridity synthesis. Without this, the paper should not be published in Climate of the past in my opinion.
→ We have added this to the discussion. But since we do not use more than one pollen and dust dataset for a region, we do not estimate the bias to be that large. We fully agree, that the requirements strongly influence the region selection, as regions with only one record type are excluded.
Chapter 4.1 compares our aridity index with a previous reconstruction from Herzschuh (2006). This reconstruction is based on various pollen records, but only with that one kind of proxy, which is pollen. Both methods reveal similar results, although Herzschuh has used a lot more records. We therefore assume that our results are representative.

Further, in the last reviews you were asked you to explain your methodology in a way that is 100% reproducible – from data to result. This still is not at all the case. As science should be reproducible, this is not acceptable as it is at the moment. I really demand from you to provide methods in detail and name where required software is available – possibly in Supplements. For speleothems you consider AGE uncertainty, for the other proxies you 'estimate' PROXY uncertainty – but you state that you use data on their original age models. This seems unlogical to mix. Please elaborate how you derive proxy uncertainty in a reproducible way.

→ We have rephrased the methodology section and additionally, provide the Matlab code and our excel template as supplementary materials.
We were asked to provide uncertainties for the aridity index. However, the aridity index is based on data sets from primary literature, which do not contain any errors in the original. Possible errors could be, however, that e.g. the individual pollen counters have miscounted. Measurement inaccuracies in dust data are also possible, for example due to the devices used. In order to be able to give at least rough error values, we have followed a method of Mudelsee (pers. communication) and Kohler (2009, as already cited in the paper). The input parameters from Table 2 for pollen and dust are all estimated - based on the data density and the method used by the author of the data set. This is now described in more detail.

Two reviewers mention that some of your your data selections are difficult or not useful for a local compilation. Please take these concerns serious and do NOT use the Palod requirements as reason to compare not-comparable datasets. These don't force you to compare different things. Please don't use the data from New Zealand and Australia together, I seriously think that mixing these is scientifically misleading. Possibly this reduces the number of regions – but that is in my opinion better than producing misleading results. The Lynch Crater is influenced by monsoons, NZ by westerlies. Although these may have similar temperature and precipitation, that is not comparable.
→ According to your and the other reviewers suggestions, we have deleted the two regions Cariaco Basin and Oceania.

'China' is a political statement, not a geographic one – what about 'east Asia'?
→ Many paper also define this region as "China". For example, see citations in our manuscript from Mingram et al., 2018; Wang et al., 2001; Stebich et al., 2015, Herzschuh, 2006; or Uno, I., Eguchi, K., Yumimoto, K. *et al.* Asian dust transported one full circuit around the globe. *Nature Geosci* **2,** 557–560 (2009); K.E. Kohfeld, S.P. Harrison, Glacial-interglacial changes in dust deposition on the Chinese Loess Plateau, Quaternary Science Reviews (2003); and many more.
In our opinion, the region should not be called East Asia, as East Asia is a much more inhomogeneous region. It includes many more countries than just China. Nor are we aware of any territorial conflict in the region of Jingyuan Loess, Hulu Cave or Sihailongwan Maar, which would require an "apolitical" statement.
Nevertheless we leave this decision to the editor.

Anonymous Referee #1

Dear Reviewer,
Thanks again for your helpful suggestions. We have changed the manuscript accordingly. Our answers to your comments are marked in red color again within this reply.

The authors indeed made some efforts to improve the manuscript from the first version. However, there are several aspects from my comments that in fact still remain unanswered, in particular concerning the methodology. Therefore I still recommend major revisions to the manuscript. This includes passages with typos and poor use of the English language.
→ We went through the whole manuscript in detail and revised the language. If this does not seem sufficient and the editor considers the manuscript appropriate, we will assign a professional proofreader to make the very last minor revisions.

SITE SELECTION
You now explain more clearly the PalMod requirements you stuck to for site selection, in particular the requirement for the datasets to be available in publicly accessible databases, and that they cover the last 60000 years. I recommend explaining also what the criteria were in terms of "high sampling resolution" and "highly cited".
→ high cited papers: more than 5 citation per year
→ high sample resolution: more than 1 sample per 250 years
→ In the beginning we looked for literature with more than 5 citations per year. But since we could not find any data for many papers, we searched the databases afterwards and in a first step we made sure that the records cover as much as possible of the last 60 000 years. From this selection, we chose those records which had a better data resolution than 1 sample per 250 years. Only the pollen record for NW-Africa does not fall under this criterion, but it is the best resolved long record publicly available for the region. Apart from that, we are not aware of any other pollen record, that covers the last 60 000 years in that region.
However, this was not possible for Speleothem data, as they do not exclusively grow continuously. Therefore, we also considered speleothem data with more than 250 years between two samples.
For clarity we have deleted the subordinate clauses " from the most cited papers" and "highly cited" as they were not necessary to anyone outside the PalMod project.

ARIDITY INDEX
You now try to better explain how the aridity index is calculated. You say it's the sum of the three scores from the individual (speleothem, pollen, dust) proxy records, each one first scaled to the 0-100% interval, and then discretized as follows: 0/1 for speleothems, and 0/1/2 for pollen and dust (0-33%, 33-66%, 66-100%), resulting in an overall aridity index score between 0 and 5 (e.g. Table 1). Yet, in Figures 2, 3, etc. you have aridity index time series with non-integer values. This is clearly inconsistent with the definition you gave of the aridity index. Aren't you by any chance linearly rescaling the 0-100% dust and pollen time series between 0 and 2?
→ The reconstructed aridity indices are smoothed with a 200-year running average (see P6/ L17) to better display the underlying structures. The actual reconstructed values are integer values, see new Supplementary material. We made this more clear and rephrased it:
"The generated error estimations are displayed in Fig. 2 and Figs. S1-S9 by grey colour shades behind the mean data. The actual reconstructed aridity index values are integer ones (see

Supplementary table) but are displayed with a 200-year running average to better illustrate the basic structures."

I also do not understand how you merge the 3 individual time series, each one representing the "aridity score". The three time series have different temporal resolution. Please explain how this is dealt with.
→ See P5/L11, but we have rephrased it for more clearness to: "Each data set of speleothem growth phases, tree pollen and dust proxies was resampled by linear interpolation to 50 years resolution."

In connection to the point just above, how do you treat "no data" versus "0 or hiatus"? For instance, in the ELSA dust stack (Fig. 2e) you see no values for the last ~3000 years. Is this because there is no dust or no dated material?
→ This particular example is a display error due to the scaling of the x-axis of the ELSA Dust Stack (2009). The values of the last 3000 years are below 3. Therefore, we have replaced Fig. 2e accordingly.
→ No data vs. hiatus is not easy to distinguish, especially in speleothems. For this reason, speleothems were divided into two parts instead of three for the aridity index. The aridity index is more robust when all proxies have similar patterns and especially when all proxies are present. This is the case, for example, for central Europe or China, so the estimated errors are smaller there.

The Central-European aridity index plotted in Fig. 2f is different (truncated) than in Fig. 3a.
→ Thank you for this suggestion. We have replaced Figure 3, where the last 3000 years were mistakenly cut off.

You claim to be using one and only one record, per type of proxy, per region (with the exception of Santa Barbara basin), but in fact I still see two speleothem records in Figure 2. Please try to be consistent.
In connection to the point just above, you have also not explained how you deal with multiple records of the same type within each region. For instance, for Central Europe I still see both Bunker Cave and Spannagel Cave (Fig. 2a,b). Which one is used for calculating the Central Europe speleothem aridity score? If you used both, please justify why and explain how you merged the two records, i.e. based on AND / OR logical operator.
→ We try to be more clear now:
We use only one kind of proxy for dust and vegetation, because there are few and these proxies are very difficult to combine. For speleothems we use several records for the regions central Europe, Arabian Sea, Mediterranean Sea and St. Barbara basin. Since we only use age dating for Speleothem records, they can be easily combined. In addition, the caves are close to each other or have already been compared in previous work:
Central Europe: The speleothems of the Spannagel and Bunker Cave show very similar growth patterns and can be combined (Fohlmeister et al., 2012).
Arabian Sea speleothems from Oman caves and Socotra Island can be compared (Fleitmann et al., 2007; Shakun et al., 2007).
Mediterranean Sea region, Dim Cave and Soreq cave can be compared (Ünal-Imer et al., 2015).
St.Barbara basin: Cave of the Bells and Fort Stanton speleothems show the same climate signals and can both be compared with the St. Barbara basin.
This section is added within the methodology part 2.1.

UNCERTAINTIES

→ The whole section is revised to be more precise:

We used the initial error values as displayed in Table 2. We estimated these based on the data density and the method originally used. These estimates are based on the experience of the ELSA pollen records (Sirocko et al., 2016). Errors for pollen and dust values result in estimated errors of the aridity index on the X- and Y-axis, since time errors must also be estimated. The age errors of the speleothems, however, result in an error on the Y-axis. Counting errors for pollen were considered very small, as the original investigators are very experienced. In addition, the sample rate of at least one sample every 250 years is high enough to smooth out minor errors. In our experience, the measurement inaccuracies of the devices are around 2%. We have therefore taken this value as a minimum measure for the dust error values. Furthermore, there are possible age uncertainties, which become more important for records with smaller sample intervals. Speleothem age errors were given in the original data sources. All speleothem age errors in the speleothem growth data we used for this synthesis were below 4% uncertainty.

To calculate a total error, we have randomly disturbed the original data with a probability given by the error estimates. From the perturbed data we calculated a perturbed aridity index as described in Table 1 and Chapter 2.1. The variance over 100 000 runs indicates the approximate error of our aridity index. This error simulation is based on the method of Koehler et al (2009) and personal communication with M. Mudelsee.

The generated error estimations are displayed in Fig. 2 and Figs. S1-S9 by grey colour shades behind the mean data. The actual reconstructed aridity index values are integer ones (see Table S2 in the Supplement) but are smoothed with a 200-year running average to better display the underlying structures. Smoothed aridity index values below 1.5 account for arid conditions, values between 1.5 and 3.5 show intermediate aridity and values larger then 3.5 show more humid conditions (see Fig. 4).

This section is still too generic. What is an error for pollen and dust? (You use all kinds of dust proxies by the way, and I am not sure how you deal with the different cases). Mentioning that you learn from the experience of the ELSA stack is just not enough. Okay the description of the Montecarlo procedure, but where do you get the perturbations from in the first place? This needs to be spelled out clearly, and the actual values/ranges of these perturbations properly justified. → See reply to Uncertainties.

The uncertainties in Table 2 are expressed as percentages. With respect to what? Age or value of the proxy variable (i.e. x or y axis)? To the actual value of the aridity index in the 0-1 or 0-2 range for the individual proxies?

→ The percentages refer to the original values of the data. This means that all values are considered for example as ± 2% → Dust concentration of 42% ±2% estimated uncertainty.

How do you combine these individual uncertainties into the overall aridity index uncertainty (the grey shaded area)? → See reply to Uncertainties in general

RESULTS

In this section (and the corresponding supplementary sections for the different regions) you could indeed introduce in the discussion the relevant records that are not used for the calculation of the aridity index, for instance the records of Nussloch and Dunaszecsko you

cited, and compare qualitatively with the records you actually used for the calculation of the aridity index.

→ We have added a paragraph about this to the discussion, according to your suggestion.

Anonymous Referee#4

Review of revised paper by Fuhrmann et al. “Aridity synthesis for 10 selected key regions of the global climate system during the last 60 000 years”
Thanks again for your helpful suggestions. We have revised the manuscript according to your suggestions. Our answers to your comments are marked in red.

The manuscript by Fuhrmann et al. has been substantially improved. However, there are a few remaining issues that I strongly recommend to revise:

-P1/L26: “This paper emerges from the PalMod project which develops a long GCM time series of past global temperatures...”. PalMod is doing much more than just a long GCM time series of past temperatures!
→ changed to „This paper emerges from the PalMod project, which among other things is developing a long GCM time series of past global temperatures (www.palmod.de).”

-P1/L27: “One prerequisite of the project was to work only with publically available datasets from the most cited papers”. I doubt that “most cited” was a PalMod prerequisite. Personally, I also think that this is a very questionable criterion. Generally, the number of citations is not a faithful quality indicator.
Comment of F.Sirocko:
This was indeed not a prerequisite of the Palmod programm, but was discussed with the group leader of WG3 to be a good aproach, when we realised how little published data are accessable indeed. It was decided in the first WG3 meeting at Mainz by F.Sirocko and M.Kucera.
The data mining prerequiste was insisted on by M.Kucera and S.Mulitza, even if we expressed our sincere problems with a 100% data mining aproach several times - from the very beginning of Palmod planning to the proposal for the second funding phase.

→ We agree that the citation number is not an indicator of quality. However, the synthesis is based on publicly available datasets, since data mining with the most cited papers produced very few publicly available datasets. These few datasets have then been sorted by citation for the project. For clarity we have deleted the subordinate clause " from the most cited papers" and we have rephrased the section on methodology to provide more clarity.

-P2/L8: Note that the “...the boundaries of the MIS have been developed by Imbrie et al. (1984) and Martinson et al. (1987)” are outdated. The stacks provided by Lisiecki and Raymo (2005, Paleoceanography, 20, doi:10.1029/2004PA001071) or Lisiecki and Stern (2016, Paleoceanography, 10.1002/2016pa003002) are up to date.
→ We have taken the updated boundaries from Spratt & Lisiecki (2016, CP), as they have refined the MIS 2 borders furthermore.

-P2/L13: What is “highly cited”?
→ In the beginning we looked for literature with more than 5 citations per year. But since we could not find any data for many papers, we searched the databases afterwards and in a first step we made sure that the records cover as much as possible of the last 60 000 years. From this selection, we chose those records which had a better data resolution than 1 sample per 250 years. Only the pollen record for NW-Africa does not fall under this criterion, but it is the

best resolved long record publicly available for the region. Apart from that, we are not aware of any other pollen record, that covers the last 60 000 years in that region.
However, this was not possible for Speleothem data, as they do not exclusively grow continuously. Therefore, we also considered speleothem data with more than 250 years between two samples. For clarity we have deleted the subordinate clauses " from the most cited papers" and “highly cited” as they were not necessary to anyone outside the PalMod project.

-P3/Fig 1: It seems that the location of the Susah Cave is wrong in Fig. 1 (c.f. Rogerson et al., Clim. Past, 15, 1757–1769, https://doi.org/10.5194/cp-15-1757-2019.). Also, it seems that Susah Cave is actually in the Mediterranean group? In Fig. 5, Susah Cave is listed under NW-Africa.

→ You are right, there we made a mistake. We wrote down the place wrong and did not notice this. Therefore we removed Susah Cave from the regional synthesis NW-Africa and adjusted the chapter accordingly.

-P4/L19: “The global climate evolution is well documented within Greenland and Antarctica ice cores”. I still disagree. For example, tropical precipitation is not represented in ice cores.

→ according to your suggestion, we have deleted the sentence.

-P5/L3: “In sediments from the Cariaco Basin, the Al/Ti ratio gives the proportion between terrigenous river sediments with higher Al/Ti ratios and Saharan dust with respective lower Al/Ti ratios.” Please back this statement up by a citation or robust evidence. Yes, there is some Saharan dust arriving in the Caribbean, but this is negligible compared to river input, and I doubt that the dust signal is visible in the Cariaco Basin.

→ The reference was directly after the second sentence: “In sediments from the Cariaco Basin, the Al/Ti ratio gives the proportion between terrigenous river sediments with higher Al/Ti ratios and Saharan dust with respective lower Al/Ti ratios. Ratio of 14 represent pure Saharan dust (Yarincik et al., 2000).” But according to your and another referees suggestions, we have deleted Cariaco Basin and Oceania as regions, so you can’t find this section anymore.

-P7/L25: “The Atlantic sea surface temperature pattern (caused by the Atlantic meridional overturning circulation - AMOC) strongly influence the whole European continent today”. Please revise this sentence. The Atlantic sea surface temperature pattern is not only caused by the AMOC.

→ We agree, that AMOC is not the only cause. We have accordingly deleted this.

-P7/L28/29; “... of central ??..”, “...with varved ??”

→ An established geoarchive to reconstruct the climate of central Europe are the volcanic maar lakes of the Eifel, which cover the Holocene with varves (…).

-P10/Fig. 3, P13/Fig. 5: As already argued in my first review I still find it very unreasonable to merge the Bahamas cave with the records from the Cariaco Basin and potentially (see comment on Fig 5 above) the Susah Cave (located at 33N/22E close to the Mediterranean) with NW African records. The prerequisites from PalMod cannot be relevant for my assessment of this paper.

→ According to your and the other referees suggestions, we have deleted Cariaco Basin and Oceania as regions. Susah Cave has been removed from NW-Africa.

Aridity synthesis for ~~10~~8 selected key regions of the global climate system during the last 60 000 years

Florian Fuhrmann[1], Benedikt Diensberg[1], Xun Gong[2], Gerrit Lohmann[2], Frank Sirocko[1]

[1]Department for Geoscience, Johannes-Gutenberg-Universität, Mainz, 55099, Germany

[2]Alfred Wegener Institute for Polar and Marine Research, Bremerhaven, Germany

Correspondence to: Florian Fuhrmann, (flfuhrma@uni-mainz.de)

Abstract. A compilation of published literature on ~~the~~ dust content in terrestrial and marine sediment cores ~~are synchronised on the basis of~~ was synchronized with pollen data and speleothem growth phases ~~within~~on the GICC05 ~~age constrain.~~time axis. Aridity patterns for ten key areas of the global climate system ~~are~~have been reconstructed ~~over~~for the ~~past~~last 60~~-~~,000 years. These records have different time resolutions and different dating methods, ~~thus various~~i.e. different types of stratigraphy. Nevertheless, all ~~the~~ regions analysed in this study show humid conditions during ~~the~~ early ~~Marine Isotope Stage~~marine isotope stage 3 (MIS3) and the early Holocene, but not always ~~with~~at the same ~~timing~~time. Such discrepancies have been interpreted as regional effects, although stratigraphic uncertainties may affect some of the proposed interpretations. In comparison, most of the MIS2 interval becomes arid in all of the northern hemisphere records, but the peak arid conditions of the Last Glacial Maximum (LGM) and Heinrich event 1 differ in duration and intensity among regions. In addition, we also compare the aridity synthesis with modelling results using a Global Climate Model (GCM). Indeed, geological archives and GCMs show agreement of aridity pattern for the Holocene, LGM and for the late MIS3.

1 Introduction

Paleoclimate research today has two main foci: i) well dated, high resolution archives of past climate (e.g., marine and terrestrial sediments, speleothems, tree rings and ice cores), ii) modelling of global and regional characteristics with Global Climate Models (GCM), which include main processes in atmosphere, ocean, land and cryosphere as well as their coupling. Geological archives have the potential to provide information on the past states of climate variables at the global and regional level, and their evolution in time. The strength of modelling approach, on the other hand, is to understand the processes of climate change and global teleconnections. A reliable model of past climate change should faithfully reproduce the observed climate patterns as reconstructed from geo-archives. We will test this prerequisite for a set of records that approximating past global aridity.

This paper emerges from the PalMod project, which ~~develops~~among other things is developing a long GCM time series of past global temperatures ~~(www.palmod.de),~~(www.palmod.de). One prerequisite of the project was to work only with

~~publically~~publicly available datasets~~ from the most cited papers.~~. Thus, we had to use only available datasets from ~~publically~~publicly accessible databases (PANGAEA, NOAA-NCDC, Neotoma (global pollen database), ice core database from Copenhagen university, SISAL (speleothem database) and EPD (European pollen database~~)) by citation count. The~~)). For the calculation of the aridity index, the most complete~~, highly cited~~ and ~~well~~best dated ~~(~~records, dating back to 60~~-~~ 000 ~~yr~~years b2k~~) records~~ with ~~high~~the highest possible sample resolution were used~~ for the aridity index calculation.~~. We could not ~~incorporate those~~include the records ~~into~~that do not meet these requirements in the calculation of the aridity index ~~calculation, which do not fulfil this prerequisites (see the compilation of prerequisites above).~~. All data were plotted on the age scale b2k.

~~We use continuous time series that cover the Holocene, 0 - 11 700 years before 2000 CE (yr b2k), Marine Isotope Stage 2 (MIS2) (24 000 - 12 500 yr b2k) and also the flickering climate of MIS3 (60 000 – 24 000 yr b2k).The boundaries of the MIS have been developed by Imbrie et al. (1984) and Martinson et al. (1987) with refinements by Thompson and Goldstein (2006).~~ We use continuous time series covering as much as possible of Holocene, 0 - 11 700 years before 2000 CE (yr b2k), Marine Isotope Stage 2 (MIS2) (25 000 - 18 000 yr b2k) and also the flickering climate of MIS3 (60 000 – 25 000 yr b2k, with MIS boundaries revised by (Spratt and Lisiecki, 2016)).

In this paper, we concentrate on published paleoclimate reconstructions for aridity, which is one of the most important indicators of climate change. We have screened published paleoclimate literature of the last 30 years to detect and select ~~10~~ key areas. These key areas were defined by the proxy availability, i.e. pollen, dust and speleothem growth must provide three independent sources of information related to past precipitation. These areas were selected because they were the smallest possible regions meeting the following criteria: i) ~~publically~~publicly available ~~datasets~~records from data repositories, ii) highly cited, iii) well dated, iv) sufficient sample resolution ~~(~~of at least 1 sample per 250 years and as far back as possible up to 60~~-~~ 000 yr b2k~~). Many important records of paleoclimatic research are thus not included in these 10 key regions, because only one or two of the aridity proxies are available or they are far away from complementary aridity records.~~. Several high~~-~~-resolution ~~records which extend into~~data sets reaching as far as MIS3 (see~~.~~ Fig. S11, ~~dotted~~dashed lines) are ~~accessible from~~ available in the literature, but ~~were~~have not ~~incorporated into~~been included in this synthesis, ~~because these cores were~~ either because these archives are too far away from the ~~chosen ten~~selected key regions to fit into a suitable synthesis or because they cover only a small part of the last 60~~-~~ 000 years. Some important records of paleoclimatic research are not included because only one or two of the aridity proxies for the region are available and complementary data are not available. Many other cores are excellent archives~~ and will be discussed in this paper~~, but cannot be incorporated into the numerical calculation of the aridity index~~ if~~, because the data are not accessible from official data repositories. Sediment cores from e.g. Lake Tulane (Grimm et al., 2006), Bear Lake (Jiménez-Moreno et al., 2007), Lake Suigetsu (Bronk Ramsey et al., 2012), Petén-Itzá (Correa-Metrio et al., 2012) and Potrok Aike (Kliem et al., 2013) were not included in the aridity index as there were no other long time series with ~~publically~~publicly available datasets beside pollen within the region of the archive. The excellent loess archive of Nussloch (Antoine et al., 2001; Moine et al., 2017) could not be used for the synthesis because no accessible data were available in official data repositories. ~~Even the excellent~~The record of Dunaszekcso loess (Újvári et al., 2015) or pollen records from

Tenaghi Phillipon (Pross et al., 2015) are not incorporated, because no data are available that covered at least a longer period of the last 60 000 years.

Dust is deflated only in regions with less than 200 mm/a precipitation, and thus indicate an arid climate (either subtropical or polar) (Pye, 1987). Speleothem growth needs dripping water in a cave, and thus rain or snow melt (Spötl and Mangini, 2002). Arboreal pollen implies more precipitation than in a landscape with abundant grass pollen. Accordingly, we do not evaluate the full width of information from these paleoclimate proxies, but just reduce the evidence to its basic structure, which is aridity. The most faithful aridity indicator is dust, which indicates deserts, whereas grass indicates steppic landscapes. Throughout this synthesis, we use 'climate improvement' for warmer and wetter climate conditions, whereas 'climate deterioration' (or similar terms) accord for colder and drier climate.

Figure 1 present the ~~10~~ key regions. The detailed evidence for each of the selected ~~10~~ key regions and their well dated and high-resolution proxy records are presented in Fig. 2 and Supplement S1-~~S9~~S7. The discussion compares the synoptic aridity reconstruction for the time of LGM (26 500 – 19 000 yr b2k), and late MIS3 (32 000 yr b2k, Fig. 4) with GCM simulations (Fig. 7, Tab. 3). Mix et al. (2001) define the LGM from comparably stable conditions during the time interval of 23 000 to 19 000 yr b2k. Clark et al. (2009) define the LGM by the maximum extend of the ice sheets and sea level low stand to 26 500 to 19 000 yr b2k for most parts of northern and southern hemisphere. We follow the wider definition of Clark et al. (2009), which encompasses the regional differences in the results of this work.

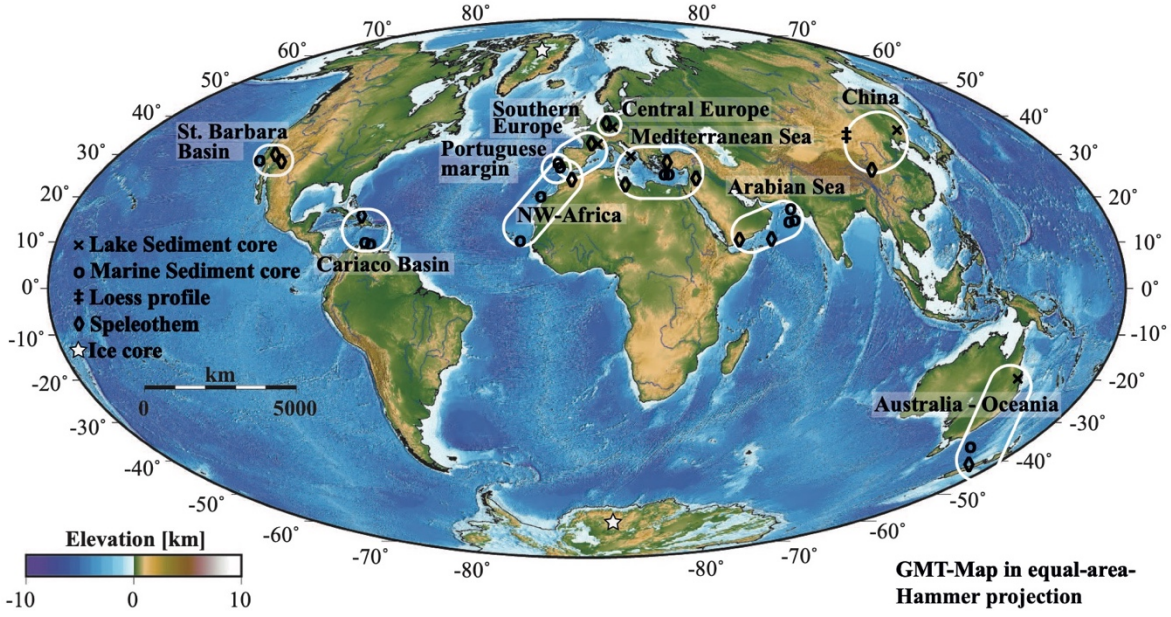

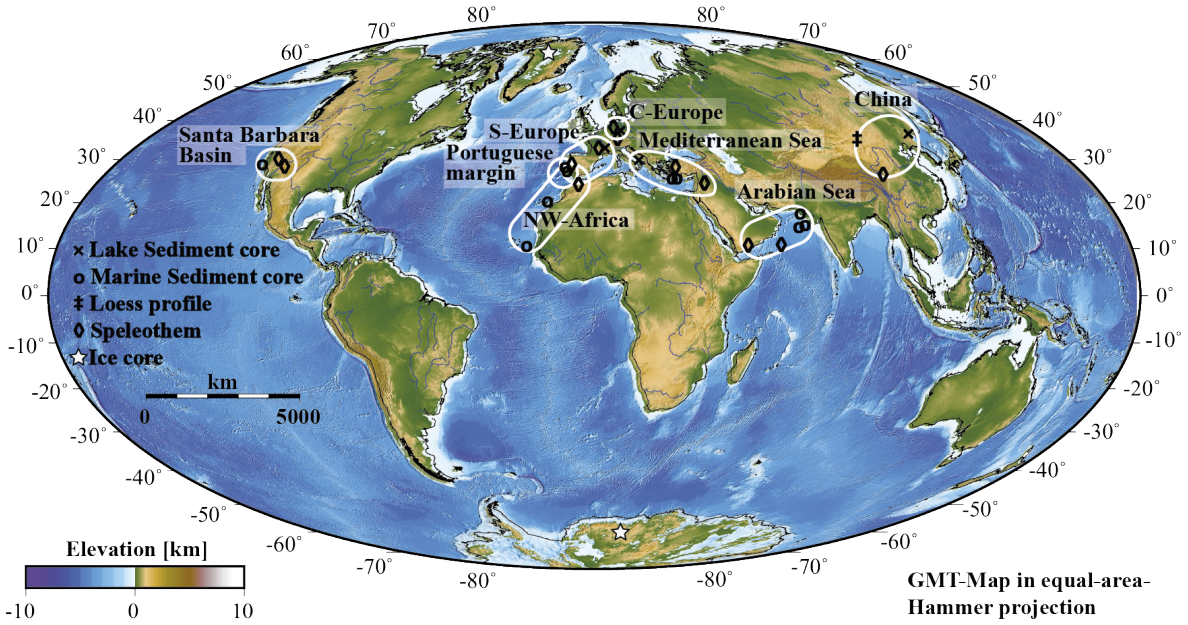

Figure 1: Global map with the 10 selected key regions and archive type, Generic Mapping Tool (GMT) (Wessel and Smith, 1991). Regions are indicated with white boundaries. Crosses sign lake sediment cores; open circles marine sediment cores; double sharp marks loess profile; Diamonds mark speleothems and white stars ice cores. The map is colour coded for the elevation.

We start the synthesis with Central Europe: Dust and pollen records from Eifel (Seelos et al., 2009; Sirocko et al., 2016), which we compare with speleothem data from nearby Bunker Cave (Fohlmeister et al., 2012, 2013; Weber et al., 2018) as well as the Spannagel Cave in Austria (Holzkämper et al., 2004, 2005; Spötl and Mangini, 2002)~~, which shows a similar speleothem growth pattern~~. The speleothems of the Spannagel and Bunker Cave show very similar growth patterns and can be combined (Fohlmeister et al., 2012). The maar sediment cores of the Eifel Laminated Sediment Archive (ELSA)-project (Sirocko et al., 2016) show all Greenland Stadials (GS) and Greenland Interstadials (GI) in the time series of eolian dust content (Dietrich and Sirocko, 2011; Seelos et al., 2009). Central Europe shows accordingly the same climatic structures, which are well known in North Atlantic marine sediments (e.g. Hodell et al., 2013; McManus et al., 1994; Naafs et al., 2013) and Greenland ice cores (North Greenland Ice Core Project Members et al., 2004; Rasmussen et al., 2014; Svensson et al., 2008). This Central European climate time series is then compared with the respective time series from all other ~~9~~ key regions, which data evidence is documented in the supplement.

2 Methods

The synthesis is based on pollen profiles from sediment cores, growth phases of speleothems and several dust proxies like grain size of eolian fraction within sediment cores.~~ Also, isotope data like $\delta^{18}O$, Sea Surface Temperature (SST) reconstructions or Ice Raft Debris (IRD) data are added to complete the interpretations within Figure 4 (for more details, see the supplement~~

~~section).~~ We used the original stratigraphy of all records on the age scale of yr b2k but we are aware of a general error of up to ± 2 000 years for all MIS 3 dates.

Especially the growth phases of speleothems are a significant indicator for presence of mobile water. If a speleothem could grow, at least some precipitation occurred over the cave. If a speleothem does not grow (hiatus), either no precipitation or a change of the drip water system above the cave could be causes. Most speleothem datasets also provide $\delta^{18}O$ or other isotope measurements (Genty et al., 2003; Hoffmann et al., 2016; Wainer et al., 2009) which often have local characteristics, thus our index only uses growth phases as the most common and robust aridity indicator.

Pollen ~~are separated in~~were divided into two classes for this work. Trees and shrubs (in the following only ~~named~~called tree pollen) ~~were combined as~~have been grouped together because they require similar ~~climate~~climatic conditions for their growth. Herbs and grasses (in the following only ~~named~~called grass pollen) were also combined. Trees ~~need~~require a ~~significantly larger~~much higher amount of ~~precipitation~~rainfall than grasses ~~to grow. So, a~~for their growth. A simple statement about the relative precipitation ~~of~~in the catchment area of the core can therefore be ~~done by looking at~~made using the tree / grass pollen ~~ratios~~ratio. In general, a higher amount of tree pollen indicates a warmer and wetter climate than high amounts of grass pollen. The ~~time~~temporal resolution of the pollen profiles is often low, but we have ~~chosen~~selected the ~~accessible~~available data with the highest resolution ~~data of~~from each selected region for ~~the~~ comparison.

~~The global climate evolution is well documented within Greenland and Antarctica ice cores (Andersen et al., 2006; EPICA community members, 2004; Grootes et al., 1993; North Greenland Ice Core Project Members et al., 2004; Rasmussen et al., 2006; Svensson et al., 2008; WAIS Divide Project Members et al., 2015; and others)~~ The best chronology for the northern hemisphere is from the annual layer counted NGRIP ice core in Greenland (Rasmussen et al., 2014). These ice core data include also dust (Ruth et al., 2003, 2007). This record is a backbone of dust records, but outside of the chosen regions of the aridity index. ~~Thus,~~Therefore, the NGRIP~~-~~ dust concentration was only used in comparison to central European dust~~.~~ from the ELSA-Dust-Stack (2009).

Several dust proxies were used for this synthesis due to a large variety in dust over the ~~several~~key regions. Calcium carbonate ($CaCO_3$) in the ocean is deposited in higher rates with warmer sea surface temperatures ~~-~~if cores are situated above the lysocline. Therefore, lower $CaCO_3$ contents of ocean sediments in regions of high dust deposition (e.g. ~~deMenocal et al., 2000; Leuschner and Sirocko, 2003)~~deMenocal et al., 2000; Leuschner and Sirocko, 2003) indicate increased mainly aridity, but is also effected by changing wind directions and ocean temperature change. This proxy is thus used only for the construction of the aridity index in Portuguese margin, off west Africa and Arabian Sea.

The grainsize record from the Jingyuan loess plateau in China shows phases of aridity. The larger the sediment grains, the lower the precipitation and temperature and the higher the wind speeds (Sun et al., 2010; Xiao et al., 1995, 2015). Dust ~~or eolian~~ content ~~of the sediment~~ in sediments off NW-Africa is given in percentages of the whole sample composition. ~~This is a very robust proxy and used for Australia – Oceania and NW-Africa regions.~~

~~In sediments from the Cariaco Basin, the Al/Ti~~The ratio ~~gives the proportion between terrigenous river sediments with higher Al/Ti ratios and Saharan dust with respective lower Al/Ti ratios. Ratio of 14 represent pure Saharan dust (Yarincik et al., 2000).~~

~~Kaolinite /~~kaolinite/chlorite (K/C) ~~ratio are~~is a dust proxy for the Mediterranean ~~Sea~~ region (Ehrmann et al., 2017). Higher K/C ratios (more kaolinite than chlorite) ~~indicates~~indicate an increased ~~eolian~~aeolian dust transport~~. During humid periods, kaolinite was stored within lakes or basins - due to increased erosion - and deflated during arid periods~~.

2.1 Data treatment and aridity index calculation

We ~~plot~~have generated all ~~chosen data~~synthesis plots for ~~a region~~the regions with ~~a~~ELSAinteractive++ (Diensberg, 2020). This software~~,~~ was written in C++ for the ~~PalMod~~ subproject PalMod at ~~Mainz~~the University ~~(‘*ELSA*interactive ++’ Diensberg, 2020).~~ of Mainz. This software ~~is~~was developed ~~to work~~for working with sediment cores on age or depth scale. ~~The time series~~ Each data set of speleothem growth phases, tree pollen and dust proxies ~~were~~was resampled ~~to 50 year resolution (~~by linear interpolation~~). Afterwards~~ to 50 years resolution. Subsequently, the resampled ~~datasets~~data sets were ~~transferred~~converted into index values. Therefore, ~~for each timeseries,~~ the data ~~has been recalculated~~for all time series were converted into percentages if the original data ~~was~~were not~~. Maximum~~ given as percentages. This was done by setting the maximum value of each ~~dataset was~~data set to 100%, the minimum value ~~was set~~ to 0%, and normalizing values in between ~~have been normalized.~~

. Speleothem growth phases give information on humid phases, however “no growth” can either indicate changes in the dripwater system or arid conditions. Grass pollen act as a counterpart to tree pollen which indicate humidity. Grass pollen values and dust values are considered to be the more robust aridity proxies, compared to speleothem growth phases. Therefore dust proxies and tree pollen index values were separated into three parts (0, 1, 2) while speleothem growth was only separated into two parts (0, 1). Speleothem growth ~~gets~~is given index values of 1, index values of 0 ~~account for~~indicate no growth. ~~For tree~~Tree pollen ~~percentages~~contents below 33~~%, index values~~ % were assigned ~~to~~index values of 0. Tree pollen contents between 33~~-~~ % and 66~~-~~ % were assigned ~~to be~~index value 1 and ~~larger than~~above 66~~% to be~~ % index value 2 (see ~~Tab.~~Table 1). ~~Dust is considered inverse to tree pollen, higher~~Higher dust values ~~get~~are assigned to lower index values, ~~as lower~~since less precipitation and ~~therefore~~thus lower soil ~~humidity~~moisture is the prerequisite for dust deflation. ~~So~~Thus dust proxy values larger than 66~~-~~% are assigned to the aridity index value 0, dust proxy values between 33~~-~~% and 66~~% are assigned~~% to the aridity index value 1 and dust proxy values below 33~~% are assigned~~% to the aridity index value ~~of~~ 2. The index values are then finally ~~summed~~added up~~.~~ (a template is available in supplementary materials). The aridity index ranges from 0 (~~highly arid~~very dry conditions) to 5 (~~highly~~very humid conditions). Speleothem growth phases, higher tree pollen values and lower dust values combined ~~therefore~~ indicate increased humidity.

The aridity index for all key regions uses ~~always~~ the three proxy types (speleothem growth, tree pollen, dust proxy), except for St. Barbara basin region, where a dust record is not available. For Arabian Sea region, we used TOC as aridity proxy instead of tree pollen, as there were no available pollen data in databases but an excellent organic carbon record. High TOC in the Arabian Sea sediments is caused by high SW-monsoon intensity, intense upwelling and surface water nutrient content, high flux rated of organic matter causing low deep water oxygen content (Schulz, et al., 1998; Sirocko et al., 1993; Sirocko and Ittekkot, 1992). We use only one record per region for dust and vegetation, because there are few and these proxy records are

very difficult to combine. For speleothems we use several records for the regions central Europe, Arabian Sea, Mediterranean Sea and St. Barbara basin. Since we only use age dating for Speleothem records, they can be easily combined. In addition, the caves are close to each other or have already been compared in previous works (Central Europe, Fohlmeister et al., 2012; Arabian Sea, Fleitmann et al., 2007; Shakun et al., 2007; Mediterranean Sea region, Ünal-Imer et al., 2015; St. Barbara basin: Cave of the Bells and Fort Stanton speleothems show the same climate signals and can both be compared with the St. Barbara basin).

Speleothems		Tree pollen		Eolian dust	
0	no speleothem growth	0	tree pollen values < 33%	0	dust values > 66%
1	speleothem growth	1	tree pollen values > 33% & < 66%	1	dust values < 66% & > 33%
		2	tree pollen values > 66%	2	dust values < 33%

Table 1. Components of the aridity index: Speleothems can either account as value 0 (no speleothem growth) or 1 (speleothem growth); Tree pollen values below 33 % do not add to the aridity index, between 33 % and 66 % they account for index value 1 and above 66 % for 2; Dust values were internally normalized and act inverse to tree pollen. Dust values above 66 % do not increase the index, between 66 % and 33 % they count as value 1 and below 33 % as value 2. The aridity index ranges from 0 (highly arid conditions) to 5 (highly humid conditions).

2.2 Error estimates

In general, the main uncertainties of the proxies are the measurements of the original data~~. In absence of uncertainties for most of the original records, we~~, but for most original data no measurement uncertainties are specified, although each measurement has inaccuracies. Sources of error can be, for example, incorrectly counted pollen or device errors of the measuring instruments. Therefore we have applied a simple Monte Carlo simulation based on error estimates to get an approximation of the total error. ~~For~~To do this, we used the initial error values as displayed in ~~Tab.~~Table 2. ~~Speleothem age errors were given in~~We estimated these based on the ~~original~~ data ~~sources. All age errors of speleothem growth data we used for this synthesis, were below 4 % uncertainty. Errors for pollen~~density and ~~eolian dust were not presented with~~ the ~~original publications; therefore, we had to estimate the uncertainties~~method originally used. These estimates are based on the experience of the ELSA pollen records (Sirocko et al., 2016). Errors for pollen and dust values result in estimated errors of the aridity index on the X- and Y-axis, since time errors must also be estimated. The age errors of the speleothems, however, result in an error on the Y-axis. Counting errors for pollen were considered very small, as the original investigators are very experienced. In addition, the sample rate of at least one sample every 250 years is high enough to smooth out minor errors. In our experience, the measurement inaccuracies of the devices are around 2%. We have therefore taken this value as a minimum measure for the dust error values. Furthermore, there are possible age uncertainties, which become more important for records with smaller sample intervals. Speleothem age errors were given in the original data sources. All speleothem age errors in the speleothem growth data we used for this synthesis were below 4% uncertainty.

To calculate a total error, we have randomly disturbed the original data with a probability given by the error estimates ~~and~~ . From the perturbed data we calculated a ~~disturbed~~perturbed aridity index ~~from the disturbed data~~ as described in ~~Tab.~~Table 1 and ~~chapter~~Chapter 2.1. The variance over 100~~-~~ 000 runs ~~gives~~indicates the approximate error of our aridity index~~.~~ (for the script, see S10). This error simulation is based on the method of Koehler et al~~.~~ (2009)~~.~~ and personal communication with M. Mudelsee.

The generated error estimations are displayed in Fig.~~-~~ 2 and Figs.~~-~~ S1-S9 by grey colour shades behind the mean data~~(~~. The actual reconstructed aridity index values are integer ones (see Supplementary table STab_2) but are displayed with a 200~~-~~-year running average~~) of~~ to better illustrate the ~~aridity index. Hence,~~basic structures. Smoothed aridity index values below 1.5 account for arid conditions, values between 1.5 and 3.5 show intermediate aridity and values larger then 3.5 show more humid conditions (see Fig.~~-~~ 4).

Regions	Speleothem age uncertainty [%]	Tree pollen uncertainty [%]	Eolian dust uncertainty [%]
Central Europe	2.66	3	5
Arabian Sea	1.5	~~1~~	3
China	2	2	2
NW-Africa	1	10	2
Southern Europe	1	4	2
Portuguese Margin	1	3	2
~~Cariaco Basin~~	~~4~~	~~3~~	~~2~~
Mediterranean Sea	2.5	2	3
St. Barbara Basin	1	3	~~no dust source~~
~~Australia - Oceania~~	~~4~~	~~3~~	~~3~~

Table 2. Error estimations as input to simulation for all ~~10~~ key regions for speleothems, tree pollen and eolian dust.

2.3 Model description

We employ the General Circulation Model COSMOS (community of earth system models) which was developed at the Max-Planck Institute for Meteorology in Hamburg (Jungclaus et al., 2006). COSMOS comprises the standardized IPCC4 model configuration which incorporates the ocean-sea ice model MPIOM (Marsland et al., 2003), the ECHAM5 atmosphere model at T31 spherical resolution (~3.75 × 3.75°) with 19 vertical levels (Roeckner et al., 2003) and the land surface model JSBACH including vegetation dynamics (Brovkin et al., 2009). The ocean model is resolved at 40 unevenly spaced vertical layers and takes advantage of a curve-linear grid at an average resolution of 3 × 1.8° on the horizontal dimension, which increases towards the grid poles at Greenland and Antarctica (~30 km). High-resolution in the realm of the grid poles advances the representation of detailed physical processes at locations of deep-water formation, as Weddell, Labrador and Greenland and Norwegian Seas. The ocean model includes a dynamic-thermodynamic sea-ice model (Hibler, 1979). Net precipitated water over land, which is not stored as snow, intercepted water or soil water, is either interpreted as surface runoff or groundwater and is redirected towards the ocean via a high-resolution river routing scheme (Hagemann and Dümenil, 1997).

Our COSMOS version (COSMOS-landveg r2413, Year 2009) has no flux correction and has been successfully applied to test a variety of paleoclimate hypotheses, ranging from the Cretaceous (Niezgodzki et al., 2017), Miocene climate (Knorr and Lohmann, 2014; Stärz et al., 2017), the Pliocene (Stepanek and Lohmann, 2012), glacial (Gong et al., 2013, 2015; Zhang et al., 2013, 2014) and interglacial climates (Lohmann et al., 2013; Pfeiffer and Lohmann, 2016; Wei and Lohmann, 2012) as well as future climates (Gierz et al., 2015; Lohmann et al., 2008).

Here, we present results obtained from model setups encompassing the Pre-industrial (PI), LGM and late MIS3 (32 000 yr b2k) climate conditions. Details of each experiment set-up have been documented in Wei and Lohmann, 2012 (for PI run), Zhang et al., 2013 (for LGM run) and Gong et al., 2013 (for 32 000 yr b2k run), with modified sea level, ice sheets, greenhouse gas concentrations and Astronomical parameters for their conditions in the past, respectively. For the late MIS3 run, the model mimics a GS due to freshwater hosing and GI with overshoot in temperature (Gong et al., 2013).

3 Results

The Central Europe region is our starting point for the comparison with the other key regions, the detailed data description of the other areas is given in the supplement S1-S7.

3.1 Central European climate for the last 60 000 years

The Atlantic sea surface temperature pattern ~~(caused by the Atlantic meridional overturning circulation – AMOC)~~ strongly influence the whole European continent today (e.g. Cassou et al., 2005). Nowadays, the annual mean temperature in Germany is about 9.6 °C and precipitation of about 800 mm/year (Deutscher Wetterdienst, 2018).

An established geoarchive to reconstruct the climate of central Europe are the volcanic maar lakes of the Eifel, which cover the Holocene with ~~varved~~varves (annually laminated sediments~~) and~~), reach far back ~~far~~ into the Pleistocene ~~covering~~and cover the entire last 60 000 years continuously (Sirocko et al., 2016). These maar lakes of the Eifel in western Germany are today up to 70 m deep, with a large water volume and anoxic bottom water, favouring the, preservation of annual layers (Negendank, 1989; Negendank and Zolitschka, 1993; Zolitschka et al., 2000). We use the long records of the ELSA Project at Mainz University (Sirocko, 2016; Sirocko et al., 2005, 2013) as a starting point for our study. Holocene cores are varved or at least laminated, which leads to a good understanding of sedimentation processes (Sirocko et al., 2016). The LGM and stadial core sections were dominated by sedimentation from annual dust storms (Schaber and Sirocko, 2005), see Figure 2.Fig. ~~2. The dust index~~ (Dietrich and Seelos, 2010; Dietrich and Sirocko, 2011; Seelos et al., 2009) calculated a dust index which reveals the GIs in detail. The closest ~~known~~to the Eifel and well-~~-~~dated speleothems ~~to the Eifel region are~~come from the Bunker Cave in the Sauerland (Fohlmeister et al., 2012; Weber et al., 2018) which can be compared to the Spannagel Cave system from western Zillertal, Austria (Fohlmeister et al., 2012; Holzkämper et al., 2004, 2005).

The timespan from 60 000 to 48 000 yr b2k (early MIS3, GIs 17-13) is characterized by ~~a~~ high precipitation visible in the fast speleothem growth of Bunker and Spannagel caves. Nearly 100 % of tree pollen combined with lowest grass and herb pollen values also indicate a wet climate during that time as well as relatively high temperatures close to present day ones (Sirocko et al., 2016). An intermediate dust content in the ELSA-Dust-Stack suggest an intermediate to low aridity, which is supported by a similar pattern of low dust concentration in the NGRIP ice core. ~~This corresponds to underlying common process affecting both regions during this time (most likely the North Atlantic AMOC changes.~~ The pollen composition change in the Eifel began around 49 000 yr b2k towards more grass and herbs pollen. A drastic change in $\delta^{18}O$ occurred at the beginning of GI12 occurred at 46 860 yr b2k (Rasmussen et al., 2014). With the beginning of Heinrich event 5 (HE5), the dust amount spikes in the ELSA-Dust-Stack as well as in the NGRIP core indicating a strong pulse of aridification around 48 000 yr b2k, ending the humid phase of early MIS3.

The period from 48 000 until 38 500 ~~yr~~years b2k ~~comprises~~includes GIs 12-9. The speleothem growth in Spannagel ended at 45 700 yr b2k. The Bunker Cave ~~speleothem shows~~speleothems show a hiatus between 50 000 and 46 000 yr b2k and a short growth recovery, with growth ending around 45 000 yr b2k. The tree pollen proportion decreased to about 50% to 60-%, still

more tree pollen than grass pollen, but a ~~considerably lower~~much smaller amount than in early MIS3. While the dust amount in the ELSA-Dust-Stack ~~rises~~increases to higher intermediate values, the pattern within the NGRIP is characterized by the stadial pulses. ELSA-Dust-Stack, NGRIP dust and NGRIP $\delta^{18}O$ show the same pattern and seem to react ~~apparently~~ to the same mechanism.

From 38 500 to 22 000 yr b2k (GIs 8-2) a change towards lower precipitation and higher aridity occurred. No speleothem growth is documented from Bunker or Spannagel cave. The pollen concentration shows higher grass and herbs content and lower tree pollen percentages, but still some birch and pine trees were present during this time (Sirocko et al., 2016). The ELSA-Dust-Stack comprises of multiple changes within this timespan and shows the general dust content as relatively high with larger variability. The NGRIP in contrast shows the highest dust concentrations in the time between 23 000 and 26 000 yr b2k, a phase where the dust content in the ELSA-Dust-Stack is high, but not at maximum values. The NGRIP $\delta^{18}O$ice whereas shows a phase of cold temperatures (-45° to -50° C) during this time (Kindler et al., 2014).

The timespan of 22 000 to 14 300 yr b2k also does show no speleothem growth as well as a complete absence of all pollen. The precipitation was at the lowest values of the aridity index for that region, while the ELSA-Dust-Stack shows the highest dust amounts from 23 000 up to 15 000 yr b2k. The biggest difference between ELSA-Dust-Stack and NGRIP-Dust can be seen in the period of 26 000 to 23 000 yr b2k, where the dust content in the NGRIP core has two distinct maxima, while the dust content in the Central European record increases only slightly. The ~~revival~~return of vegetation followed shortly after 14 300 yr b2k (Litt and Stebich, 1999). Younger Dryas (YD) is apparent in the pollen data by a grass pollen increase and the Holocene is marked by a sharp increase in tree pollen. Throughout the Holocene, tree pollen values range around 90 %. The dust content of the ELSA-Dust-Stack varies between intermediate to low levels. Speleothem growth in Spannagel and Bunker Cave started again at ~~11 197 (± 94)~~12 408 yr b2k and continues through the whole Holocene. Also, the $\delta^{18}O$ of the NGRIP shows constant high values with exception of the YD event. The time from 14 300 yr b2k up to present day can be described as a humid phase with intermediate to high precipitation and moderate temperatures.

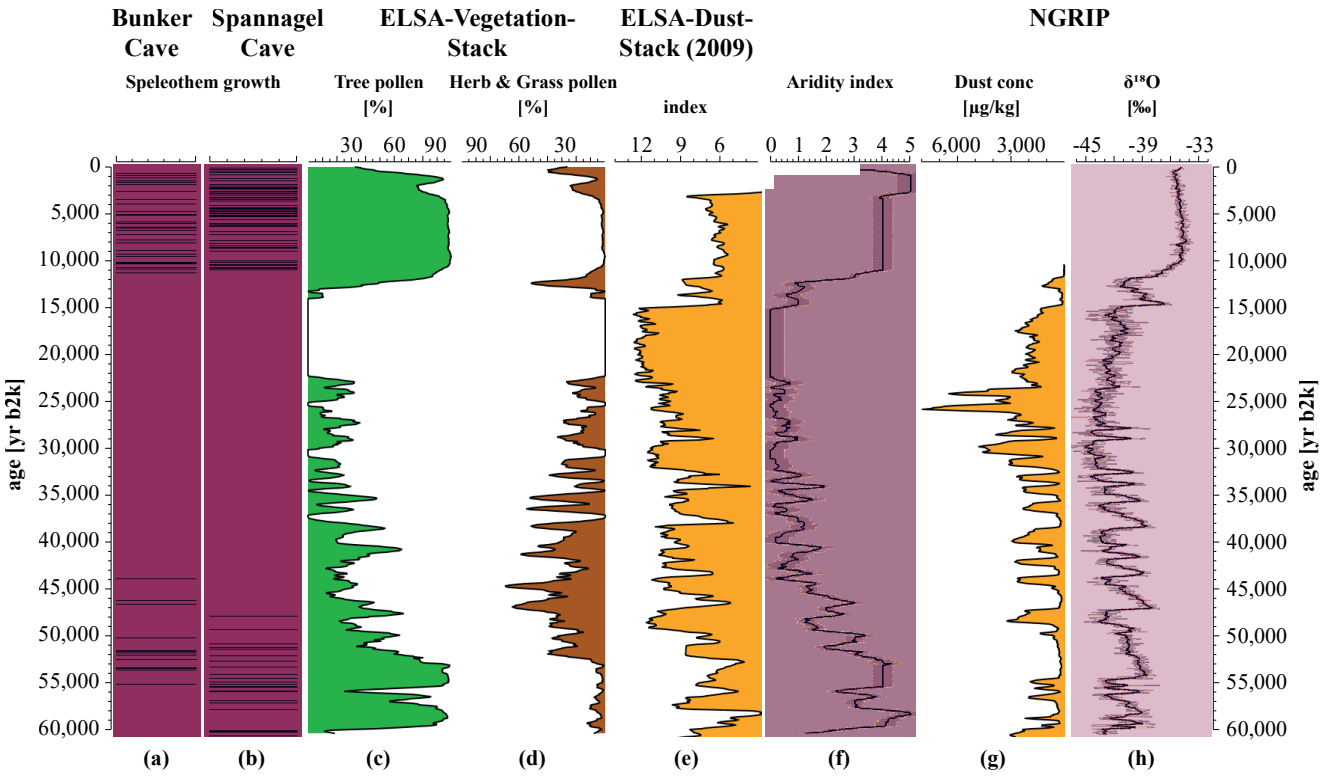
Bunker Cave
Spannagel Cave
ELSA-Vegetation-Stack
ELSA-Dust-Stack (2009)
NGRIP
Speleothem growth
Tree pollen [%]
Herb & Grass pollen [%]
index
Aridity index
Dust conc [µg/kg]
δ18O [‰]
30 60 90
90 60 30
12 9 6
0 1 2 3 4 5
6,000 3,000
-45 -39 -33
0
5,000
10,000
15,000
20,000
25,000
30,000
35,000
40,000
45,000
50,000
55,000
60,000
age [yr b2k]
(a)
(b)
(c)
(d)
(e)
(f)
(g)
(h)

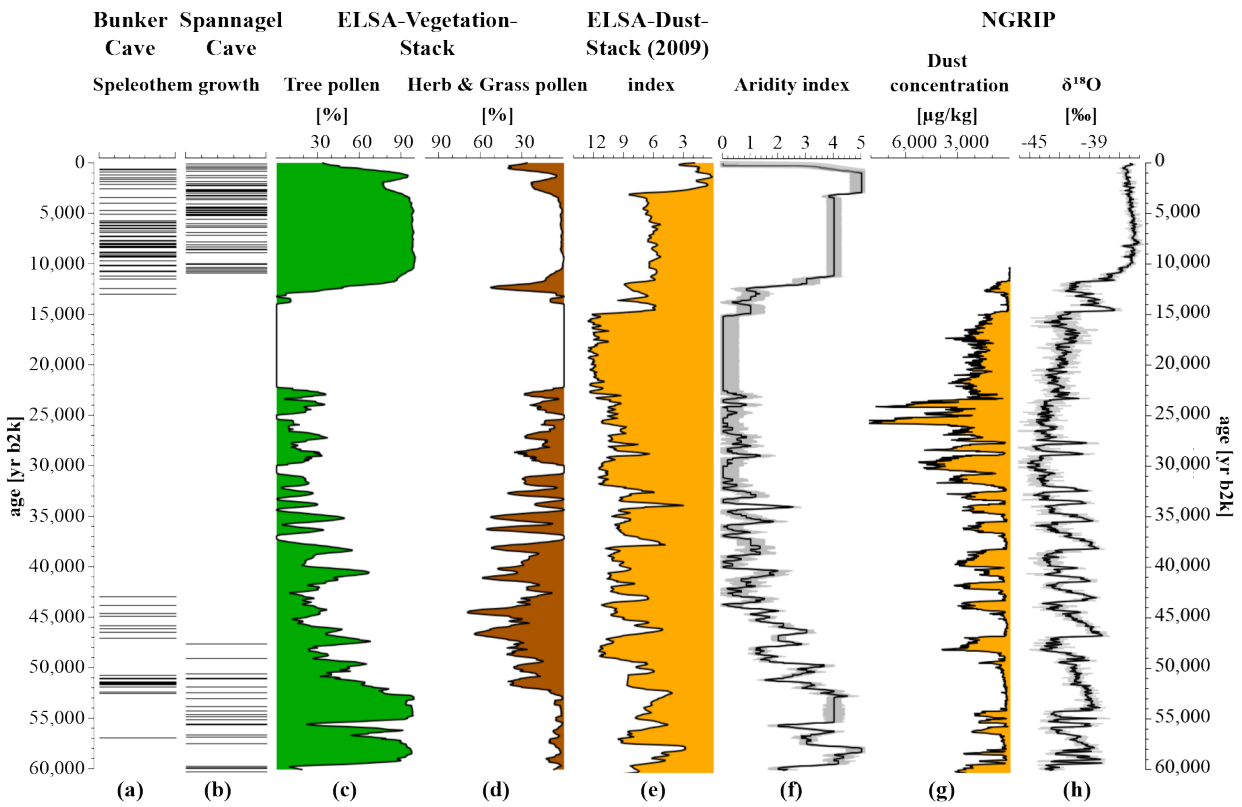

Figure 2: Central European climate over the last 60 000 years: **(a)** Bunker Cave (Fohlmeister et al., 2012, 2013; Weber et al., 2018) and **(b)** Spannagel Cave (Holzkämper et al., 2004, 2005; Spötl and Mangini, 2002) show speleothem growth phases, which require mobile water from frequent precipitation; **(c, d)** ELSA-Vegetation-Stack pollen data (Sirocko et al., 2016) are divided into tree- and herb & grass pollen. While trees require more precipitation, grasses are dominant for more arid conditions; **(e)** ELSA-Dust-Stack (Seelos et al., 2009) indicates more arid conditions with higher values, lower values account for more humid conditions. GIs are distinguishable by lower index values and are highly comparable to **(h)**; **(f)** Aridity index for Central Europe as result from **(a-e)**, for detailed information see method section; **(g)** Dust concentration from NGRIP ice core (Ruth et al., 2007); **(h)** $\delta^{18}O$ data from NGRIP ice core (North Greenland Ice Core Project Members et al., 2004) in comparison.

~~The Central Europe region is our starting point for the comparison with the nine other key regions, the detailed data description of the other areas is given in the supplement S1-S9.~~

3.2 Aridity reconstruction of the last 60 000 years

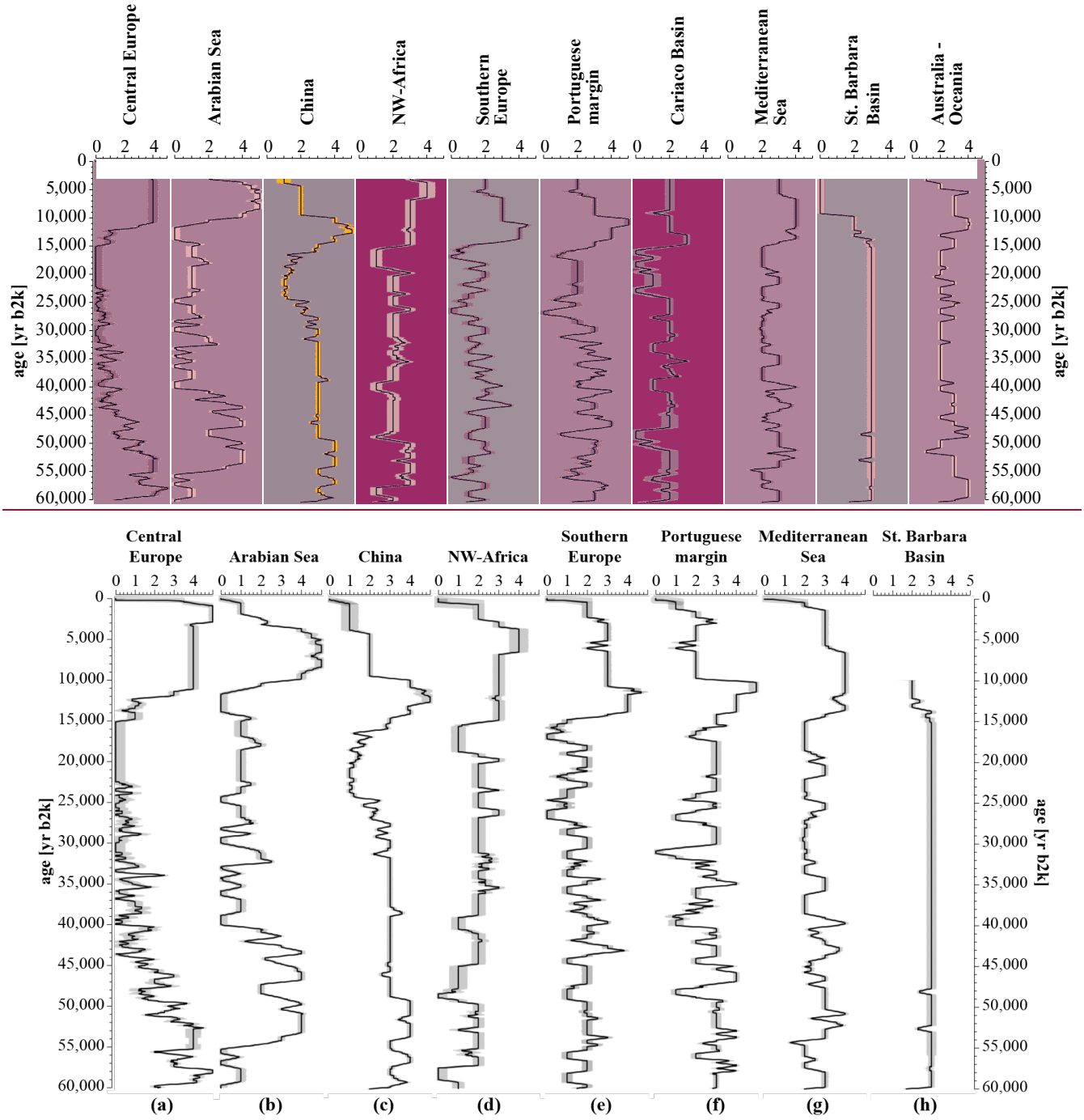

Figure 3: Aridity indices for the ~~10~~ key regions over the last 60 000 years. Smaller values indicate more arid, higher values indicate more humid conditions. An early MIS3 wet phase and a Holocene wet phase on various timings for the regions are recognisable.

Figure 3 ~~displays~~shows all aridity indices from the regional syntheses. ~~Humid~~A humid, early ~~MIS 3 is apparent~~MIS3 can be identified for all regions ~~beside Cariaco Basin and~~ adjacent to the St. Barbara Basin, ~~however~~but sometimes with ~~offset~~a time lag of several millennia ~~in timings~~. We cannot ~~ensure if~~be sure whether these ~~offset~~shifts are caused by ~~the~~ stratigraphy or whether they represent leads and lags in the climate system itself. Arid LGM conditions are identifiable for Central Europe, Arabian Sea, China~~,~~ NW-Africa, Southern Europe, Portuguese margin~~, Cariaco Basin~~ and Mediterranean Sea region. The last deglaciation is visible in all records by drastic changes around 14 700 yr b2k. A humid phase during Holocene is also apparent for all regions, apart from St. Barbara Basin, where the proxies show an opposing signal to the other archives due to regional effects ~~(~~(Heusser, 1998; see ~~S8~~S7 'St. Barbara Basin'). Fig. 3h is truncated, as no Holocene proxies are available for that region from these records (see S7).

Figure 4 is based on the aridity indices shown in Fig. 3 and additional information of the regional syntheses (see Fig. 2 and S1-~~S9~~S7). For example, ~~publically~~publicly available pollen data from Mingram et al. (2018) start at 10 150 yr b2k. Pollen reconstructions from Stebich et al. (2015) give additional holocene information on the Sihailongwan maar lake (see S3 'China'). Therefore, we have used the additional information ~~after~~following the construction of the aridity index to complete the interpretation shown in Figure 4. Blue bars ~~show~~indicate humid conditions, yellow bars ~~intermediate~~indicate medium and red bars indicate arid conditions. Transitions or subdivisions between these ~~states~~conditions are ~~marked~~indicated by ~~both bars~~ overlapping ~~each other~~bars. Figure 4 shows three large~~-~~-scale structures that ~~link~~connect all ~~10~~ selected key areas. The Holocene is ~~in general~~generally always relatively humid, but there are regional ~~variations occur~~differences between the early and late Holocene. The ~~time~~period of the LGM is arid in all selected key regions ~~of the globe~~, but the ~~begin~~beginning of the arid phase ~~starts with large offsets~~varies between ~~the 10~~ regions~~, which can~~. These may also be ~~again~~ related to stratigraphic inconsistencies or ~~present~~existing leads and lags in ~~the~~ regional climate change. The early MIS3 is quite warm and humid in all regions. The signal is strongest in Central Europe~~, south-eastern Asia~~ and China from 60 000 to around 48 000 yr b2k, and in the Arabian Sea from 55 000 to 42 000 yr b2k (Fig. 4 and S1). ~~Australia, indicating~~This indicates teleconnections between the North Atlantic and the subtropical monsoons (Sirocko et al., 1993).

~~High humidity is clearly visible for early MIS3 phase for most of the regions apart of the Cariaco basin. The signal is strongest in Central Europe~~ North-west Africa and Southern Europe were slightlyfrom 60 000 to around 48 000 yr b2k, and in the Arabian Sea from 55 000 to 42 000 yr b2k (Fig. 4 and S1). ~~North-west Africa was~~ less humid in the early MIS3, but still shows enhanced precipitation compared to mid and late MIS3. ~~China and Southern Europe were humid.~~The Portuguese margin region underwent larger changes compared to the other regions, as it was directly influenced by the North Atlantic. The Mediterranean Sea region also was more humid during mid and late MIS3 but not as humid as other regions, St. Barbara Basin shows humidity with same intensity. ~~The Oceania region shows similar patterns for early MIS3 but with a major decrease in precipitation between 55 000 and 50 000 yr b2k.~~ The early MIS3 was generally quite humid in the northern hemisphere. A pronounced aridification occurred with H5 (around 48 000 yr b2k), especially in NW-Africa, Portuguese margin region, Arabian Sea, Southern and Central Europe.

The ~~time~~period between 45 000 and 15 000 years b2k was ~~globally~~ less humid globally than the early MIS3 ~~around~~by 50 000 years b2k. ~~Variations~~During late MIS3, variations occur within ~~the~~ regions ~~during late MIS3~~, but ~~nevertheless on intermediate or~~ between medium and more arid conditions. Heinrich events ~~appear~~seem to have a strong ~~impact, especially in the Cariaco Basin where climatic conditions drastically impair during Heinrich events.~~influence. Towards the end of the LGM ~~time,~~period all regions show arid or intermediate conditions, but ~~most arid was again central~~Central Europe and the Arabian Sea~~.~~ were the most arid. The LGM is characterized by ~~decreased~~reduced precipitation, which is clearly visible by the red bars around 20 000 years b2k (Fig. ~~4). Oceania conversely shows intermediate values throughout the whole~~ 4).

The LGM ~~indicating at least some precipitation during the whole period.~~

~~Following the LGM,~~period was followed by a global climate ~~amelioration took place~~improvement, again with a different ~~timings in the onset~~ start time for each region ~~due to regional or latitudinal effects.~~. The earliest and most ~~drastic~~pronounced climate improvement took place in China, followed shortly after by the Mediterranean ~~region~~Sea, Central Europe, Southern Europe and the Portuguese margin~~. Also, Cariaco Basin,~~ regions. In the St. Barbara Basin ~~and Oceania underwent~~, too, there were climate improvements even before the Holocene ~~begun~~began. This ~~overall~~general climate improvement is most likely associated with the warming of the North Atlantic ~~warming at~~by 14 700 yr b2k (Rasmussen et al., 2014). ~~The Early Holocene Climate Optimum took place with beginning of the Holocene with a temperature and precipitation maximum~~The early Holocene climate optimum occurred around 8 000 years b2k ~~(Shakun and Carlson, 2010). This is apparent for Central Europe, Arabian Sea, north-west Africa, Mediterranean Sea, China as well as Australia - Oceania~~(Shakun and Carlson, 2010) with a temperature and precipitation maximum. This is particularly evident for Central Europe, the Arabian Sea, NW-Africa, the Mediterranean Sea and China.

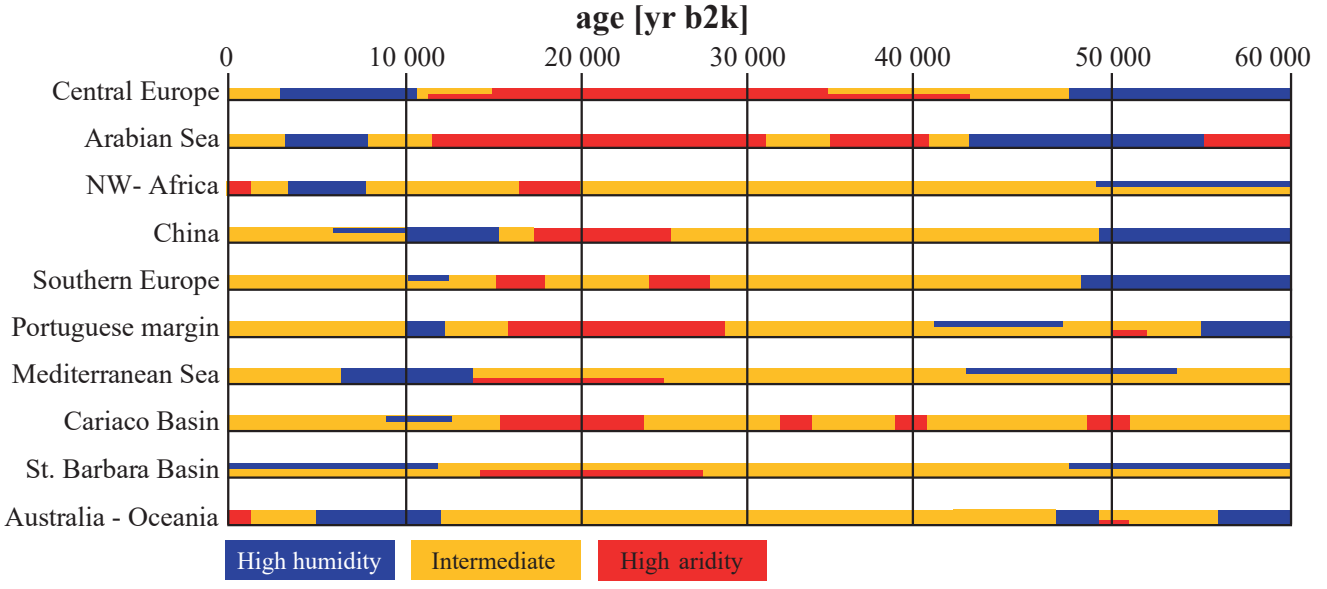

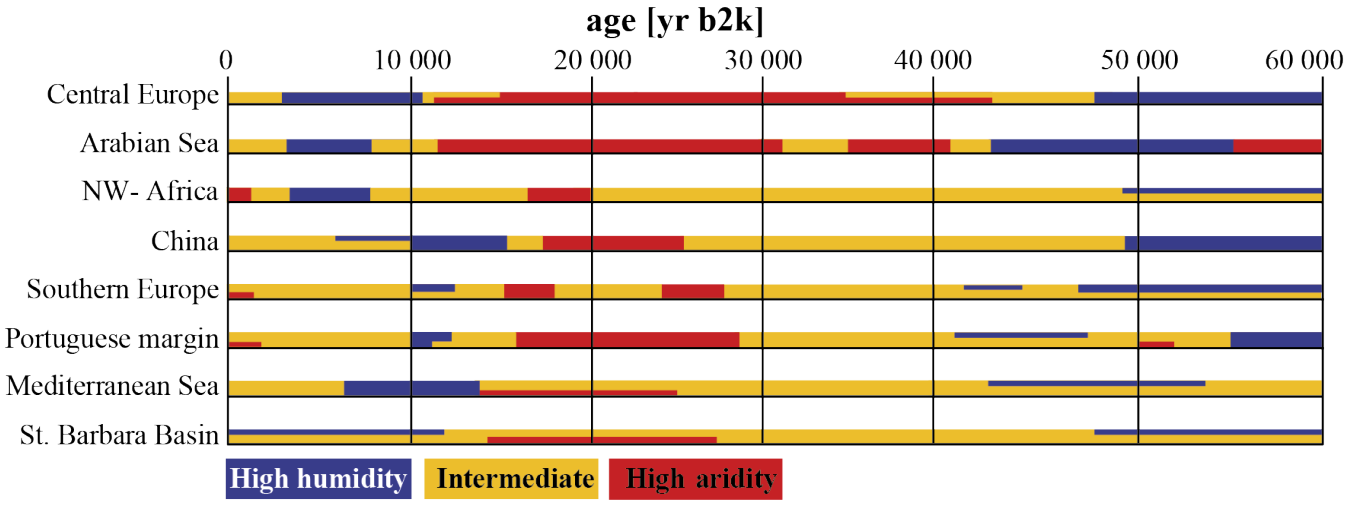

Figure 4: Aridity synthesis for the ~~10~~selected key regions for the last 60 000 years. Blue bars indicate high humidity, yellow bars intermediate humidity and red bars indicate high aridity. Overlapping half bars indicate transitions between both states. An early MIS3 wet phase and a ~~Holocene~~holocene wet phase ~~on various timings~~with different starting times for the regions ~~are recognisable~~can be identified.

3.3 Global speleothem growth pattern

Figure 5 summarizes all speleothem growth phases mentioned in the regional syntheses. A consistent pattern shows the growth of ~~most~~all speleothems except NW-Africa during the early MIS3 phase~~, apart from the Bahamas speleothem representative for the Cariaco Basin where speleothem growth started at about 45 000 years b2k. Except for New Zealand, all~~. All other regions indicate fast growth rates and corresponding humid conditions at least during interstadials. ~~New Zealand shows low growth rates indicating in general more arid conditions.~~ A ~~major~~larger change occurs around HE5 or, shortly ~~after~~afterwards, between 48 000 and 45 000 yr b2k ~~respectively~~. Speleothem growth stopped in Central Europe caves as well as in Arabian Sea region and drastically slowed down in Southern Europe, China and Mediterranean Sea region during late MIS3. The still fast growth for ~~Cariaco Basin~~ Portuguese margin region could be explained by a regional effect~~:~~ of enhanced moisture supply due to the position of the ~~speleothem on the Bahamas.~~Buraca Gloriosa Cave. These speleothems show Heinrich events H4, H3, H1 as hiatus. Climatic conditions impair with progressing time~~, growth stopped in Cariaco region as well around 23 000 yr b2k.~~. No growth is observed during LGM times for several regions including Central Europe, Arabian Sea~~,~~ and Southern Europe and ~~Cariaco Basin and~~ very slow growth rates are observed for ~~north west~~ NW- Africa, China and Mediterranean region pointing out to more arid conditions during late MIS3 and LGM times compared to early MIS3 conditions. ~~This also previously observed~~ The effect of large-scale atmospheric teleconnections, also observed previously, can also be ~~seen by~~observed with the ~~onset~~beginning of Bølling / Allerød (14 700~~-~~ yr~~-~~ b2k) or after YD (11 703 yr b2k~~), with the restart of speleothem~~). Speleothem growth starts again for Central Europe, the Arabian Sea, Southern Europe~~, Cariaco Basin and accelerating growth rates like for~~. In China, the Mediterranean ~~region~~ and the Santa Barbara Basin region~~.~~, the growth rate is again increasing significantly. The available data show climatic amelioration after the LGM period globally but especially on the northern hemisphere (NH)~~. Oceania and Southern hemisphere (SH) seem to act as a counterpart towards the NH. Fast~~

~~growth rates in Oceania correspond to no or slow growth rates on the northern hemisphere until the Holocene, when both hemispheres show enhanced moisture supply. This shows reverse behaviour between the climate of the hemispheres: If NH receives more precipitation, SHs precipitation decreases and vice versa.~~

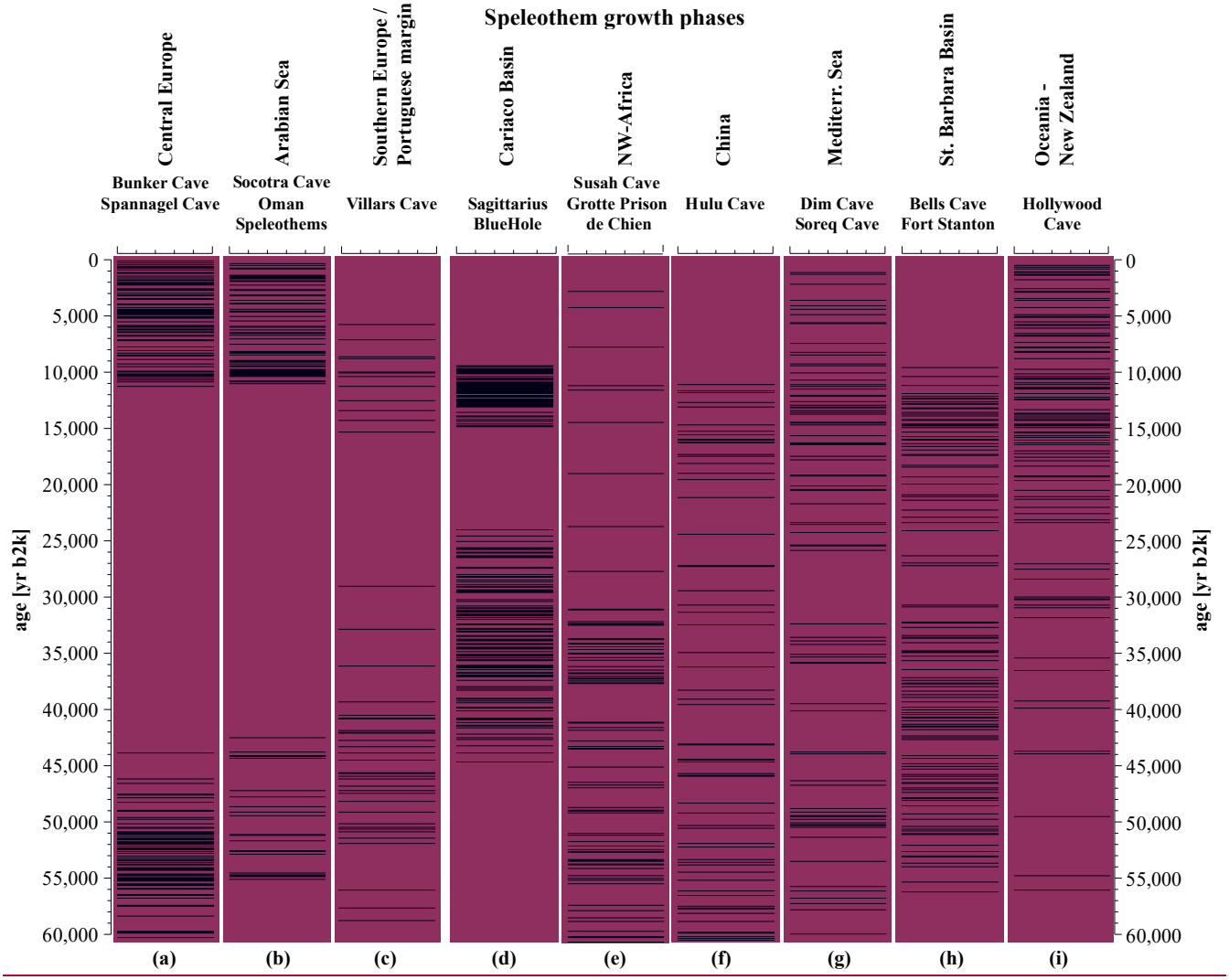
Speleothem growth phases
Central Europe
Arabian Sea
Southern Europe / Portuguese margin
Cariaco Basin
NW-Africa
China
Mediterr. Sea
St. Barbara Basin
Oceania - New Zealand
Bunker Cave
Spannagel Cave
Socotra Cave
Oman
Speleothems
Villars Cave
Sagittarius
BlueHole
Susah Cave
Grotte Prison
de Chien
Hulu Cave
Dim Cave
Soreq Cave
Bells Cave
Fort Stanton
Hollywood
Cave
age [yr b2k]
0
5,000
10,000
15,000
20,000
25,000
30,000
35,000
40,000
45,000
50,000
55,000
60,000
(a)
(b)
(c)
(d)
(e)
(f)
(g)
(h)
(i)

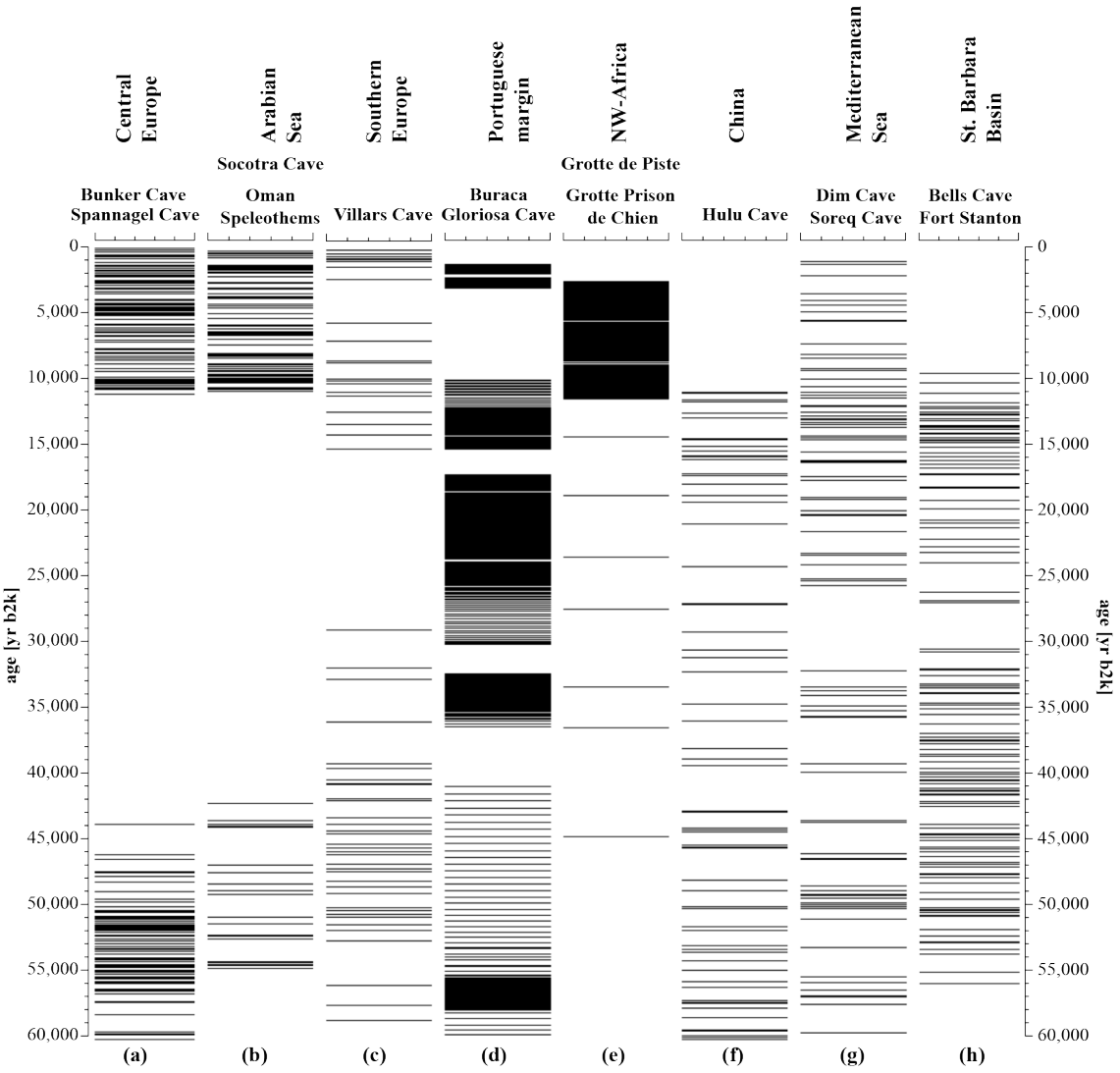

Figure 5: Speleothem growth phases, which require mobile water from frequent precipitation for the ~~10~~selected key regions. Horizontal bars show age datings. **(a)** Central Europe with Bunker Cave and Spannagel Cave (Fohlmeister et al., 2012, 2013; Holzkämper et al., 2005; Spötl and Mangini, 2002; Weber et al., 2018); **(b)** Socotra Cave and Oman Caves from Arabian Sea region (Burns et al., 2003; Fleitmann et al., 2007); **(c)** Southern Europe ~~and Portuguese margin regions represented by Villars Cave speleothems (Genty et al., 2003, 2006; Wainer et al., 2009); **(d)** Sagittarius Blue Hole Bahamas speleothem for Cariaco Basin region (Hoffmann et al., 2010); **(e)** North-West Africa with Grotte Prison de Chien and Susah Cave (Hoffmann et al., 2016; Wassenburg et al., 2012)~~represented by Villars Cave speleothems (Genty et al., 2003, 2006; Labuhn et al., 2015; Wainer et al., 2009, 2011); **(d)** Portuguese margin region with Buraca Gloriosa Cave (Denniston et al., 2018); **(e)** North-West Africa with Grotte Prison de Chien and Grotte de Piste (Wassenburg et al., 2012, 2016); **(f)** China with Hulu Cave (Liu et al., 2010; Wang et al., 2001); **(g)** Mediterranean Sea region with Dim Cave and Soreq Cave (Bar-Matthews et al., 2000; Ünal-İmer et al., 2015); **(h)** Bells Cave and Fort Stanton representing St. Barbara Basin ~~(Asmerom et al., 2010; Wagner et al., 2010); **(i)** Hollywood Cave from New Zealand for Oceania region (Hellstrom et al., 1998; Whittaker et al., 2011; Williams, 1996; Williams et al., 2005)~~(Asmerom et al., 2010; Wagner et al., 2010).

3.4 Global eolian dust pattern

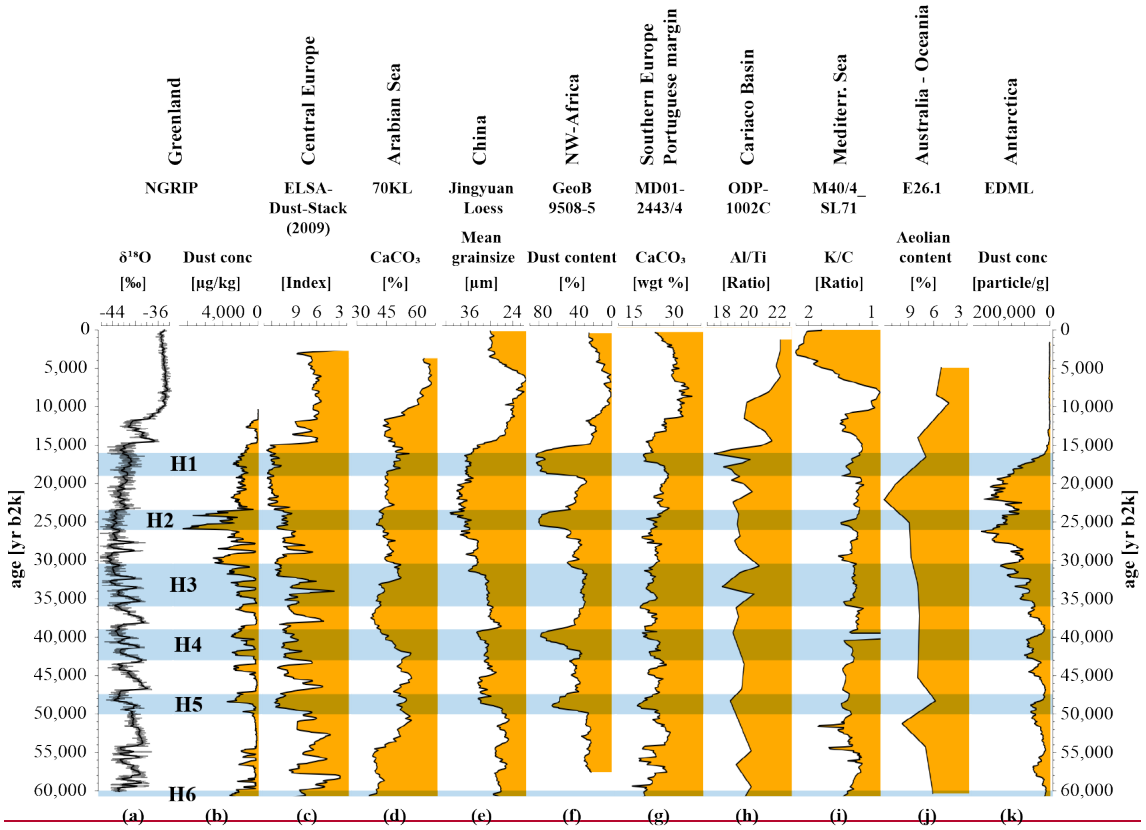

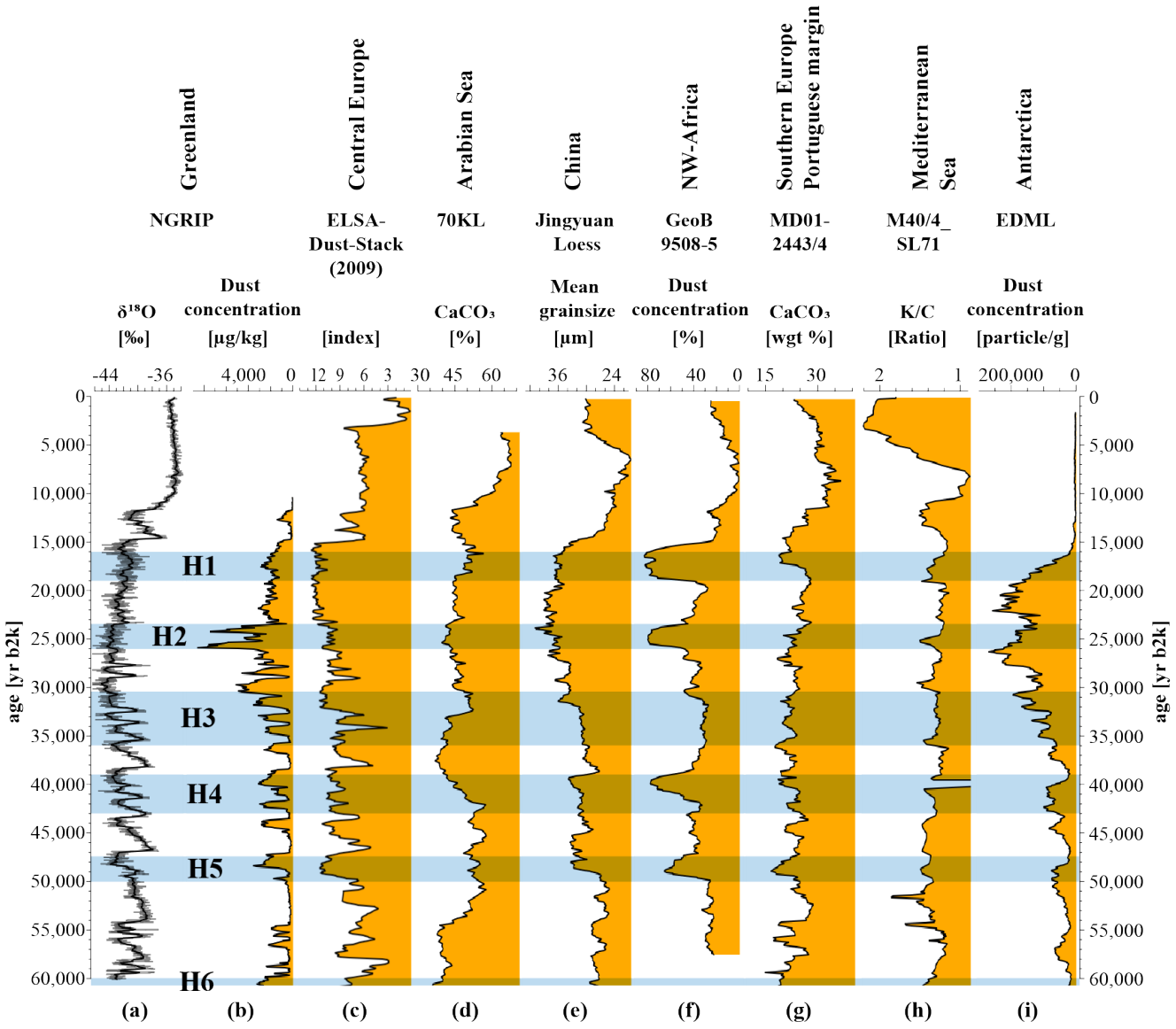

Figure 6: Global eolian dust archives over the last 60 000 years. More dust (left side of each column) indicates increased aridity, less dust indicates increased humidity. **(a)** NGRIP $\delta^{18}O$ (North Greenland Ice Core Project Members et al., 2004) in comparison and **(b)** Dust concentration (Ruth et al., 2007); **(c)** ELSA-Dust-Stack (2009) for Central European dust (Seelos et al., 2009); **(d)** $CaCO_3$ accounting for dust from Arabian Sea marine core 70KL (Leuschner and Sirocko, 2003); **(e)** Mean Grainsize from Jingyuan Chinese Loess plateau (Sun et al., 2010); **(f)** Dust content within marine core GeoB9508-5 off North-West Africa (Collins et al., 2013); **(g)** $CaCO_3$ for Southern Europe and Portuguese margin from marine core MD01-2443/4 (Hodell et al., 2013) **(h)** ~~Cariaco Basin Al/Ti ratio dust record from marine core ODP 165-1002C (Yarincik et al., 2000); (i)~~ K/C ratio from marine core M40/4_SL71 for Mediterranean Sea (Ehrmann et al., 2017); ~~(j) Aeolian content from marine core E26.1 from Tasmanian Sea for Oceania (Hesse, 1994); (k~~ **(i)** Antarctica ice core EDML Dust concentration (Wegner et al., 2015) in comparison. Light blue bars highlight Heinrich events after ~~(Naafs et al., 2013)~~(Naafs et al., 2013).

Similar patterns are visible in the dust archives used for this synthesis. For the early MIS3, low dust values ~~are discernible~~ for Central Europe, China, ~~north-west~~ NW-Africa and ~~intermediate~~medium dust values for all other regions ~~beside~~except the

Arabian Sea are visible. In general, ~~MIS3 climate shows flickering visible within~~ the dust records also show the flickering of the MIS3 climate.

Apart from ~~every region's~~the regions' own ~~pattern~~patterns, some background structures ~~are apparent~~can be seen. Heinrich events are most pronounced for NW-Africa~~, Cariaco Basin,~~ and Southern Europe ~~and~~/ Portuguese margin~~ regions~~, as these regions belong directly ~~belong~~ to the North Atlantic. Also the Mediterranean ~~Sea~~, Central Europe and China ~~also~~ show Heinrich events within the dust records. ~~Cariaco Basin,~~ China, the Arabian Sea, NW-Africa and Central Europe show a ~~distinct~~pronounced dust maximum during the LGM~~. Beside during~~ period. Apart from the Holocene, the lowest dust values ~~are apparent~~ in the early MIS3 show for Central Europe, Arabian Sea, China, NW-Africa and Mediterranean ~~Sea~~ - but ~~on various timings.~~at different times.

The NGRIP dust concentration and the ELSA~~-Dust-Stack~~ dust concentration (Seelos et al., 2009) are in good ~~accordance~~agreement for early and ~~mid~~intermediate MIS3. Tipping points show ~~stepped appearance~~stepwise changes in both archives at several ~~times~~points in time (~49 000, ~36 500, ~23 000, ~14 700 yr b2k~~) which are also visible~~), and are described ~~as Landscape Evolution Zones (LEZ)~~ in ~~Sirocko et al. (2016). The good consistency of both regions indicates a close connection to the North Atlantic climate variations. Arabian Sea sediments also are closely coupled to North Atlantic variability as known since Schultz et al.~~Sirocko et al. (2016) as Landscape Evolution Zones. The good agreement of both regions indicates a close connection with the North Atlantic climate variations. The sediments of the Arabian Sea are also closely linked to the North Atlantic variability, as known since Schultz et al. (1998) and visible ~~within~~in Fig. 6.

Sun et al. (2010) also ~~shows~~showed a correlation of Chinese loess ~~to~~with North Atlantic climate ~~variations~~fluctuations. High dust contents during ~~mid~~mean MIS3 and LGM are visible in most archives, often ~~related to~~in connection with dustier Heinrich events or stadials in general. Increasing dust ~~values~~levels around 30~~-~~ 000~~ yr~~ years b2k ~~towards the~~up to LGM show ~~nearly~~an almost global distribution, but regional differences ~~are observable~~can be observed: ELSA-Dust-Stack and NGRIP differ in the timing of the maximum dust values~~.~~ This could be explained by a process similar ~~process like~~to the blocking of ~~westerly~~western winds by ice ~~shield~~sheet growth ~~which is~~ described in~~ Schenk (Schenk et al., 2018) and Schiemann~~Schenk et al. (2018) and ~~(Schiemann et al., 2017)~~Schiemann et al. (2017).

~~From~~Between 30 000 ~~to~~and 17 000~~ yr~~ years b2k, ~~the~~ conditions were ~~mainly~~mostly arid, ~~discernible~~recognizable by the dust maxima in Greenland, Central Europe, China~~,~~ and the Portuguese margin~~, Australia - Oceania and Antarctica for~~ during the LGM. With the YD and the onset ~~towards~~of the Holocene, ~~global climate ameliorates and~~ dust values decrease ~~globally~~ until the end of the Altithermal~~. Afterwards~~ period. After that, dust increases in the Arabian Sea, China, NW~~-~~ Africa, the Portuguese margin and the Mediterranean Sea, indicating ~~increased~~increasing aridification of the large desert areas in Africa, the Arabian Peninsula and China. ~~Large~~During the last 60 000 years of climate evolution, major changes occurred simultaneously on the globe~~ during the last 60 000 years of climate history~~, indicating atmospheric teleconnections (Bjerknes, 1969; Markle et al., 2017; Sirocko, 2003; Sirocko et al., 1993, 1996; Zhou et al., 1999).

4 Discussion

The PalMod requirements limit the creation of the Aridity index partially. In particular, not all high-resolution archives could be taken into account in the selection of the regions, since too few further data from other archives in the proximity are publicly accessible. The requirements strongly influence the region selection, as regions with only one record type were excluded. Records that would also fall within the selected regions are e.g. Nussloch loess sequence as dust record for Central Europe / Southern Europe or the pollen record of Tenaghi Philippon for Mediterranean Sea region.

Since we use only one dust or pollen record per region to calculate the aridity index, these records would replace the existing ones. The ELSA-Dust-Stack (2009) and Nussloch are very similar with respect to the processes that formed these records. Therefore their climatic patterns are very similar. The aridity index would therefore not be completely different from the version now generated with freely available data. The situation would be similar for Tenaghi Philippon and Lago Grande di Monticchio. The archives show similar patterns and were subject to similar processes. These aridity indices would therefore also be very similar. To utilize more than one data set for pollen or dust from different archives would require a much more complex method to compare the different data.

The ELSA dust stack by Seelos et al. (2009) see Fig. 2e, shows all Greenland Interstadials of the last 60 000 years. The resolution of the ELSA-Dust-Stack (2009) is very high and the data are publicly available. For Nussloch, among other things, grain size index data have been collected, which show the GIs. These data from Nussloch (e.g. Antoine et al., 2009; Rousseau et al., 2007) can basically be compared with the ELSA-Dust-Stack (2009), as both archives show paleo dust. Although the data are not accessible, the figures of the original papers can be used for comparison. The disadvantage of a loess archives compared to terrestrial archives is an often discontinuous sedimentation. Nevertheless, it is clear that both archives are well suited to study paleoclimate developments. Both archives can be used for aridity reconstructions due to their paleo dust sedimentation.

The following chapter 4.1 compares our aridity index with a previous reconstruction from Herzschuh (2006). This reconstruction is based on various pollen records, but only with that one kind of proxy, which is pollen. Both methods reveal similar results, although Herzschuh has used a lot more records. Chapter 4.2 compares the aridity index with different climate simulations. Since the overall agreement is quite good as well, we consider our aridity reconstructions to be representative.

4.1 Comparison of aridity index and previous aridity reconstruction

Aridity reconstructions of ~~Herzschuh (Herzschuh, 2006)~~Herzschuh (2006) for the last 50 000 years for Central Asia are in excellent agreement to the aridity reconstructions of this synthesis of the China region (S3). Herzschuh ~~solely~~ used only pollen data for the reconstruction, while our aridity index is based on three ~~distinct~~different proxies to refine the ~~picture. The~~ image. On the other hand, Herzschuh used several pollen records of one region to calculate her aridity index ~~in addition~~on a broader basis. Our aridity index consists of longer records and reaches until the beginning of MIS3 (60 000 yr b2k). It shows a humid early MIS3 and a decrease in humidity around 50 000 yr b2k to intermediate conditions. Moderate dry conditions are

reconstructed for 50 000 to 45 000 yr b2k from Herzschuh, similar to the aridity index, followed by an increase in humidity until 40 000 yr b2k. Minor differences between 45 000 and 30 000 yr b2k are ~~apparent~~visible, but the general trend shows broad consensus between both reconstructions for this ~~time. Mid~~period. The middle to late MIS3 are relatively humid in both reconstructions. ~~Aridity~~ In both reconstructions the aridity increases ~~drastically~~rapidly towards the LGM~~ in both reconstructions~~, with a strong LGM aridity maximum ~~from~~of 21 000 to 18 000~~-~~ yr~~-~~ b2k. ~~Stepwise~~A gradual climate ~~amelioration~~improvement after ~~the~~ LGM is clearly ~~expressed~~evident in both reconstructions, with a first increase in humidity ~~occurs until~~up to 13 000~~-~~ yr~~-~~ b2k with ~~following~~subsequent optimal climate conditions during the early Holocene (11 000 ~~–~~ - 7 000~~-yr-~~ years b2k). The aridity index lacks ~~in~~pollen values in the Holocene data (see S3~~)~~), but the ~~accordance~~agreement of Herzschuh compared to the published Holocene pollen data of ~~Stebich (Stebich et al., 2015)~~Stebich et al. (2015) is ~~evident~~obvious and shows an early Holocene climate optimum ~~until~~up to 4 000~~-yr-~~ years b2k in both reconstructions. A wet early Holocene can also be observed in ~~Central~~central Chinese speleothem growth rates from ~~'Sanbao Cave'~~the 'Sanbao Cave', which are highest from 9 500 to 6 500~~-yr-~~ years b2k (Dong et al., 2010).

4.2 Comparison of proxy synthesis with model results

The above records describe the structure of past aridity globally, but do not ~~present causal mechanism, which Global Climate Models (GCM) can be used to simulate~~show the mechanisms of past, present and future climate changes~~. In order~~, which can be simulated by global climate models (GCM). Compared to our reconstructed ~~precipitation~~aridity indices, we ~~employ~~use the coupled climate model COSMOS. ~~Fig.~~Figure 7 ~~displays~~shows the precipitation changes and anomalies from ~~Late~~the late MIS3 time slice with respect to pre-industrial (PI) and LGM conditions. Panel A and C show stadial conditions and ~~panels~~panel B and D ~~show~~ interstadial conditions. Panels A and B show the time slice 32 000 ~~yr~~years b2k ~~time slice with respect~~compared to pre-industrial ~~times~~time, while panels C and D ~~are with respect to~~show LGM conditions.

Model runs for late MIS3 interstadial times show ~~enhanced~~increased precipitation for Europe, the North Atlantic, the Arabian Sea and large parts of the equatorial Pacific, while the remaining parts of the equator in Asia, the Central Atlantic and the northern parts of South America show ~~decreased~~lower precipitation. ~~Stadial~~The stadial MIS3 state ~~in general~~generally shows the same spatial trends, but with ~~general~~a generally higher aridity. Model and ~~aridity~~drought reconstructions ~~match in nearly equal~~are consistent under almost identical conditions for PI and MIS3. ~~Barron and Pollard (2002)~~Barron and Pollard (2002) simulated a ~~42 000 yr b2k~~ time slice of 42 000 years b2k for European precipitation. The results are comparable ~~to~~with our aridity index, but Central Europe, Southern Europe and the Portuguese margin were ~~more humid~~wetter in our reconstruction than in the ~~simulation of~~ Barron and Pollard simulation. In contrast, these results show that the 42 000~~-yr-~~ year b2k time slice was more humid than the 32 000~~-yr-~~ year b2k time slice for Europe. Our reconstruction ~~estimates~~assumes that precipitation ~~even higher~~ during early and ~~mid~~ middle MIS3 was even higher than during late MIS3 and ~~to be~~ as high as during the early Holocene optimum. This ~~could~~statement can be ~~said~~made for all regions ~~beside the Cariaco Basin, regarding~~if the different ~~timings~~starting times of the wet periods~~. In current models, late~~ are included. Late MIS3 and especially comparisons between ~~the~~ early and late MIS3 ~~were~~have not been investigated in current models so far.

Table 3 summarizes the results from the model simulations (transferred to symbols) from Fig. 7~~, converted into symbols.~~. This model ~~setup~~structure is divided ~~in~~into GI and GS state and is compared for each of the key regions with the results for the ~~aridity~~drought reconstructions from Fig.~~ 4 for each of the ten key regions.~~. Relatively ~~larger~~greater aridity ~~with respect to~~in terms of PI or LGM for each region is ~~shown with~~represented by a minus (-), approximately ~~the same~~equal conditions ~~with~~by a circle (o) and more humid conditions ~~with~~by a small plus (+). ~~The~~Additionally, the agreement of each simulation and the aridity reconstructions of this work are shown. A bad agreement is shown in ~~addition. Bad congruence is displayed in~~ red ~~colour,~~color, a medium one with yellow ~~and~~, a light ~~and intense~~ green for good and ~~even better accordance respectively.~~dark green for very good agreement. The overall ~~consistence~~consistency of model and reconstruction is good. Most ~~of the~~ precipitation changes of the ~~aridity~~drought index are ~~observable~~also captured in the simulation ~~as well~~.

The aridity reconstructions show that Central Europe was humid during the early MIS3, followed by ~~an intermediate~~a medium to ~~highly~~very arid period until the end of the LGM.

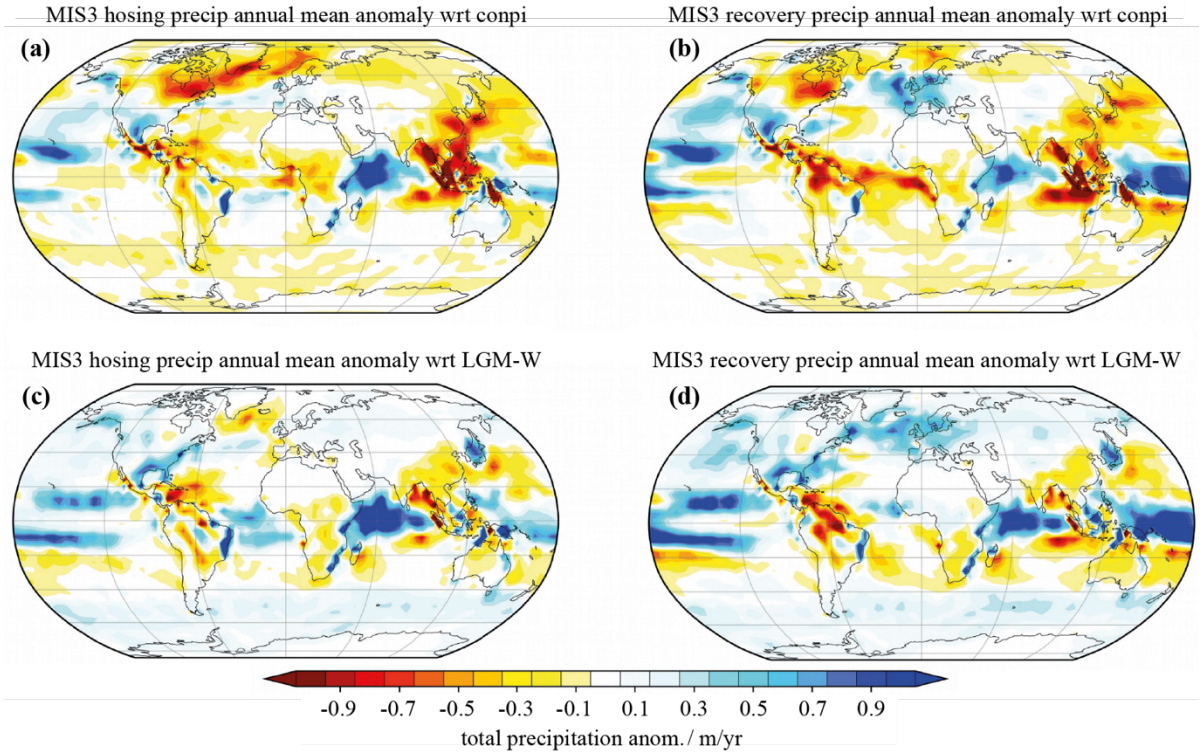

Figure 7: Simulated total precipitation anomalies for the late MIS3 climate relative to pre-industrial times (a, b) or LGM (c, d). Panel **(a, c)** show stadial conditions (hosing) and panels **(b, d)** show interstadial conditions (recovery). Simulation is compiled of various model simulations with COSMOS for pre-industrial (Wei and Lohmann, 2012), LGM (Zhang et al., 2013) and Late MIS3 (32 000 yr b2k) simulations (Gong et al., 2013).

	MIS 3 wrt. PI	MIS 3 wrt. LGM
	32 000 [a]	32 000 [a]

	GS	GI	GS	GI
Central Europe	o	+	o	+
Southern Europe	+	+	o	+
Portuguese margin	o	+	o	o
Mediterranean Sea	o	o	o	o
NW Africa	o	o	o	o
China	-	-	-	o
Arabian Sea	+	+	+	o
~~Cariaco basin~~	-	-	-	-
St. Barbara basin	o	o	o	o
~~Australia – Oceania~~	~~o~~	~~o~~	~~o~~	~~o~~

Table 3. Comparison of model simulation with reconstructed aridity index. Relatively larger aridity with respect to PI or LGM for each region is shown with a minus (-), approximately the same conditions with an open circle (o) and more humid conditions with a small plus (+). ~~Bad~~A bad agreement ~~of simulation and~~ between aridity index and simulation is shown ~~with~~in red ~~colour,~~color, a medium ~~by~~one with yellow ~~colour,~~, a light ~~and intense~~ green ~~account~~ for good ~~or even better accordance respectively~~and dark green for very good agreement.

5 Conclusions

The aridity synthesis for the ~~ten key~~selected regions of the ~~world's~~world climate allows ~~six~~five main conclusions ~~to be drawn~~:

(1) All regions analysed here ~~gone through~~underwent a wet phase during ~~early MIS3, as well as during~~both the early MIS3 and the early Holocene. The timing of ~~this humid MIS3 phase~~ these wet phases varied considerably from region to region.

(2) ~~Atmospheric~~There were atmospheric teleconnections ~~occurred~~ from the North Atlantic (Greenland) ~~over~~across Central Europe, the Arabian Sea ~~until~~to China. The changes in these regions ~~took place within~~occurred at similar ~~timings~~times and with similar ~~strength~~intensity. The other regions also ~~went through~~underwent these changes, but with temporal differences ~~in timing~~. We do indeed attribute this to ~~indeed~~ regional effects ~~rather than simply dating~~ and not exclusively to uncertainties in the stratigraphy.

(3) Eolian dust, tree pollen and speleothem growth phases show congruent climatic ~~pattern~~patterns for the ~~individual~~different regions and can be easily compared ~~easily regarding~~with regard to precipitation analyses.

(4) The aridity index and the precipitation simulations shown are generally consistent.

(5) The quality of the aridity index is mainly limited ~~mostly~~ by the original stratigraphy and sample resolution. ~~It~~Therefore, it is ~~accordingly~~ only a useful tool to observe large-scale changes in precipitation ~~changes.~~.

~~(6) The aridity suggests a general antiphase behaviour between LGM and early MIS3 for northern hemisphere and Australia – Oceania.~~

Author contributions

FF generated the aridity index, processed the data and prepared the manuscript. GL and XG developed and performed the climate simulation. BD developed the *ELSA*interactive++ program for data visualisation and analysis. ~~Fs~~FS stimulated the discussion on the global teleconnections within the climate system.

Acknowledgments

We would like to thank all four anonymous referees which have greatly improved the manuscript. This work was supported by German Federal Ministry of Education and Research (BMBF) as Research for Sustainability initiative (FONA); www.fona.de through PalMod project (FKZ: 01LP1510B). The authors thank Manfred Mudelsee for input on the error estimations, Hannes Knapp, Philip Süßer and Jennifer Klose for data mining, Michael Weber, Johannes Albert, Sarah Britzius for discussion contributions to the manuscript.

References

~~Andersen, K. K., Svensson, A., Johnsen, S. J., Rasmussen, S. O., Bigler, M., Röthlisberger, R., Ruth, U., Siggaard-Andersen, M. L., Peder Steffensen, J. and Dahl-Jensen, D.: The Greenland Ice Core Chronology 2005, 15–42ka. Part 1: constructing the time scale, Quaternary Science Reviews, 25(23–24), 3246–3257, doi:10.1016/j.quascirev.2006.08.002, 2006.~~

Antoine, P., Rousseau, D.-D., Zöller, L., Lang, A., Munaut, A.-V., Hatté, C. and Fontugne, M.: High-resolution record of the last Interglacial–glacial cycle in the Nussloch loess–palaeosol sequences, Upper Rhine Area, Germany, Quaternary International, 76–77, 211–229, doi:10.1016/S1040-6182(00)00104-X, 2001.

Antoine, P., Rousseau, D.-D., Moine, O., Kunesch, S., Hatté, C., Lang, A., Tissoux, H. and Zöller, L.: Rapid and cyclic aeolian deposition during the Last Glacial in European loess: a high-resolution record from Nussloch, Germany, Quaternary Science Reviews, 28(25), 2955–2973, doi:10.1016/j.quascirev.2009.08.001, 2009.

Asmerom, Y., Polyak, V. J. and Burns, S. J.: Variable winter moisture in the southwestern United States linked to rapid glacial climate shifts, Nature Geoscience, 3(2), 114–117, doi:10.1038/ngeo754, 2010.

Bar-Matthews, M., Ayalon, A. and Kaufman, A.: Timing and hydrological conditions of Sapropel events in the Eastern Mediterranean, as evident from speleothems, Soreq cave, Israel, Chemical Geology, 169(1–2), 145–156, 2000.

Barron, E. and Pollard, D.: High-Resolution Climate Simulations of Oxygen Isotope Stage 3 in Europe 1, Quaternary Research, 58(3), 296–309, doi:10.1006/qres.2002.2374, 2002.

Bjerknes, J.: Atmospheric teleconnections from the equatorial pacific, Mon. Wea. Rev., 97(3), 163–172, doi:10.1175/1520-0493(1969)097<0163:ATFTEP>2.3.CO;2, 1969.

Bronk Ramsey, C., Staff, R. A., Bryant, C. L., Brock, F., Kitagawa, H., van der Plicht, J., Schlolaut, G., Marshall, M. H., Brauer, A., Lamb, H. F., Payne, R. L., Tarasov, P. E., Haraguchi, T., Gotanda, K., Yonenobu, H., Yokoyama, Y., Tada, R. and

Nakagawa, T.: A Complete Terrestrial Radiocarbon Record for 11.2 to 52.8 kyr B.P., Science, 338(6105), 370–374, doi:10.1126/science.1226660, 2012.

Brovkin, V., Raddatz, T., Reick, C. H., Claussen, M. and Gayler, V.: Global biogeophysical interactions between forest and climate, Geophysical Research Letters, 36(7), doi:10.1029/2009GL037543, 2009.

Burns, S. J., Fleitmann, D., Matter, A., Kramers, J. and Al-Subbary A. A: Indian Ocean Climate and a Absolute Chronology over Dansgaard/Oescher Events 9 to 13, Science, 301, 1365–1367, 2003.

Cassou, C., Terray, L. and Phillips, A. S.: Tropical Atlantic Influence on European Heat Waves, J. Climate, 18(15), 2805–2811, doi:10.1175/JCLI3506.1, 2005.

Clark, P. U., Dyke, A. S., Shakun, J. D., Carlson, A. E., Clark, J., Wohlfarth, B., Mitrovica, J. X., Hostetler, S. W. and McCabe, A. M.: The Last Glacial Maximum, Science, 325(5941), 710–714, doi:10.1126/science.1172873, 2009.

Collins, J. A., Govin, A., Mulitza, S., Heslop, D., Zabel, M., Hartmann, J., Röhl, U. and Wefer, G.: Abrupt shifts of the Sahara-Sahel boundary during Heinrich stadials, Climate of the Past, 9(3), 1181–1191, doi:10.5194/cp-9-1181-2013, 2013.

Correa-Metrio, A., Bush, M. B., Hodell, D. A., Brenner, M., Escobar, J. and Guilderson, T.: The influence of abrupt climate change on the ice-age vegetation of the Central American lowlands: Abrupt climate change in ice-age Central America, Journal of Biogeography, 39(3), 497–509, doi:10.1111/j.1365-2699.2011.02618.x, 2012.

deMenocal, P., Ortiz, J., Guilderson, T., Adkins, J., Sarnthein, M., Baker, L. and Yarusinsky, M.: Abrupt onset and termination of the African Humid Period: rapid climate responses to gradual insolation forcing, Quaternary science reviews, 19(1), 347–361, 2000.

Denniston, R. F., Houts, A. N., Asmerom, Y., Wanamaker Jr., A. D., Haws, J. A., Polyak, V. J., Thatcher, D. L., Altan-Ochir, S., Borowske, A. C., Breitenbach, S. F. M., Ummenhofer, C. C., Regala, F. T., Benedetti, M. M. and Bicho, N. F.: A stalagmite test of North Atlantic SST and Iberian hydroclimate linkages over the last two glacial cycles, Climate of the Past, 14(12), 1893–1913, doi:https://doi.org/10.5194/cp-14-1893-2018, 2018.

Deutscher Wetterdienst: Wetter und Klima - Deutscher Wetterdienst - Klimadaten weltweit, [online] Available from: https://www.dwd.de/DE/leistungen/klimadatenwelt/klimadatenwelt_node.html (Accessed 17 July 2018), 2018.

Dietrich, S. and Seelos, K.: The reconstruction of easterly wind directions for the Eifel region (Central Europe) during the period 40.3––12.9 ka BP, Climate of the Past, 6(2), 145–154, doi:10.5194/cp-6-145-2010, 2010.

Dietrich, S. and Sirocko, F.: The potential of dust detection by means of μXRF scanning in Eifel maar lake sediments, Quaternary Science Journal, 60(1), 90–104, doi:10.3285/eg.60.1.06, 2011.

Dong, J., Wang, Y., Cheng, H., Hardt, B., Edwards, R. L., Kong, X., Wu, J., Chen, S., Liu, D., Jiang, X. and Zhao, K.: A high-resolution stalagmite record of the Holocene East Asian monsoon from Mt Shennongjia, central China, The Holocene, 20(2), 257–264, doi:10.1177/0959683609350393, 2010.

Ehrmann, W., Schmiedl, G., Beuscher, S. and Krüger, S.: Intensity of African Humid Periods Estimated from Saharan Dust Fluxes, edited by S.-P. Xie, PLOS ONE, 12(1), e0170989, doi:10.1371/journal.pone.0170989, 2017.

~~EPICA community members: Eight glacial cycles from an Antarctic ice core, Nature, 429(6992), 623–628,~~

doi:10.1038/nature02599, 2004.

Fleitmann, D., Burns, S. J., Mangini, A., Mudelsee, M., Kramers, J., Villa, I., Neff, U., Al-Subbary, A. A., Buettner, A., Hippler, D. and Matter, A.: Holocene ITCZ and Indian monsoon dynamics recorded in stalagmites from Oman and Yemen (Socotra), Quaternary Science Reviews, 26(1–2), 170–188, doi:10.1016/j.quascirev.2006.04.012, 2007.

Fohlmeister, J., Schröder-Ritzrau, A., Scholz, D., Spötl, C., Riechelmann, D. F. C., Mudelsee, M., Wackerbarth, A., Gerdes, A., Riechelmann, S., Immenhauser, A., Richter, D. K. and Mangini, A.: Bunker Cave stalagmites: an archive for central European Holocene climate variability, Climate of the Past, 8(5), 1751–1764, doi:10.5194/cp-8-1751-2012, 2012.

Fohlmeister, J., Vollweiler, N., Spötl, C. and Mangini, A.: COMNISPA II: Update of a mid-European isotope climate record, 11 ka to present, The Holocene, 23(5), 749–754, doi:10.1177/0959683612465446, 2013.

Genty, D., Blamart, D., Ouahdi, R., Gilmour, M., Baker, A., Jouzel, J. and Van-Exter, S.: Precise dating of Dansgaard–Oeschger climate oscillations in western Europe from stalagmite data, Nature, 421(6925), 833–837, doi:10.1038/nature01391, 2003.

Genty, D., Blamart, D., Ghaleb, B., Plagnes, V., Causse, Ch., Bakalowicz, M., Zouari, K., Chkir, N., Hellstrom, J. and Wainer, K.: Timing and dynamics of the last deglaciation from European and North African δ13C stalagmite profiles—comparison with Chinese and South Hemisphere stalagmites, Quaternary Science Reviews, 25(17–18), 2118–2142, doi:10.1016/j.quascirev.2006.01.030, 2006.

Gierz, P., Lohmann, G. and Wei, W.: Response of Atlantic overturning to future warming in a coupled atmosphere-ocean-ice sheet model, Geophysical Research Letters, 42(16), 6811–6818, doi:10.1002/2015GL065276, 2015.

Gong, X., Knorr, G., Lohmann, G. and Zhang, X.: Dependence of abrupt Atlantic meridional ocean circulation changes on climate background states, Geophysical Research Letters, 40(14), 3698–3704, doi:10.1002/grl.50701, 2013.

Gong, X., Zhang, X., Lohmann, G., Wei, W., Zhang, X. and Pfeiffer, M.: Higher Laurentide and Greenland ice sheets strengthen the North Atlantic ocean circulation, Clim Dyn, 45(1), 139–150, doi:10.1007/s00382-015-2502-8, 2015.

Grimm, E. C., Watts, W. A., Jacobson Jr., G. L., Hansen, B. C. S., Almquist, H. R. and Dieffenbacher-Krall, A. C.: Evidence for warm wet Heinrich events in Florida, Quaternary Science Reviews, 25(17–18), 2197–2211, doi:10.1016/j.quascirev.2006.04.008, 2006.

Grootes, P. M., Stuiver, M., White, J. W. C., Johnsen, S. and Jouzel, J.: Comparison of oxygen isotope records from the GISP2 and GRIP Greenland ice cores., Nature, 366, 552–554, 1993.

Hagemann, S. and Dümenil, L.: A parametrization of the lateral waterflow for the global scale, Climate Dynamics, 14(1), 17–31, doi:10.1007/s003820050205, 1997.

Hellstrom, J., McCulloch, M. and Stone, J.: A Detailed 31,000-Year Record of Climate and Vegetation Change, from the Isotope Geochemistry of Two New Zealand Speleothems, Quaternary Research, 50(2), 167–178, doi:10.1006/qres.1998.1991, 1998.

Herzschuh, U.: Palaeo-moisture evolution in monsoonal Central Asia during the last 50,000 years, Quaternary Science Reviews, 25(1), 163–178, doi:10.1016/j.quascirev.2005.02.006, 2006.

Hesse, P. P.: The record of continental dust from Australia in Tasman Sea Sediments, Quaternary Science Reviews, 13(3), 257–272, doi:10.1016/0277-3791(94)90029-9, 1994.

Heusser, L.: Direct correlation of millennial-scale changes in western North American vegetation and climate with changes in the California Current System over the past ~60 kyr, Paleoceanography, 13(3), 252–262, doi:10.1029/98PA00670, 1998.

Hibler, W. D.: A Dynamic Thermodynamic Sea Ice Model, J. Phys. Oceanogr., 9(4), 815–846, doi:10.1175/1520-0485(1979)009<0815:ADTSIM>2.0.CO;2, 1979.

Hodell, D., Crowhurst, S., Skinner, L., Tzedakis, P. C., Margari, V., Channell, J. E. T., Kamenov, G., Maclachlan, S. and Rothwell, G.: Response of Iberian Margin sediments to orbital and suborbital forcing over the past 420 ka, Paleoceanography, 28(1), 185–199, doi:10.1002/palo.20017, 2013.

Hoffmann, D. L., Beck, J. W., Richards, D. A., Smart, P. L., Singarayer, J. S., Ketchmark, T. and Hawkesworth, C. J.: Towards radiocarbon calibration beyond 28ka using speleothems from the Bahamas, Earth and Planetary Science Letters, 289(1–2), 1–10, doi:10.1016/j.epsl.2009.10.004, 2010.

Hoffmann, D. L., Rogerson, M., Spötl, C., Luetscher, M., Vance, D., Osborne, A. H., Fello, N. M. and Moseley, G. E.: Timing and causes of North African wet phases during the last glacial period and implications for modern human migration, Scientific Reports, 6, 36367, doi:10.1038/srep36367, 2016.

Holzkämper, S., Mangini, A., Spötl, C. and Mudelsee, M.: Timing and progression of the Last Interglacial derived from a high alpine stalagmite: TIMING OF THE LAST INTERGLACIAL, Geophysical Research Letters, 31(7), n/a-n/a, doi:10.1029/2003GL019112, 2004.

Holzkämper, S., Spotl, C. and Mangini, A.: High-precision constraints on timing of Alpine warm periods during the middle to late Pleistocene using speleothem growth periods, Earth and Planetary Science Letters, 236(3–4), 751–764, doi:10.1016/j.epsl.2005.06.002, 2005.

Imbrie, J., Hays, J. D., Martinson, D. G., McIntyre, A., Mix, A. C., Morley, J. J., Pisias, N. G., Prell, W. L. and Shackleton, N. J.: The orbital theory of pleistocene climate: support from a revised chronology of the marine δ18O record, in Milankovitch and Climate, Part 1, edited by A. L. Berger et al, pp. 269–305., 1984.

Jiménez-Moreno, G., Anderson, S. R. and Fawcett, P.: Orbital- and millennial-scale vegetation and climate changes of the past 225ka from Bear Lake, Utah–Idaho (USA), Quaternary Science Reviews, 26(13–14), 1713–1724, doi:10.1016/j.quascirev.2007.05.001, 2007.

Jungclaus, J. H., Keenlyside, N., Botzet, M., Haak, H., Luo, J.-J., Latif, M., Marotzke, J., Mikolajewicz, U. and Roeckner, E.: Ocean Circulation and Tropical Variability in the Coupled Model ECHAM5/MPI-OM, J. Climate, 19(16), 3952–3972, doi:10.1175/JCLI3827.1, 2006.

Kindler, P., Guillevic, M., Baumgartner, M., Schwander, J., Landais, A., Leuenberger, M., Spahni, R., Capron, E. and Chappellaz, J.: Temperature reconstruction from 10 to 120 kyr b2k from the NGRIP ice core, Climate of the Past, 10(2), 887–902, doi:10.5194/cp-10-887-2014, 2014.

Kliem, P., Enters, D., Hahn, A., Ohlendorf, C., Lisé-Pronovost, A., St-Onge, G., Wastegård, S. and Zolitschka, B.: Lithology,

radiocarbon chronology and sedimentological interpretation of the lacustrine record from Laguna Potrok Aike, southern Patagonia, Quaternary Science Reviews, 71, 54–69, doi:10.1016/j.quascirev.2012.07.019, 2013.

Knorr, G. and Lohmann, G.: Climate warming during Antarctic ice sheet expansion at the Middle Miocene transition, Nature Geoscience, 7(5), 376–381, doi:10.1038/ngeo2119, 2014.

Koehler, E., Brown, E. and Haneuse, S. J.-P. A.: On the Assessment of Monte Carlo Error in Simulation-Based Statistical Analyses, Am Stat, 63(2), 155–162, doi:10.1198/tast.2009.0030, 2009.

Labuhn, I., Genty, D., Vonhof, H., Bourdin, C., Blamart, D., Douville, E., Ruan, J., Cheng, H., Edwards, R. L., Pons-Branchu, E. and Pierre, M.: A high-resolution fluid inclusion δ18O record from a stalagmite in SW France: modern calibration and comparison with multiple proxies, Quaternary Science Reviews, 110, 152–165, doi:10.1016/j.quascirev.2014.12.021, 2015.

Leuschner, D. C. and Sirocko, F.: Orbital insolation forcing of the Indian Monsoon - a motor for global climate changes?, Palaeogeography Palaeoclimatology Palaeoecology, 197(1–2), 83–95, 2003.

Litt, T. and Stebich, M.: Bio- and chronostratigraphy of the lateglacial in the Eifel region, Germany, Quaternary International, 61(1), 5–16, doi:10.1016/S1040-6182(99)00013-0, 1999.

Liu, D., Wang, Y., Cheng, H., Lawrence Edwards, R., Kong, X., Wang, X., Hardt, B., Wu, J., Chen, S., Jiang, X., He, Y., Dong, J. and Zhao, K.: Sub-millennial variability of Asian monsoon intensity during the early MIS 3 and its analogue to the ice age terminations, Quaternary Science Reviews, 29(9), 1107–1115, doi:10.1016/j.quascirev.2010.01.008, 2010.

Lohmann, G., Haak, H. and Jungclaus, J. H.: Estimating trends of Atlantic meridional overturning circulation from long-term hydrographic data and model simulations, Ocean Dynamics, 58(2), 127–138, doi:10.1007/s10236-008-0136-7, 2008.

Lohmann, G., Pfeiffer, M., Laepple, T., Leduc, G. and Kim, J.-H.: A model-data comparison of the Holocene global sea surface temperature evolution, Climate of the Past, 1807–1839, doi:Lohmann, G. ORCID: https://orcid.org/0000-0003-2089-733X <https://orcid.org/0000-0003-2089-733X>, Pfeiffer, M. , Laepple, T. ORCID: https://orcid.org/0000-0001-8108-7520 <https://orcid.org/0000-0001-8108-7520>, Leduc, G. and Kim, J. H. (2013) A model-data comparison of the Holocene global sea surface temperature evolution , Climate of the Past, (9), pp. 1807-1839 . doi:https://doi.org/10.5194/cp-9-1807-2013 <https://doi.org/10.5194/cp-9-1807-2013> , hdl:10013/epic.41917, 2013.

Markle, B. R., Steig, E. J., Buizert, C., Schoenemann, S. W., Bitz, C. M., Fudge, T. J., Pedro, J. B., Ding, Q., Jones, T. R., White, J. W. C. and Sowers, T.: Global atmospheric teleconnections during Dansgaard–Oeschger events, Nature Geoscience, 10(1), 36–40, doi:10.1038/ngeo2848, 2017.

Marsland, S. J., Haak, H., Jungclaus, J. H., Latif, M. and Röske, F.: The Max-Planck-Institute global ocean/sea ice model with orthogonal curvilinear coordinates, Ocean Modelling, 5(2), 91–127, doi:10.1016/S1463-5003(02)00015-X, 2003.

~~Martinson, D. G., Pisias, N. G., Hays, J. D., Imbrie, J., Moore jr., T. C. and Shackelton, N. J.: Age Dating and the Orbital Theory of the Ice Ages: Development of a High-Resolution 0 to 300,000-Year Chronostratigraphy, Quaternary Researche, 27, 1–29, 1987.~~

McManus, J. F., Bond, G. C., Broecker, W. S., Johnsen, S., Labeyrie, L. and Higgins, S.: High-resolution climate records from the North Atlantic during the last interglacial, Nature, 371(6495), 326, doi:10.1038/371326a0, 1994.

Mingram, J., Stebich, M., Schettler, G., Hu, Y., Rioual, P., Nowaczyk, N., Dulski, P., You, H., Opitz, S., Liu, Q. and Liu, J.: Millennial-scale East Asian monsoon variability of the last glacial deduced from annually laminated sediments from Lake Sihailongwan, N.E. China, Quaternary Science Reviews, 201, 57–76, doi:10.1016/j.quascirev.2018.09.023, 2018.

Mix, A. C., Bard, E. and Schneider, R.: Environmental processes of the ice age: land, oceans, glaciers (EPILOG), Quaternary Science Reviews, 20(4), 627–657, doi:10.1016/S0277-3791(00)00145-1, 2001.

Moine, O., Antoine, P., Hatté, C., Landais, A., Mathieu, J., Prud'homme, C. and Rousseau, D.-D.: The impact of Last Glacial climate variability in west-European loess revealed by radiocarbon dating of fossil earthworm granules, Proceedings of the National Academy of Sciences, 114(24), 6209–6214, doi:10.1073/pnas.1614751114, 2017.

Naafs, B. D. A., Hefter, J., Grützner, J. and Stein, R.: Warming of surface waters in the mid-latitude North Atlantic during Heinrich events: ~~HIGH SSTs DURING HEINRICH EVENTS~~High SST during Heinrich Events, Paleoceanography, 28(1), 153–163, doi:10.1029/2012PA002354, 2013.

Negendank, J. F. W.: Pleistozäne und holozäne Maarsedimente der Eifel, Zeitschrift der Deutschen Geologischen Gesellschaft, 13–24, 1989.

Negendank, J. F. W. and Zolitschka, B.: Maars and maar lakes of the Westeifel Volcanic Field, in Paleolimnology of European Maar Lakes, edited by J. F. W. Negendank and B. Zolitschka, pp. 61–80, Springer Berlin Heidelberg, Berlin, Heidelberg., 1993.

Niezgodzki, I., Knorr, G., Lohmann, G., Tyszka, J. and Markwick, P. J.: Late Cretaceous climate simulations with different CO2 levels and subarctic gateway configurations: A model-data comparison, Paleoceanography, 32(9), 980–998, doi:10.1002/2016PA003055, 2017.

North Greenland Ice Core Project Members, Andersen, K. K., Azuma, N., Barnola, J.-M., Bigler, M., Biscaye, P., Caillon, N., Chappellaz, J., Clausen, H. B., Dahl-Jensen, D., Fischer, H., Flückiger, J., Fritzsche, D., Fujii, Y., Goto-Azuma, K., Grønvold, K., Gundestrup, N. S., Hansson, M., Huber, C., Hvidberg, C. S., Johnsen, S. J., Jonsell, U., Jouzel, J., Kipfstuhl, S., Landais, A., Leuenberger, M., Lorrain, R., Masson-Delmotte, V., Miller, H., Motoyama, H., Narita, H., Popp, T., Rasmussen, S. O., Raynaud, D., Rothlisberger, R., Ruth, U., Samyn, D., Schwander, J., Shoji, H., Siggard-Andersen, M.-L., Steffensen, J. P., Stocker, T., Sveinbjörnsdóttir, A. E., Svensson, A., Takata, M., Tison, J.-L., Thorsteinsson, T., Watanabe, O., Wilhelms, F. and White, J. W. C.: High-resolution record of Northern Hemisphere climate extending into the last interglacial period, Nature, 431(7005), 147–151, doi:10.1038/nature02805, 2004.

Pfeiffer, M. and Lohmann, G.: Greenland Ice Sheet influence on Last Interglacial climate: global sensitivity studies performed with an atmosphere–ocean general circulation model, Climate of the Past, 1313–1338, 2016.

Pross, J., Koutsodendris, A., Christanis, K., Fischer, T., Fletcher, W. J., Hardiman, M., Kalaitzidis, S., Knipping, M., Kotthoff, U., Milner, A. M., Müller, U. C., Schmiedl, G., Siavalas, G., Tzedakis, P. C. and Wulf, S.: The 1.35-Ma-long terrestrial climate archive of Tenaghi Philippon, northeastern Greece: Evolution, exploration, and perspectives for future research, , doi:info:doi/10.1127/nos/2015/0063, 2015.

Pye, K.: Aeolian dust and dust deposits., Academic Press, University of Cambridge., 1987.

Rasmussen, S. O., ~~Andersen, K. K., Svensson, A. M., Steffensen, J. P., Vinther, B. M., Clausen, H. B., Siggaard-Andersen, M.-L., Johnsen, S. J., Larsen, L. B., Dahl-Jensen, D., Bigler, M., Röthlisberger, R., Fischer, H., Goto-Azuma, K., Hansson, M. E. and Ruth, U.: A new Greenland ice core chronology for the last glacial termination, Journal of Geophysical Research, 111(D6), doi:10.1029/2005JD006079, 2006.~~

~~Rasmussen, S. O.,~~ Bigler, M., Blockley, S. P., Blunier, T., Buchardt, S. L., Clausen, H. B., Cvijanovic, I., Dahl-Jensen, D., Johnsen, S. J., Fischer, H., Gkinis, V., Guillevic, M., Hoek, W. Z., Lowe, J. J., Pedro, J. B., Popp, T., Seierstad, I. K., Steffensen, J. P., Svensson, A. M., Vallelonga, P., Vinther, B. M., Walker, M. J. C., Wheatley, J. J. and Winstrup, M.: A stratigraphic framework for abrupt climatic changes during the Last Glacial period based on three synchronized Greenland ice-core records: refining and extending the INTIMATE event stratigraphy, Quaternary Science Reviews, 106, 14–28, doi:10.1016/j.quascirev.2014.09.007, 2014.

Roeckner, E., Bäuml, G., Bonaventura, L., Brokopf, R., Esch, M., Giorgetta, M., Hagemann, S., Kirchner, I., Kornblueh, L., Manzini, E., Rhodin, A., Schlese, U., Schulzweida, U. and Tompkins, A.: The atmospheric general circulation model ECHAM 5. PART I: Model description, , doi:10.17617/2.995269, 2003.

Rousseau, D.-D., Sima, A., Antoine, P., Hatté, C., Lang, A. and Zöller, L.: Link between European and North Atlantic abrupt climate changes over the last glaciation, Geophysical Research Letters, 34(22), doi:10.1029/2007GL031716, 2007.

Ruth, U., Wagenbach, D., Steffensen, J. P. and Bigler, M.: Continuous record of microparticle concentration and size distribution in the central Greenland NGRIP ice core during the last glacial period: CONTINUOUS RECORD OF MICROPARTICLE CONCENTRATION, Journal of Geophysical Research: Atmospheres, 108(D3), n/a-n/a, doi:10.1029/2002JD002376, 2003.

Ruth, U., Bigler, M., Röthlisberger, R., Siggaard-Andersen, M.-L., Kipfstuhl, S., Goto-Azuma, K., Hansson, M. E., Johnsen, S. J., Lu, H. and Steffensen, J. P.: Ice core evidence for a very tight link between North Atlantic and east Asian glacial climate, Geophysical Research Letters, 34(3), doi:10.1029/2006GL027876, 2007.

Schaber, K. and Sirocko, F.: Lithologie und Stratigraphie der spätpleistozänen Trockenmaare der Eifel, Mainzer geowissenschaftliche Mitteilungen, 33, 295–340, 2005.

Schenk, F., Väliranta, M., Muschitiello, F., Tarasov, L., Heikkilä, M., Björck, S., Brandefelt, J., Johansson, A. V., Näslund, J.-O. and Wohlfarth, B.: Warm summers during the Younger Dryas cold reversal, Nature Communications, 9(1), doi:10.1038/s41467-018-04071-5, 2018.

Schiemann, R., Demory, M.-E., Shaffrey, L. C., Strachan, J., Vidale, P. L., Mizielinski, M. S., Roberts, M. J., Matsueda, M., Wehner, M. F. and Jung, T.: The resolution sensitivity of Northern Hemisphere blocking in four 25-km atmospheric global circulation models, Journal of Climate, 30, 337–358, 2017.

Schulz, H., von Rad, U., Erlenkeuser, H. and von Rad, U.: Correlation between Arabian Sea and Greenland climate oscillations of the past 110,000 years, Nature, 393(6680), 54–57, doi:10.1038/31750, 1998.

Seelos, K., Sirocko, F. and Dietrich, S.: A continuous high-resolution dust record for the reconstruction of wind systems in central Europe (Eifel, Western Germany) over the past 133 ka, Geophysical Research Letters, 36(20),

doi:10.1029/2009GL039716, 2009.

Shakun, J. D. and Carlson, A. E.: A global perspective on Last Glacial Maximum to Holocene climate change, Quaternary Science Reviews, 29(15), 1801–1816, doi:10.1016/j.quascirev.2010.03.016, 2010.

Sirocko, F.: What Drove Past Teleconnections?, Science, 301(5638), 1336–1337, doi:10.1126/science.1088626, 2003.

Sirocko, F.: The ELSA - Stacks (Eifel-Laminated-Sediment-Archive): An introduction, Global and Planetary Change, 142, 96–99, doi:10.1016/j.gloplacha.2016.03.011, 2016.

Sirocko, F. and Ittekkot, V.: Organic carbon accumulation rates in the Holocene and Glacial Arabian Sea: Implications for the global CO2 budget., Climate Dynamics, 7, 167–172, 1992.

Sirocko, F., Sarnthein, M., Erlenkeuser, H., Lange, H., Arnold, M. and Duplessy, J. C.: Century-scale events in monsoonal climate over the past 24,000 years, Nature, 364(6435), 322, doi:10.1038/364322a0, 1993.

Sirocko, F., Garbe-Schönberg, D., McIntyre, A. and Molfino, B.: Teleconnections Between the Subtropical Monsoons and High-Latitude Climates During the Last Deglaciation, Science, 272(5261), 526–529, doi:10.1126/science.272.5261.526, 1996.

Sirocko, F., Seelos, K., Schaber, K., Rein, B., Dreher, F., Diehl, M., Lehne, R., Jager, K., Krbetschek, M. and Degering, D.: A late Eemian aridity pulse in central Europe during the last glacial inception, Nature, 436(7052), 833–836, doi:10.1038/nature03905, 2005.

Sirocko, F., Dietrich, S., Veres, D., Grootes, P. M., Schaber-Mohr, K., Seelos, K., Nadeau, M.-J., Kromer, B., Rothacker, L., Roehner, M., Krbetschek, M., Appleby, P., Hambach, U., Rolf, C., Sudo, M. and Grim, S.: Multi-proxy dating of Holocene maar lakes and Pleistocene dry maar sediments in the Eifel, Germany, Quat. Sci. Rev., 62, 56–76, doi:10.1016/j.quascirev.2012.09.011, 2013.

Sirocko, F., Knapp, H., Dreher, F., Förster, M. W., Albert, J., Brunck, H., Veres, D., Dietrich, S., Zech, M., Hambach, U., Röhner, M., Rudert, S., Schwibus, K., Adams, C. and Sigl, P.: The ELSA-Vegetation-Stack: Reconstruction of Landscape Evolution Zones (LEZ) from laminated Eifel maar sediments of the last 60,000years, Global and Planetary Change, 142, 108–135, doi:10.1016/j.gloplacha.2016.03.005, 2016.

Spötl, C. and Mangini, A.: Stalagmite from the Austrian Alps reveals Dansgaard–Oeschger events during isotope stage 3: Implications for the absolute chronology of Greenland ice cores, Earth and Planetary Science Letters, 203(1), 507–518, doi:10.1016/S0012-821X(02)00837-3, 2002.

Spratt, R. M. and Lisiecki, L. E.: A Late Pleistocene sea level stack, Climate of the Past, 12(4), 1079–1092, doi:10.5194/cp-12-1079-2016, 2016.

Stärz, M., Jokat, W., Knorr, G. and Lohmann, G.: Threshold in North Atlantic-Arctic Ocean circulation controlled by the subsidence of the Greenland-Scotland Ridge, Nature Communications, 8(1), 1–13, doi:10.1038/ncomms15681, 2017.

Stebich, M., Rehfeld, K., Schlütz, F., Tarasov, P. E., Liu, J. and Mingram, J.: Holocene vegetation and climate dynamics of NE China based on the pollen record from Sihailongwan Maar Lake, Quaternary Science Reviews, 124, 275–289, doi:https://doi.org/10.1016/j.quascirev.2015.07.021, 2015.

Stepanek, C. and Lohmann, G.: Modelling mid-Pliocene climate with COSMOS, Geosci. Model Dev., 5, 1221–1243,

doi:Stepanek, C. ORCID: https://orcid.org/0000-0002-3912-6271 <https://orcid.org/0000-0002-3912-6271> and Lohmann, G. ORCID: https://orcid.org/0000-0003-2089-733X <https://orcid.org/0000-0003-2089-733X> (2012) Modelling mid-Pliocene climate with COSMOS , Geosci. Model Dev., 5 , pp. 1221-1243 . doi:https://doi.org/10.5194/gmd-5-1221-2012 <https://doi.org/10.5194/gmd-5-1221-2012> , hdl:10013/epic.39137, 2012.

Sun, Y., Wang, X., Liu, Q. and Clemens, S. C.: Impacts of post-depositional processes on rapid monsoon signals recorded by the last glacial loess deposits of northern China, Earth and Planetary Science Letters, 289(1–2), 171–179, doi:10.1016/j.epsl.2009.10.038, 2010.

Svensson, A., Andersen, K. K., Bigler, M., Clausen, H. B., Dahl-Jensen, D., Davies, S. M., Johnsen, S. J., Muscheler, R., Parrenin, F., Rasmussen, S. O., Röthlisberger, R., Seierstad, I., Steffensen, J. P. and Vinther, B. M.: A 60 000 year Greenland stratigraphic ice core chronology, Clim. Past, 12, 2008.

~~Thompson, W. G. and Goldstein, S. L.: A radiometric calibration of the SPECMAP timescale, Quaternary Science Reviews, 25(23), 3207–3215, doi:10.1016/j.quascirev.2006.02.007, 2006.~~

Újvári, G., Stevens, T., Svensson, A., Klötzli, U. S., Manning, C., Németh, T., Kovács, J., Sweeney, M. R., Gocke, M., Wiesenberg, G. L. B., Markovic, S. B. and Zech, M.: Two possible source regions for central Greenland last glacial dust: SOURCE REGIONS OF GREENLAND GLACIAL DUST, Geophysical Research Letters, 42(23), 10,399-10,408, doi:10.1002/2015GL066153, 2015.

Ünal-İmer, E., Shulmeister, J., Zhao, J.-X., Tonguç Uysal, I., Feng, Y.-X., Duc Nguyen, A. and Yüce, G.: An 80 kyr-long continuous speleothem record from Dim Cave, SW Turkey with paleoclimatic implications for the Eastern Mediterranean, Scientific Reports, 5(1), doi:10.1038/srep13560, 2015.

Wagner, J. D. M., Cole, J. E., Beck, J. W., Patchett, P. J., Henderson, G. M. and Barnett, H. R.: Moisture variability in the southwestern United States linked to abrupt glacial climate change, Nature Geoscience, 3(2), 110–113, doi:10.1038/ngeo707, 2010.

Wainer, K., Genty, D., Blamart, D., Hoffmann, D. and Couchoud, I.: A new stage 3 millennial climatic variability record from a SW France speleothem, Palaeogeography, Palaeoclimatology, Palaeoecology, 271(1–2), 130–139, doi:10.1016/j.palaeo.2008.10.009, 2009.

~~WAIS Divide Project Members, Buizert, C., Adrian, B., Ahn, J., Albert, M., Alley, R. B., Baggenstos, D., Bauska, T. K., Bay, R. C., Bencivengo, B. B., Bentley, C. R., Brook, E. J., Chellman, N. J., Clow, G. D., Cole-Dai, J., Conway, H., Cravens, E., Cuffey, K. M., Dunbar, N. W., Edwards, J. S., Fegyveresi, J. M., Ferris, D. G., Fitzpatrick, J. J., Fudge, T. J., Gibson, C. J., Gkinis, V., Goetz, J. J., Gregory, S., Hargreaves, G. M., Iverson, N., Johnson, J. A., Jones, T. R., Kalk, M. L., Kippenhan, M. J., Koffman, B. G., Kreutz, K., Kuhl, T. W., Lebar, D. A., Lee, J. E., Marcott, S. A., Markle, B. R., Maselli, O. J., McConnell, J. R., McGwire, K. C., Mitchell, L. E., Mortensen, N. B., Neff, P. D., Nishiizumi, K., Nunn, R. M., Orsi, A. J., Pasteris, D. R., Pedro, J. B., Pettit, E. C., Buford Price, P., Priscu, J. C., Rhodes, R. H., Rosen, J. L., Schauer, A. J., Schoenemann, S. W., Sendelbach, P. J., Severinghaus, J. P., Shturmakov, A. J., Sigl, M., Slawny, K. R., Souney, J. M., Sowers, T. A., Spencer, M. K., Steig, E. J., Taylor, K. C., Twickler, M. S., Vaughn, B. H., Voigt, D. E., Waddington, E. D., Welten, K. C., Wendricks, A.~~

W., White, J. W. C., Winstrup, M., Wong, G. J. and Woodruff, T. E.: Precise interpolar phasing of abrupt climate change during the last ice age, Nature, 520(7549), 661–665, doi:10.1038/nature14401, 2015.

Wainer, K., Genty, D., Blamart, D., Daëron, M., Bar-Matthews, M., Vonhof, H., Dublyansky, Y., Pons-Branchu, E., Thomas, L., van Calsteren, P., Quinif, Y. and Caillon, N.: Speleothem record of the last 180 ka in Villars cave (SW France): Investigation of a large δ18O shift between MIS6 and MIS5, Quaternary Science Reviews, 30(1–2), 130–146, doi:10.1016/j.quascirev.2010.07.004, 2011.

Wang, Y. J., Cheng, H., Edwards, R. L., An, Z. S., Wu, J. Y., Shen, C.-C. and Dorale, J. A.: A High-Resolution Absolute-Dated Late Pleistocene Monsoon Record from Hulu Cave, China, Science, 294(5550), 2345, doi:10.1126/science.1064618, 2001.

Wassenburg, J. A., Immenhauser, A., Richter, D. K., Jochum, K. P., Fietzke, J., Deininger, M., Goos, M., Scholz, D. and Sabaoui, A.: Climate and cave control on Pleistocene/Holocene calcite-to-aragonite transitions in speleothems from Morocco: Elemental and isotopic evidence, Geochimica et Cosmochimica Acta, 92, 23–47, doi:10.1016/j.gca.2012.06.002, 2012.

Wassenburg, J. A., Dietrich, S., Fietzke, J., Fohlmeister, J., Jochum, K. P., Scholz, D., Richter, D. K., Sabaoui, A., Spötl, C., Lohmann, G., Andreae, M. O. and Immenhauser, A.: Reorganization of the North Atlantic Oscillation during early Holocene deglaciation, Nature Geoscience, 9(8), 602–605, doi:10.1038/ngeo2767, 2016.

Weber, M., Scholz, D., Schroeder-Ritzrau, A., Deininger, M., Spoetl, C., Lugli, F., Mertz-Kraus, R., Jochum, K. P., Fohlmeister, J., Stumpf, C. F. and Riechelmann, D. F. C.: Evidence of warm and humid interstadials in central Europe during early MIS 3 revealed by a multi-proxy speleothem record, Quat. Sci. Rev., 200, 276–286, doi:10.1016/j.quascirev.2018.09.045, 2018.

Wegner, A., Fischer, H., Delmonte, B., Petit, J.-R., Erhardt, T., Ruth, U., Svensson, A., Vinther, B. and Miller, H.: The role of seasonality of mineral dust concentration and size on glacial/interglacial dust changes in the EPICA Dronning Maud Land ice core: EPICA DML DUST RECORD, Journal of Geophysical Research: Atmospheres, 120(19), 9916–9931, doi:10.1002/2015JD023608, 2015.

Wei, W. and Lohmann, G.: Simulated Atlantic Multidecadal Oscillation during the Holocene, J. Climate, 25(20), 6989–7002, doi:10.1175/JCLI-D-11-00667.1, 2012.

Wessel, P. and Smith, W. H. F.: Free software helps map and display data, Eos, Transactions American Geophysical Union, 72(41), 441–446, doi:10.1029/90EO00319, 1991.

Whittaker, T. E., Hendy, C. H. and Hellstrom, J. C.: Abrupt millennial scale changes in intensity of Southern Hemisphere westerly winds during marine isotope stages 2–4, Geology, 39(5), 455–458, doi:10.1130/G31827.1, 2011.

Williams, P. W.: A 230 ka record of glacial and interglacial events from Aurora Cave, Fiordland, New Zealand, New Zealand Journal of Geology and Geophysics, 39(2), 225–241, doi:10.1080/00288306.1996.9514707, 1996.

Williams, P. W., King, D. N. T., Zhao, J. X. and Collerson, K. D.: Late Pleistocene to Holocene composite speleothem 18O and 13C chronologies from South Island, New Zealand—did a global Younger Dryas really exist?, Earth and Planetary Science Letters, 230(3–4), 301–317, doi:10.1016/j.epsl.2004.10.024, 2005.

Xiao, J., Porter, S. C., An, Z., Kumai, H. and Yoshikawa, S.: Grain Size of Quartz as an Indicator of Winter Monsoon Strength on the Loess Plateau of Central China during the Last 130,000 Yr, Quaternary Research, 43(1), 22–29, doi:10.1006/qres.1995.1003, 1995.

Xiao, M., Zhang, Q. and Singh, V. P.: Influences of ENSO, NAO, IOD and PDO on seasonal precipitation regimes in the Yangtze River basin, China, International Journal of Climatology, 35(12), 3556–3567, doi:10.1002/joc.4228, 2015.

~~Yarincik, K. M., Murray, R. W. and Peterson, L. C.: Climatically sensitive eolian and hemipelagic deposition in the Cariaco Basin, Venezuela, over the past 578,000 years: Results from Al/Ti and K/Al, Paleoceanography, 15(2), 210–228, doi:10.1029/1999PA900048, 2000.~~

Zhang, X., Lohmann, G., Knorr, G. and Xu, X.: Different ocean states and transient characteristics in Last Glacial Maximum simulations and implications for deglaciation, Climate of the Past, 9(5), 2319–2333, doi:10.5194/cp-9-2319-2013, 2013.

Zhang, X., Lohmann, G., Knorr, G. and Purcell, C.: Abrupt glacial climate shifts controlled by ice sheet changes, Nature, 512(7514), 290–294, doi:10.1038/nature13592, 2014.

Zhou, W., Head, M. J., Lu, X., An, Z., Jull, A. J. T. and Donahue, D.: Teleconnection of climatic events between East Asia and polar, high latitude areas during the last deglaciation, Palaeogeography, Palaeoclimatology, Palaeoecology, 152(1), 163–172, doi:10.1016/S0031-0182(99)00041-3, 1999.

Zolitschka, B., Brauer, A., Negendank, J. F. W., Stockhausen, H. and Lang, A.: Annually dated late Weichselian continental paleoclimate record from the Eifel, Germany, Geology, 28(9), 783–786, doi:10.1130/0091-7613(2000)28<783:ADLWCP>2.0.CO;2, 2000.

Aridity synthesis for 10 selected key regions of the global climate system during the last 60 000 years

Florian Fuhrmann[1], Benedikt Diensberg[1], Xun Gong[2], Gerrit Lohmann[2], Frank Sirocko[1]

[1]Department for Geoscience, Johannes-Gutenberg-Universität, Mainz, 55099, Germany
[2]Alfred Wegener Institute for Polar and Marine Research, Bremerhaven, Germany

Correspondence to: Florian Fuhrmann, (flfuhrma@uni-mainz.de)

Supplements:

S1 Arabian Sea:

The Arabian Sea comprises the region from the Persian Gulf to the Indian Sea and is characterized by warm and high saline waters ~~as well as~~and fluvial input from the Indus River. ~~In addition, high~~High dust fluxes mainly from Arabian desert are preserved in the sediments. The high surface-water productivity from monsoonal inputs into the ocean and upwelling offshore west Pakistan lead to a stable oxygen minimum zone (OMZ) in water depths between 200 m and 1200 m. This OMZ results in excellent preservation conditions for dark, organic-carbon rich, laminated sediments during mild interstadials and in contrast to light colored, bioturbated sediments during stadials and especially Heinrich events (Schulz, et al., 1998). Arabian Sea and North Atlantic regions are closely coupled by atmospheric teleconnections (Burns et al., 2003; Deplazes et al., 2014; Leuschner and Sirocko, 2000, 2003; Schulz, et al., 1998; Sirocko et al., 1996a and others). There is evidence for a general relationship between these two regions on timescales of the last 110 000 years within low-latitude monsoonal variability and high northern latitude records of Greenland ice cores (Schulz, et al., 1998). The sediment cores SO130-289KL and SO90-136KL are from very close positions and show nearly the same pattern within Reflectance and Total Organic Carbon (TOC) content. Furthermore, they can be correlated one-to-one to the NGRIP ice core (North Greenland Ice Core Project Members et al., 2004) on every GI from 17 to 1 and the YD cold event. In Addition, the Heinrich events 6 to 1 (H6 - H1) appear in superposition (see Fig. S1). The speleothem growth in this region can be correlated to the Greenland ice cores as well (Burns et al., 2003). Speleothems from Oman and Socotra Cave in Yemen are very close to the Arabian Sea and hence used for this synthesis. The sediment core 70KL shows $CaCO_3$ content in percent as a dust indicator. High $CaCO_3$ values show low dust contents from Arabian Peninsula desert and vice versa – more dust accounts for lower $CaCO_3$ values due to higher dilution of the sediment because of increased sedimentation rates.

From 60 000 to 55 000 yr b2k no speleothem growth is apparent for the Arabian sea region while the dust values show a maximum. The Reflectance data simultaneously show very high values (according to bioturbation) indicating the extend of H6 to this region. The TOC content is on small values resulting from only slight upwelling and low bioproduction but still all

GIs are visible with less expression compared to the NGRIP ice core. The dust reconstruction from $CaCO_3$ content shows high amounts in dust values. A high aridity is reconstructed for this period.

From 55 000 to 41 800 yr b2k, the GIs 14 to 11 are visible in the TOC. High variations between stadial and interstadial times occur with the highest values of about 5% TOC during GI14 and 12. The lowest values go along with H5, but in general, stadials account for lower TOC values. In the time of 55 000 to 41 800 yr b2k, the mean TOC values were on the highest values for the last 60 000 years. Also, the Reflectance data show this pattern with clearly visible H5 and GI expression. Within the dust content, a minimum during this period is apparent (lowest values beside the Holocene) and speleothem growth occurred in the Socotra Cave during this early MIS3 time indicating high precipitation and strong monsoonal variability resulting in low aridity as visible in the aridity index (see Fig. S1e).

From 41 800 to 27 700 yr b2k the GIs 10 to 3 are present within Reflectance and TOC data and comparable to the NGRIP ice core. Intermediate TOC values and the large ~~variations~~differences between interstadial and stadial, especially at H4 and H3 ~~event~~ times, are remarkable. The dust content varies between high and medium values through this period with higher values around 35 000 yr b2k and lower values during GI5. This interstadial seems to be nearly as strong as GI12, which is known as one of the 'warmest interstadials' for several regions within TOC and Reflectance data. No speleothem growth is observed during the high glacial period. The aridity was high at the beginning of this phase. GI5 and the double GI3 and 4 appear to have had strong impact on the precipitation, so the aridity was lower during this time with an increase to stronger aridity afterwards. Between 27 700 and 11 700 yr b2k are GI2 and 1 as well as H2 and H1 and the YD apparent. The TOC decreases from high values at the end of GI3 to very low ones during LGM and especially H1 and YD. The dust remains on intermediate to high values with dust pulses within H1 and H2. These events increased aridity to very high values but the aridity within the rest of this time phase was high nevertheless.

With the onset of the Holocene at 11 700 yr b2k, speleothem growth in Oman caves started. The dust values decrease to minimum during the Holocene climate optimum around 8 000 to 6 000 yr b2k. The Reflectance and TOC data increase drastically and show higher temperature as well during early Holocene, with a slight decrease towards present day. During early Holocene times the precipitation seems very strong with low aridity. Towards present day, the aridity increases strongly.

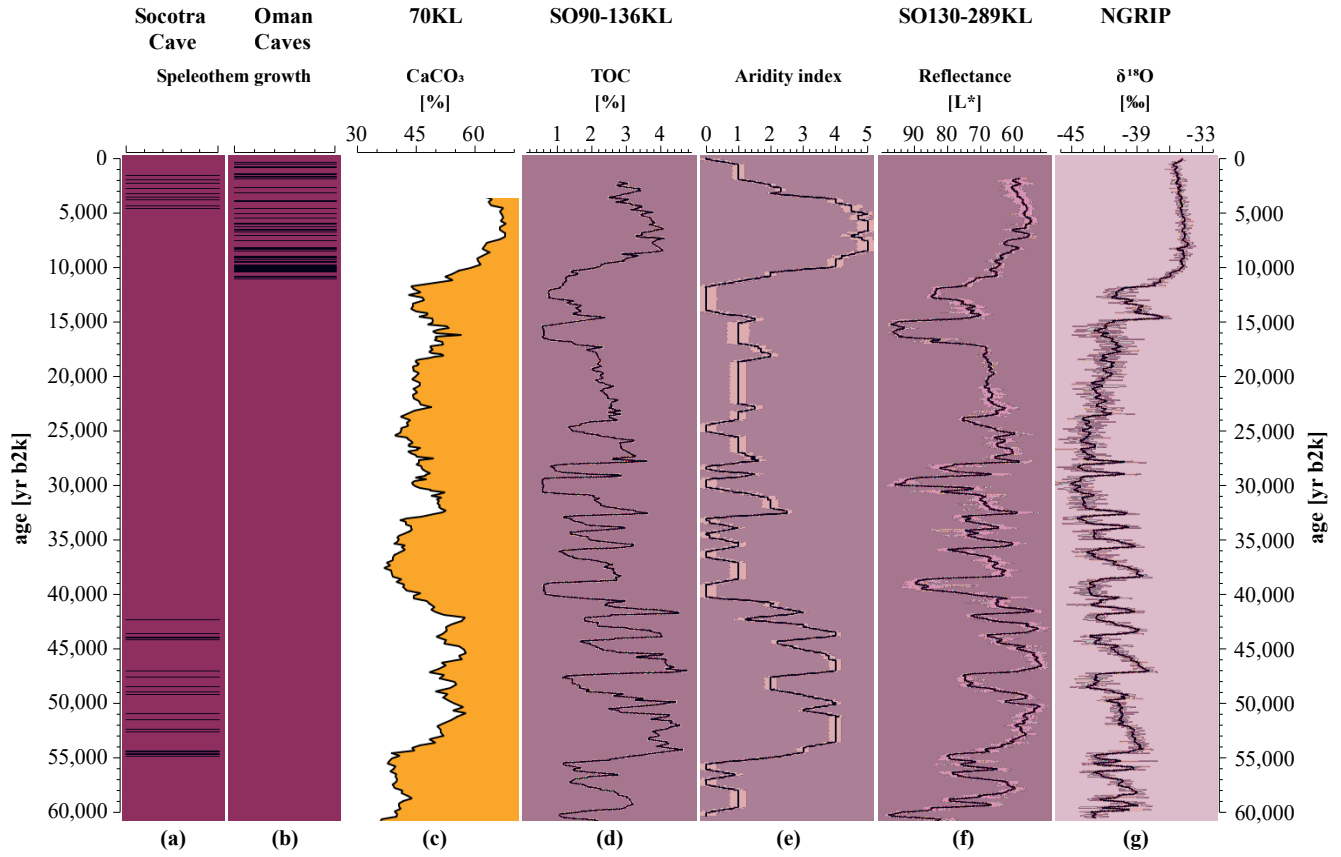
Socotra Cave
Oman Caves
70KL
SO90-136KL
SO130-289KL
NGRIP
Speleothem growth
CaCO3 [%]
TOC [%]
Aridity index
Reflectance [L*]
δ18O [‰]
30 45 60
1 2 3 4
0 1 2 3 4 5
90 80 70 60
-45 -39 -33
0 5,000 10,000 15,000 20,000 25,000 30,000 35,000 40,000 45,000 50,000 55,000 60,000
age [yr b2k]
(a) (b) (c) (d) (e) (f) (g)

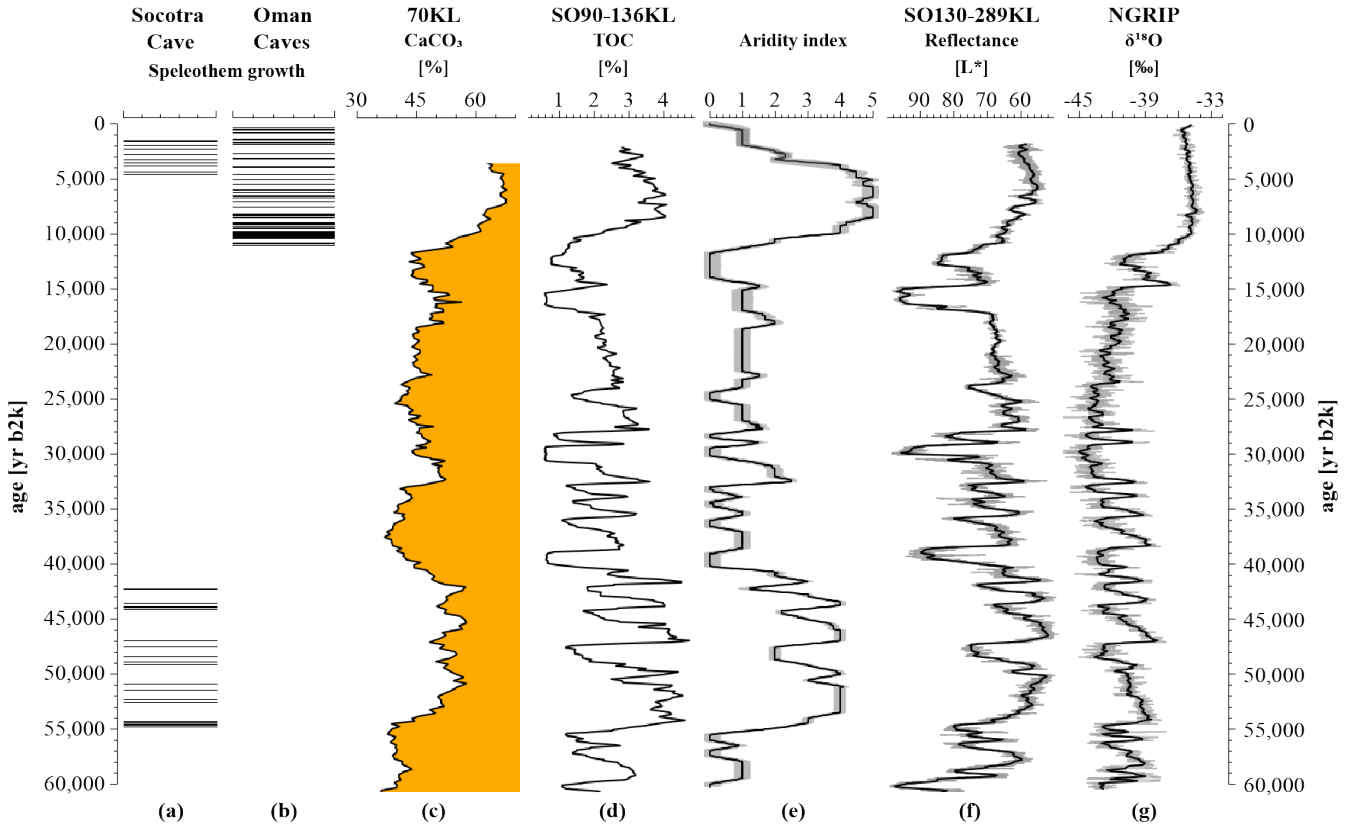

Figure S1: Arabian Sea climate over the last 60 000 years: **(a)** Socotra Cave and **(b)** Oman Caves (Burns et al., 2003; Fleitmann et al., 2007) show speleothem growth phases, which require mobile water from frequent precipitation; **(c)** 70KL $CaCO_3$ (Leuschner and Sirocko, 2003) indicates more arid conditions with lower values, higher values account for more humid conditions; **(d)** SO90-136KL (Schulz, et al., 1998) TOC content exhibits the GIs comparable to **(g)** in total by higher carbon values; **(e)** Aridity index for Central Europe as result from **(a-d),** for detailed information see method section; **(f)** SO130-289KL Reflectance data (Deplazes et al., 2014) resembling **(d)** and **(g); (g)** $\delta^{18}O$ data from NGRIP ice core (North Greenland Ice Core Project Members et al., 2004) in comparison.

S2 North-West Africa:

To understand the climate history of North-West Africa and the continental margin off West Africa is important for understanding changes in Sahara – Sahel aridification as induced by changes in Atlantic water sea surface temperatures (SST) or large scale mechanisms like for example AMOC, North Atlantic Oscillation (NAO), Inter Tropical Convergence Zone (ITCZ). Life in this region strongly depends on the availability of water. Nowadays, the mean annual temperature ranges between 12 and 15 °C and mean annual precipitation is about 468 mm/yr for Atlas Mountain ranges related to the Azores high position (Wassenburg et al., 2012). Sediment core GIK15627-3 from offshore Morocco reveals the time from 250 000 to 5 000 years b2k of paleovegetation for NW-Africa (Hooghiemstra et al., 1992). No long pollen time series are available from terrestrial archives right now, hence this record was chosen despite a relatively low sample resolution. Nearby speleothems are

known from Atlas mountain range like Grotte Prison de Chien (Wassenburg et al., 2012) or ~~from Central North Africa Susah Cave, where speleothem growth stopped 32 000 yr b2k but shows growth phases during all GIs from 17 to 5, except a hiatus during the time of GI8 and GI9. Today, the speleothems are dust covered and the growth is inactive for a long time~~Grotte de Piste ~~(Hoffmann et al., 2016)~~(Wassenburg et al., 2016). ~~Another~~GeoB9508-5, a sediment core from offshore Senegal, West Africa, ~~(GeoB9508-5,~~ (Collins et al., 2013; Mulitza et al., 2008)~~)~~ reveals strong Heinrich Stadials in dust content during times of reduced AMOC ~~related to cold North Atlantic sea surface temperatures resulting in arid mega droughts for West Africa (~~(Mulitza et al., 2008; see Fig. S2). ~~The majority of deposited eolian dust grains is larger than 10 µm (Stuut et al., 2005), while 95 % of river suspended sediments are smaller than 10 µm (Gac and Kane, 1986).~~

The timespan from 60 000 to 50 000 yr b2k comprises GI17~~—~~ - 14 ~~within the Susah Cave speleothem.~~. No Speleothem growth is apparent during the whole timespan ~~beside a small hiatus around 50 000 yr b2k~~. The amount of tree pollen decreases from values around 60 % to 0 % (53 000 yr b2k) and rises again during a wet period from 52 500 to 50 500 yr b2k~~, which is also visible within the speleothem growth phases (Hoffmann et al., 2016). The dust content shows no larger variabilities during this phase and is on it's lowest values until the onset of the Holocene. With speleothem growth, low~~. The dust content shows no major fluctuations during this phase and remains at its lowest levels until the beginning of the Holocene. Low dust values and varying tree pollen amounts, the aridity is on intermediate to lower values. Between 50 000 and 37 000 yr b2k with GI13 – 8, aridity is increased. ~~The speleothem shows a hiatus during GI9 and 8 but showing all other GIs within the growth phases. The hiatus falls within the phase of Heinrich Stadial 4.~~A first speleothem age is known to be around 45 000 yr b2k, shortly after the end of H5. Tree pollen amount is constantly on lower values (~ 30 %) with a little decrease during H5. Dust values peak strongly during Heinrich Stadials 5 and 4~~, synchronously to the speleothem hiatus at H4 times~~ indicating intermediate to high aridity. From 37 000 to 27 000 yr b2k (GIs 7-3) NW-Africa underwent increasing aridity. Speleothem growth ~~ended after 33 000 yr b2k, alike a wet period for NW-Africa (Hoffmann et al., 2016). GIs 7 to 5 are visible within the speleothem growth phases indicating at least a moderate humidity for this time phase. Tree pollen remain on lower values between 20 and 30 % with a small increase during the wet phase known from the speleothem.~~was only sporadic but comes along with higher tree pollen values for the same times. Tree pollen remain on lower values between 20 and 30 % with a small increase during the growth phases known from the speleothem. Dust content is on intermediate values with a small increase during H3 at the end of this period. The climate of this time phase appears cold and moderate arid. The onset to H2 marks the begin of the next period (27 000 to 14 800 yr b2k, GI2 within). ~~No speleothem growth is known for Susah Cave, but~~ Grotte Prison de Chien shows at least ~~shows~~ some ~~datings~~dating indicating sporadic precipitation for this ~~time phase~~period. In general, tree pollen values decrease to very low values indicating even more arid conditions between 20 000 and 15 000 yr b2k (Hooghiemstra et al., 1992). The dust values are on a maximum during this phase in general but H2 and H1 are clearly identifiably within the record. With all that information combined, the period expresses the impact of the LGM ~~on global climate systems~~period and shows arid and cold conditions. With the end of H1 and the onset of warming towards the Holocene, the amount of tree pollen increases again (14 800 yr b2k until present, GI1 and YD), while speleothems from North Morocco also show some growth phases. Gradually, less arid conditions show a climate amelioration until 8 500 yr b2k, the 'African Humid Period' (AHP) or

EHTO (Early Holocene Temperature Optimum~~)~~.), where lots of age datings can be found indicating fast speleothem growth. Dust shows a small peak during YD cold event. However, the general strong decrease from the end of LGM until EHTO is evident. Little dust was mobile during this phase. In the last 4 000 years, dust values rise again, indicating an aridity increase for youngest times.

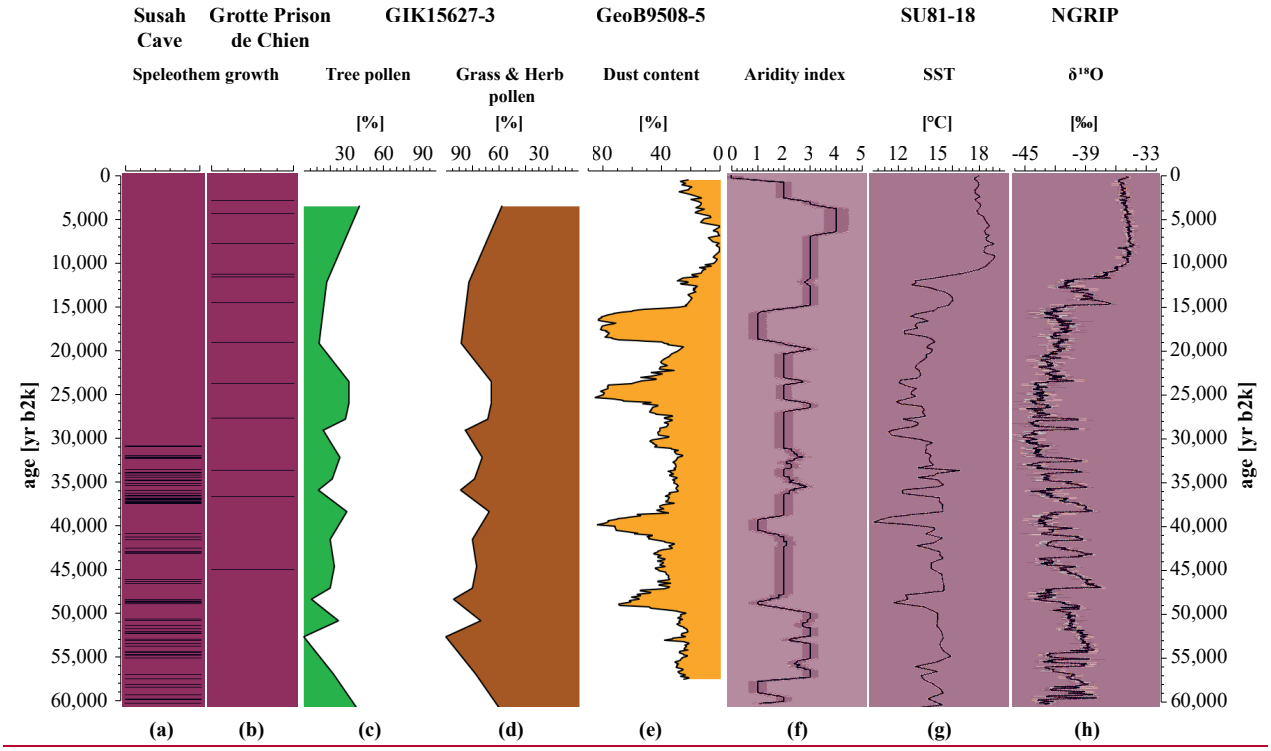

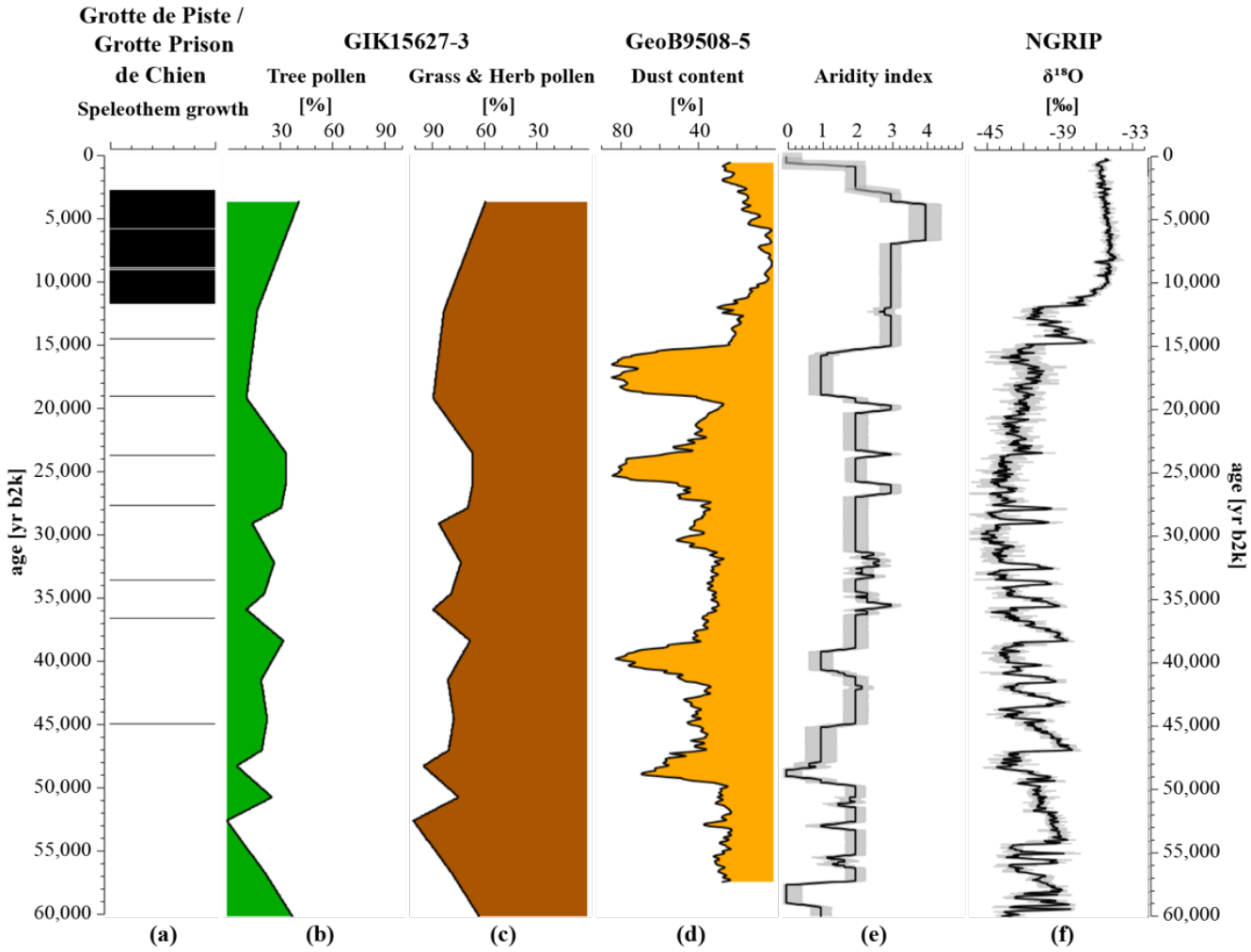

Figure S2: ~~NW-Africa climate over the last 60 000 years: **(a)** Susah Cave (Hoffmann et al., 2016) and **(b:**~~ NW-Africa climate over the last 60 000 years: **(a)** Grotte Prison de Chien (Wassenburg et al., 2012) ~~show speleothem growth phases, which require mobile water from frequent precipitation; **(c, d**~~ and Grotte de Prison (Wassenburg et al., 2016) show speleothem growth phases, which require mobile water from frequent precipitation; **(b, c)** GIK15627-3 marine core pollen data (Hooghiemstra et al., 1992) are divided into tree- and herb & grass pollen. While trees require more precipitation, grasses are dominant for more arid conditions; **(**~~c~~**d)** GeoB9508-5 (Collins et al., 2013) indicates more arid conditions with higher values, lower values account for more humid conditions. ~~HE are distinguishable by higher dust concentrations; **(f)** Aridity index for NW-Africa as result from **(a)-(c)**, for detailed information see method section; **(g)** SST reconstructions from marine core SU81-18 (Bard, 2002) with all HE, and less distinct GIs, apparent; **(h**~~HE are distinguishable by higher dust concentrations; **(e)** Aridity index for NW-Africa as result from **(a)-(d)**, for detailed information see method section; **(f)** $\delta^{18}O$ data from NGRIP ice core (North Greenland Ice Core Project Members et al., 2004) in comparison.

S3 China:

Most of the Asian continent is influenced by the East Asian Monsoon, which is the most important moisture source. Most of annual precipitation (~ 80 %) falls in summer season (e.g. Mingram et al., 2018; Wang et al., 2001) with mean annual

precipitation about 1015 mm/yr at Hulu Cave and 715 mm/yr at Sihailongwan maar lake (Stebich et al., 2015). The mean annual temperature is about 2.9 °C (Schettler et al., 2006), varying from -18.1 °C for January and + 20.7 °C for July at Sihailongwan site and 15.4 °C at Hulu Cave (Wang et al., 2001).

Hulu Cave is one of the most popular east Asian monsoon records through the last glacial cycle. For this record, five speleothems from the cave were stacked together to compile a continuous record for the timespan of 11 000 – 75 000 yr b2k. The long-term trend follows summer insolation pattern, suggesting an increased summer continent-ocean temperature difference and so, enhanced summer monsoon (Wang et al., 2001). The Hulu record shows a link between East Asia Monsoon and North Atlantic climate by apparent GI-variations within the $\delta^{18}O$ record. The Sihailongwan maar lake (SHL) lies within the Long Gang Volcanic Field in NE-China. The SHL-core is continuously warved until 65 000 yr b2k, providing an excellent stratigraphy for climate reconstructions by not only paleovegetation. The tree pollen amount replicates the stadial / interstadial variations of the North Atlantic (see Fig. S3) as well as the total organic carbon. Stadials and especially Heinrich events are characterized by steppic plants like Artemisia. Interstadials in general show higher amounts of tree pollen (Mingram et al., 2018). However, the Holocene pollen data are not publically available for this paper but kept in mind for the discussion of this synthesis. The China Loess Plateau is well known for its loess paleosol sequences. Jingyuan and Weinan sections from Sun et al. (2010) and Lu et al. (2007) are established and show reliable indications for North Atlantic - China climate teleconnections with “loess interstadial / loess stadial” within the mean grainsize of the Jingyuan record.

The timespan from 60 000 yr b2k until 50 000 yr b2k (GI17 - GI13, early MIS3) is regarded as the most humid period of the record (Liu et al., 2010; Lu et al., 2007; Mingram et al., 2018). Speleothem growth is apparent and $\delta^{18}O$ values are on minimum (more negative equals higher temperatures, see (Liu et al., 2010; Wang et al., 2001)) during this period. The tree pollen show high values in order of 60 % with identifiable GI variability. Also, dust values from the Jingyuan loess section show small grainsizes according to a lower dust content. In result, the archives account for humid climate conditions through the early MIS3 phase. Within the period of 50 000 yr b2k to 34 000 yr b2k, GIs 12 to 5 are comprised. This phase also shows continuous speleothem growth with intermediate $\delta^{18}O$ values, GIs are easy to identify. Also, the tree pollen show medium contents with still relative high values during interstadials but lower compared to early MIS3 times. The dust content rises to intermediate values until 38 000 yr b2k indicating stronger winds and lower temperatures combined with a higher aridity. Towards the end of this phase, lower $\delta^{18}O$ values combined with the sharp GI-type increases in tree pollen and lower dust contents are visible, suggesting a phase of stagnation within the climate conditions.

From 34 000 yr b2k to 14 800 yr b2k (GIs 4-2) the climate is characterized by glacial conditions, especially during last glacial maximum and the Heinrich events 3 to 1. The growth rates of the Hulu Cave speleothems went down while the $\delta^{18}O$ values rise to their highest values of the record. Synchronously, the tree pollen decrease to about 20 % during LGM, with high contents of Artemisia especially during Heinrich events, the GIs during this phase are less expressive with general lower temperatures and shorter durations. Between 29 550 yr b2k and 18 250 yr b2k, the minimum of thermophilous plants and tree pollen is apparent (Mingram et al., 2018). The dust values are on a maximum during this time span. The large grainsize comes along

with low temperatures and precipitation values. All that combined is clearly visible in the aridity index with a strong expressed LGM. The deglaciation and the Holocene itself (14 800 yr b2k to present, GI1) can be characterized by the amelioration of the climate conditions, in China as well as on a global scale. The $\delta^{18}O$ values decrease while the growth rate increases. The tree pollen rise up to 80 % while synchronously the dust content lessens to the minimum of the record during the Holocene temperature optimum (6 000 yr b2k – 4 000 yr b2k). According to Stebich et al. (2015) the Sihailongwan Maar pollen indicate a maximum precipitation at 4 550 yr b2k (not included into Fig. S3). The aridity decreased during the Holocene transition to intermediate values, but a lack in data for the Holocene period makes it complicated to draw further estimates.

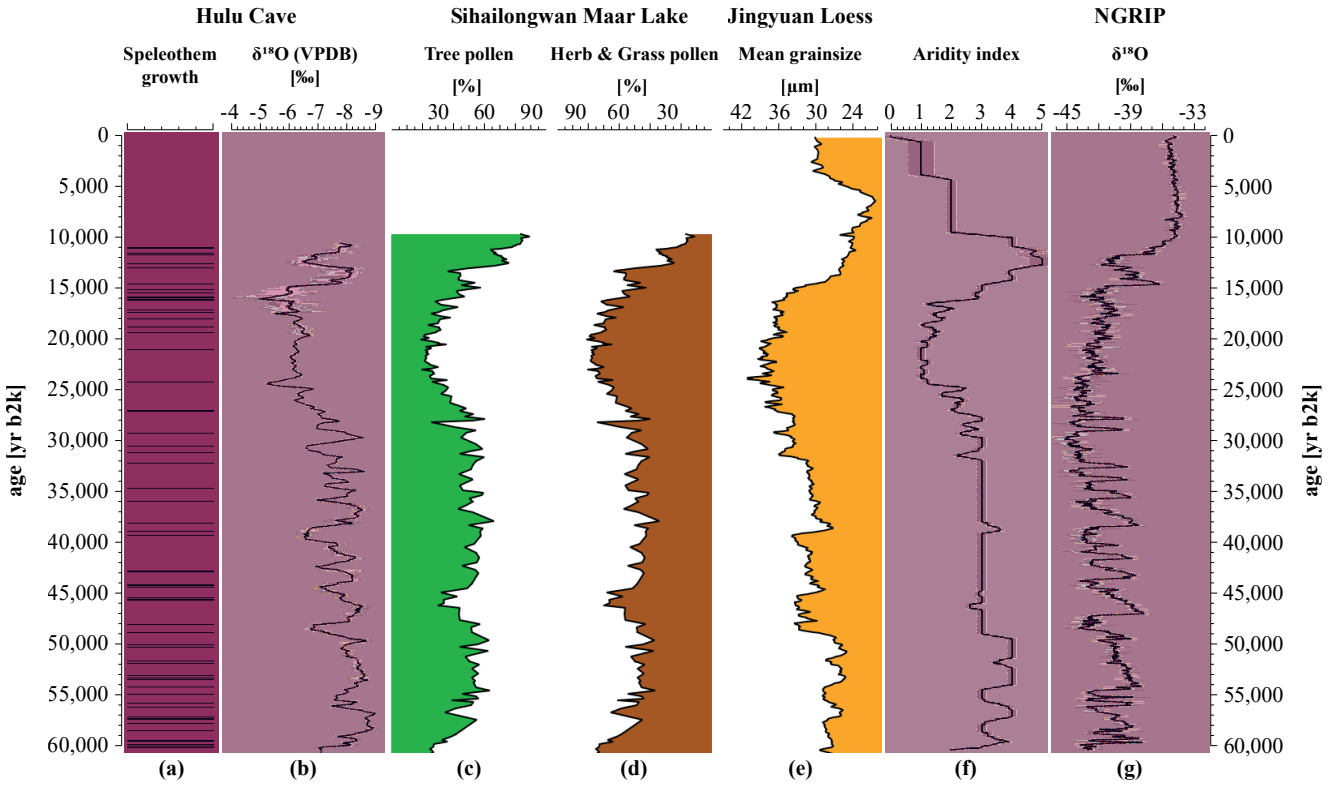

Figure S3: China climate over the last 60 000 years: **(a)** Hulu Cave (Liu et al., 2010; Wang et al., 2001) show speleothem growth phases, which require mobile water from frequent precipitation; **(b)** $\delta^{18}O$ data with apparent GIs comparable to **(g)**, more negative $\delta^{18}O$ values account for more humid conditions (Wang et al., 2001); **(c, d)** Sihailongwan Maar Lake pollen data (Mingram et al., 2018) are divided into tree- and herb & grass pollen. While trees require more precipitation, grasses are dominant for more arid conditions; **(e)** Jingyuan Loess mean grainsize (Sun et al., 2010) indicates more arid conditions with larger grains, smaller grains account for more humid conditions; **(f)** Aridity index for China as result from **(a-e)**, for detailed information see method section; **(g)** $\delta^{18}O$ data from NGRIP ice core (North Greenland Ice Core Project Members et al., 2004) in comparison.

S4 Southern Europe

Southern Europe is affected by the Atlantic Ocean water masses as well as from the Mediterranean Sea and so, influenced by changes in AMOC, NAO, ITCZ and other large-scale mechanisms. Nowadays, the mean annual temperature close to the Villars Cave (in southern France) speleothem site is 12.1 °C and mean annual precipitation 1020 mm/yr, evenly spread through the whole year (Wainer et al., 2009). A sediment core of volcanic maar lake Lac du Bouchet (Lake Bouchet) shows pollen spectra until the end of the last interglacial (Reille and de Beaulieu, 1988, 1990). ~~Although 'Nussloch paleosol loess sequence' is well established but publically available data are not accessible.~~Although 'Nussloch paleosol loess sequence' (Antoine et al., 2001) is well established but publicly available data are not accessible. MD01-2443 marine sediment core (Hodell et al., 2013) is the closest dust archive with sufficient stratigraphy for Southern Europe. SST, L* (color reflectance) and $\delta^{18}O$ of the core show GIs (Hodell et al., 2013; Martrat et al., 2007). Well dated speleothem data are available for the Villars Cave, 200 km away from the Atlantic coast, with speleothem growth between 52 000 and 29 000 yr b2k and for the Holocene (see Fig. S4). The growth speed significantly slowed down between 42 000 and 29 000 yr b2k and finally stopped with the onset to LGM conditions. Also, a hiatus from 55 700 to 52 000 yr b2k is present within the record. GIs 14, 13, 12 and on minor extend GI11 are preserved as well as H5 ~~(Genty et al., 2003a; Wainer et al., 2009). Additional information for this region come from SST (uk'37) record of Martrat et al. (2007) with all Heinrich events as well as from an Ice Raft Debris (IRD) content time series from Naafs et al. (2013) from Central Atlantic derived from Dolomite/Calcite ratio. Higher values show IRD layers and Heinrich events are clearly distinguishable (see Fig. S4). IRD layers consist of coarse-grained lithic clasts from iceberg discharge and low foraminifer contents (Heinrich, 1988). They were climatically interpreted as extreme cooling of the SSTs before Greenland interstadials (Bond et al., 1998).The timespan from 60 000 to 44 000 yr b2k incorporates GIs 17 to 12 within the records of this region.~~(Genty et al., 2003; Wainer et al., 2009).

The timespan from 60 000 to 44 000 yr b2k incorporates GIs 17 to 12 within the records of this region. Speleothem growth in the Villars Cave is evident with a hiatus between 55 700 to 52 000 yr b2k. $\delta^{18}O$ values indicate warm and moist conditions with more negative values than during later phases of the record. The GIs 17, 16, 13 and 12 are identifiable within the data. According to Wainer et al. (2009) the temperature optimum of the recorded time phase was during early MIS3 at around 52 000 yr b2k. In contrast, the highest amount of tree pollen for this period (with about 50 %) falls within the hiatus of the speleothem but still indicating warm and wet early MIS3 conditions for this region. Also, dust content from marine sediment core MD01-2443 are on relatively low values with minor variations. Their lowest values until the Holocene were during the tree pollen maximum. ~~Heinrich events are clearly visible in SST and IRD records. SST are on a maximum during this period, with coldspikes during Heinrich events and IRD layers are only well expressed during those.~~ Until the end of this time phase towards 45 000 yr b2k, conditions tend to get worse as indicated by rising dust content, decreasing amount of tree pollen, lower $\delta^{18}O$ values from Villars Cave and with H5 from the marine cores. The aridity is low during the early MIS3 phase and rises towards the end of the time phase.

The period from 44 000 to 30 000 yr b2k (GIs 11-5) shows general aridity (Reille and de Beaulieu, 1990). The speleothem $\delta^{18}O$ values are very low, only GI8 stands out a bit. The speleothem growth was significantly slower and stopped at the end of this time phase. The tree pollen show high variations and high absolute values, but high amount of steppe vegetation and a small remaining tree population complete the in general increased aridity for Southern Europe. The dust values replicate the interstadial / stadial changes with stronger impression on Heinrich events. ~~The SST decreases in general within this time and IRD layers show H4.~~

From 30 000 to 15 000 yr b2k (GIs 4-2) no speleothem growth is known from Villars Cave. The tree pollen show low values with a minimum around 25 000 yr b2k, were no tree pollen occur within the record. During LGM, grasses (60 to 100 %) replace the last Pinus woodland, which was still apparent ~~during~~at GI3 and 4. Dust values~~, SST and IRD~~ show arid conditions and low temperatures, Heinrich events are well expressed, apart from a low variability. Dust values are highest at the end of this period from 17 000 to 14 000 yr b2k during the same time, were Ruth et al. (2007) detected most eolian dust in NGRIP ice cores (cf. Fig. 2 and Fig. ~~5~~ 6). The aridity was strongest during LGM especially during the end of this phase. With the onset ~~of~~towards the Holocene ~~towards~~around 15 000 yr b2k, speleothem growth restarted in the Villars cave, the amount of tree pollen drastically increases and dust values decrease with a delay of approximately 4 000 years after YD cold event. The Altithermal is displayed by precipitation and temperature increase visible in the records. The aridity decreases with the onset of the Holocene and stays relatively constant on lower values throughout.

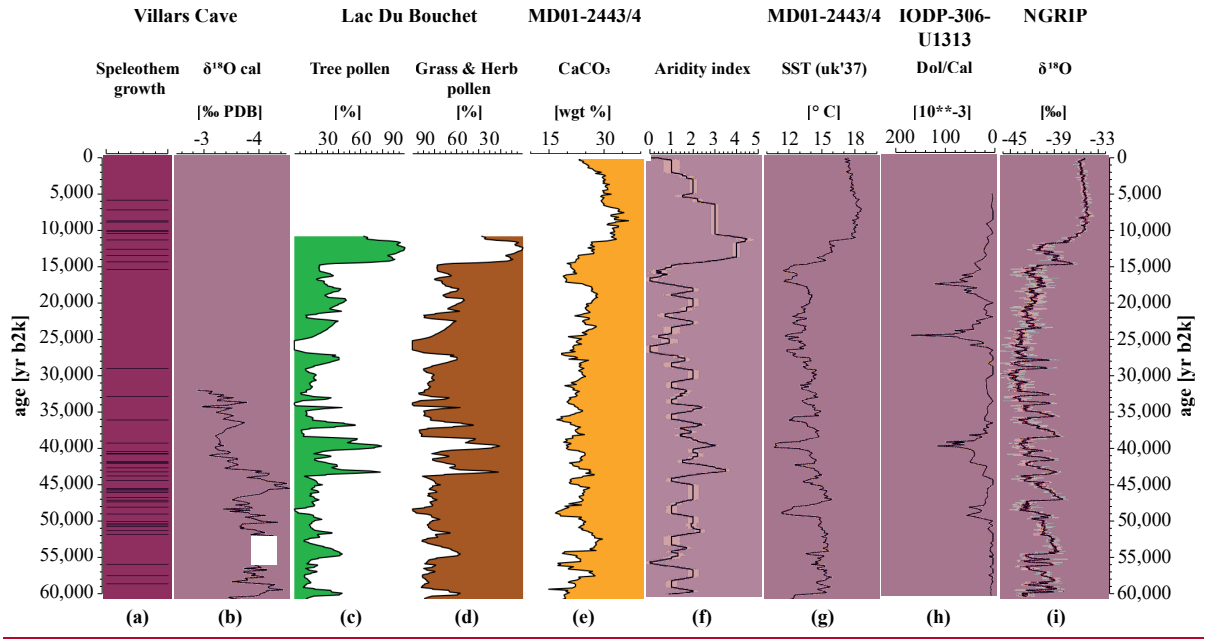

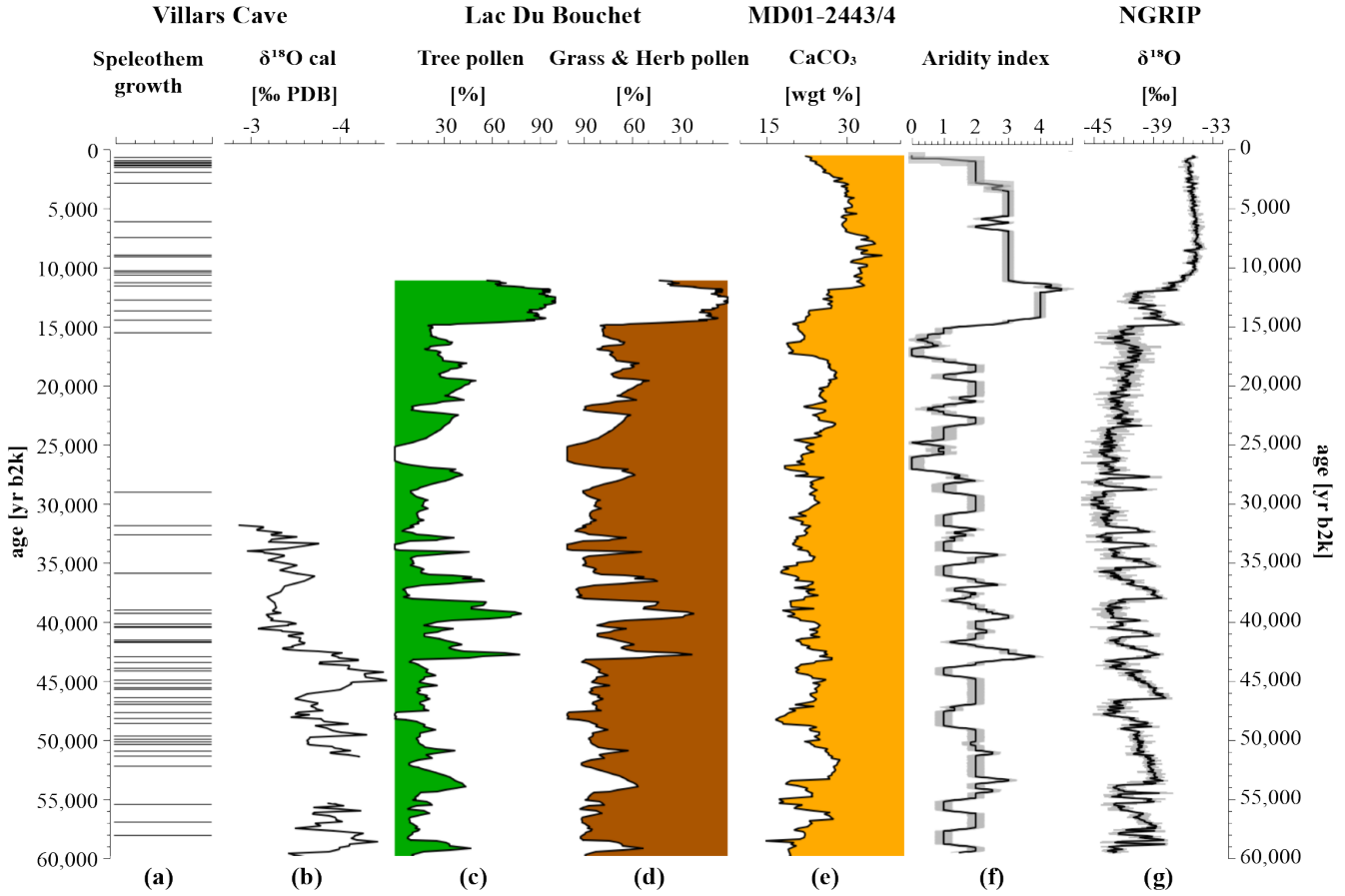

Figure S4: ~~Southern European climate over the last 60 000 years: **(a)** Villars Cave (Genty et al., 2003a, 2006; Wainer et al., 2009) show speleothem growth phases, which require mobile water from frequent precipitation; **(b)** $\delta^{18}O$ data with few apparent GIs comparable to **(g)**, more negative $\delta^{18}O$ values account for more humid conditions (Genty et al., 2003a); **(c, d)** Lac Du Bouchet pollen data~~ **:** Southern European climate over the last 60 000 years: **(a)** Villars Cave (Genty et al., 2003, 2006; Labuhn et al., 2015; Wainer et al., 2009) show speleothem growth phases, which require mobile water from frequent precipitation; **(b)** $\delta^{18}O$ data with few apparent GIs comparable to **(g)**, more negative $\delta^{18}O$ values account for more humid conditions (Genty et al., 2003); **(c, d)** Lac Du Bouchet pollen data (Reille and de Beaulieu, 1990) are divided into tree- and herb & grass pollen. While trees require more precipitation, grasses are dominant for more arid conditions; **(e)** MD01-2443/4 marine cores $CaCO_3$ (Hodell et al., 2013) ~~indicates more arid conditions with lower values, higher values account for more humid conditions; **(f)** Aridity index for Southern Europe as result from **(a-e),** for detailed information see method section; **(g)** SST from marine cores MD01-2443/4 (Martrat et al., 2007) resembling HE and most GIs; **(h)** Dol/Cal ration from IODP-306-U1313 (Naafs et al., 2013) show detailed HE structure; **(i)** $\delta^{18}O$ data from NGRIP ice core (North Greenland Ice Core Project Members et al., 2004) in comparison.~~

~~**S5 Portuguese Margin:**~~

~~**The Portuguese margins sediment cores are known to be highly impacted by climate change on both timescales,**~~ indicates more arid conditions with lower values, higher values account for more humid conditions; **(f)** Aridity index for Southern Europe as result from **(a-e),** for detailed information see method section; **(g)** $\delta^{18}O$ data from NGRIP ice core (North Greenland Ice Core Project Members et al., 2004) in comparison.

S5 Portuguese Margin:

The Portuguese margins sediment cores are known to be highly impacted by climate change on orbital and millennial timescales. Constant sedimentation rates are responsible for good stratigraphies and they are influenced by high- and low-latitude processes (Hodell et al., 2013). Today's mean annual temperatures are about 15~~-~~ °C, winters are mild (10~~-~~ - 13 °C) and summers are moderate (18~~—~~ - 22- °C) with up to 3 000 mm yearly precipitation. Portuguese margin and Southern Europe ~~- France are similar considering~~contain the ~~records, besides~~same dust record, the ~~Paleovegetation one (see Fig. S5).~~MD01-2443 sediment core shows dust in the $CaCO_3$ content. For Portuguese margin, a marine sediment core with terrestrial pollen input can be used to reconstruct the vegetation of the coast. Tree populations of sediment core MD95-2039 show rapid shifts, following GI-scheme. During Heinrich events 1 - 6, SST's dropped in order of 5 – 10 °C. ~~For periods of SST decrease, also the amount of tree pollen decreases and vice versa.~~ Short GIs show less impact on the extend of woodland (Roucoux et al., 2005). ~~For all other records in Fig. S5, see section 'Southern Europe – France'. Villars Cave is the closest, well dated speleothem for this region. The MD01-2443 sediment core shows $CaCO_3$ dust values and SST's (uk'37). In addition, Dol/Cal ratio from IODP-306-U1313 as Heinrich event proxy are used to complete the picture~~Buraca Gloriosa Cave speleothems show the climate evolution of the last 220 000 years (Denniston et al., 2018). The cave is located 30 km from the Atlantic coast, near the both marine cores used for this region.

Within the timespan from 60 000 to 50 000 yr b2k (GIs 17-13), ~~δ^{18}O values shows~~ humid conditions can be reconstructed for Portuguese Iberian margin. ~~Beside the hiatus, speleothem~~Speleothem growth was continuous in ~~Villars~~Buraca Gloriosa Cave and shows ~~very low δ^{18}O values accounting for~~ high ~~humidity and temperature.~~growth rates. The tree pollen in general ~~are~~were on a maximum during this time phase, showing high amplitude fluctuations between cooler and drier stadials and warmer and wetter interstadials (Roucoux et al., 2005), as well as a decline in dust content from 60 000 towards 50 000 yr b2k from relatively high values to lowest values until the Holocene. ~~SST's also show warm temperatures and IRD is apparent primary during H6.~~ The high amount of tree pollen, speleothem growth and the decline in the dust content indicates a general warmer and wetter early MIS3 and consequently, low aridity with the begin of the phase and an intermediate aridity towards the end. During the period from 50 000 to 32 000 yr b2k (GIs 12-5) an intermediate aridity is estimated for the region. H5 and H4 are visible within all records indicating a rapid climate change throughout the region. Speleothem growth ~~is significantly~~rates were lower than before ~~and δ^{18}O values show higher values (equal~~. Around H4 a hiatus of 41 000 to ~~cooler / drier conditions) with only a strongly expressed GIs 12 and 8. Villars cave~~ 36 000 years b2k in speleothem ~~exhibits a strong H5 event, which is also evident in the paleovegetation record MD95-2039.~~growth can be seen. Heinrich events 5 and 4 ~~spike~~are strongly expressed within ~~this~~the MD95-2039 core indicating a dramatic decrease in climate conditions (Roucoux et al., 2005). A minor rise in dust is visible within the $CaCO_3$ content of MD01-2443 from in general intermediate dust values throughout this period for H5 and ~~4. The SST values show rapid decreases during interstadials with strongest impression in Heinrich events and IRD layers show synchronously Heinrich events.~~H4. Regarding all this, an intermediate aridity is estimated throughout this time phase with strong variability between interstadials and stadials for Portuguese margin region.

Between 32 000 and 15 000 yr b2k (GIs 4-2~~) no~~), the speleothem growth ~~is known for Villars~~at Buraca Gloriosa Cave~~.~~ shows two hiatus during H3 and H1 (from 32 000 to 30 000 and 17 000 to 15 000). The amount of tree pollen was very low, open, herb-dominated steppic vegetation indicates cool and arid conditions. Less aridity towards the end of the phase is indicated from a slight increase in tree pollen and heath population, which required amelioration in climate (Roucoux et al., 2005). Intermediate dust values with a decrease towards the end are visible, again with stronger impressed Heinrich events compared to the other stadials. ~~SST and IRD supplement the picture.~~ The LGM, which falls into this period, can be characterized by intermediate aridity but surprisingly low dust values towards the end.

The time phase from 15 000 yr b2k (GI1, YD) to present is marked by the onset of the Holocene with Bølling / Allerød. Speleothem growth restarted and remains constant ~~through the early Holocene.~~until 10 000 yr b2k, a growth recovery from 3 000 to 1 000 yr b2k is also apparent. A rapid increase in tree pollen ~~and SST~~ around 15 000 yr b2k marks a strong increase in temperature and precipitation. Younger Dryas cold event reduced that for a short duration, but afterwards the climate ~~climbed~~improved to Holocene and present day conditions. The dust values were highest during the begin of the time phase around 15 000 yr b2k and declines through the early Holocene temperature optimum. ~~SST's stay constantly high after the initial increase following YD cold event.~~ Aridity was very low with the begin of this phase but in the past 5 000 years, dust values increase again indicating higher aridity than during Altithermal.

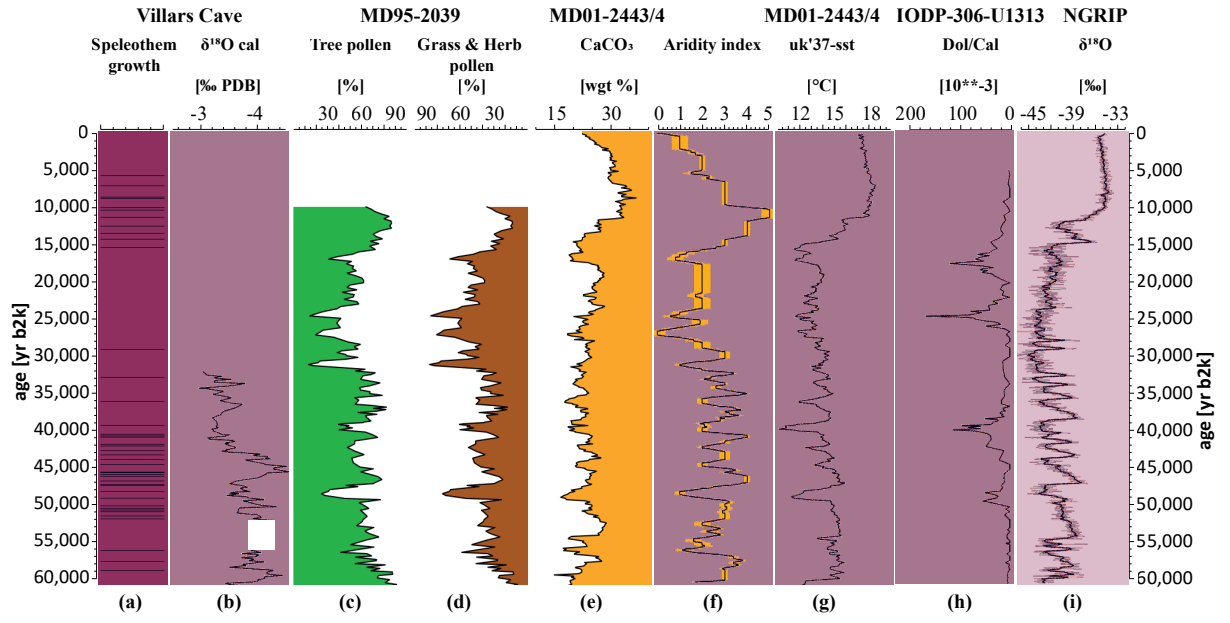

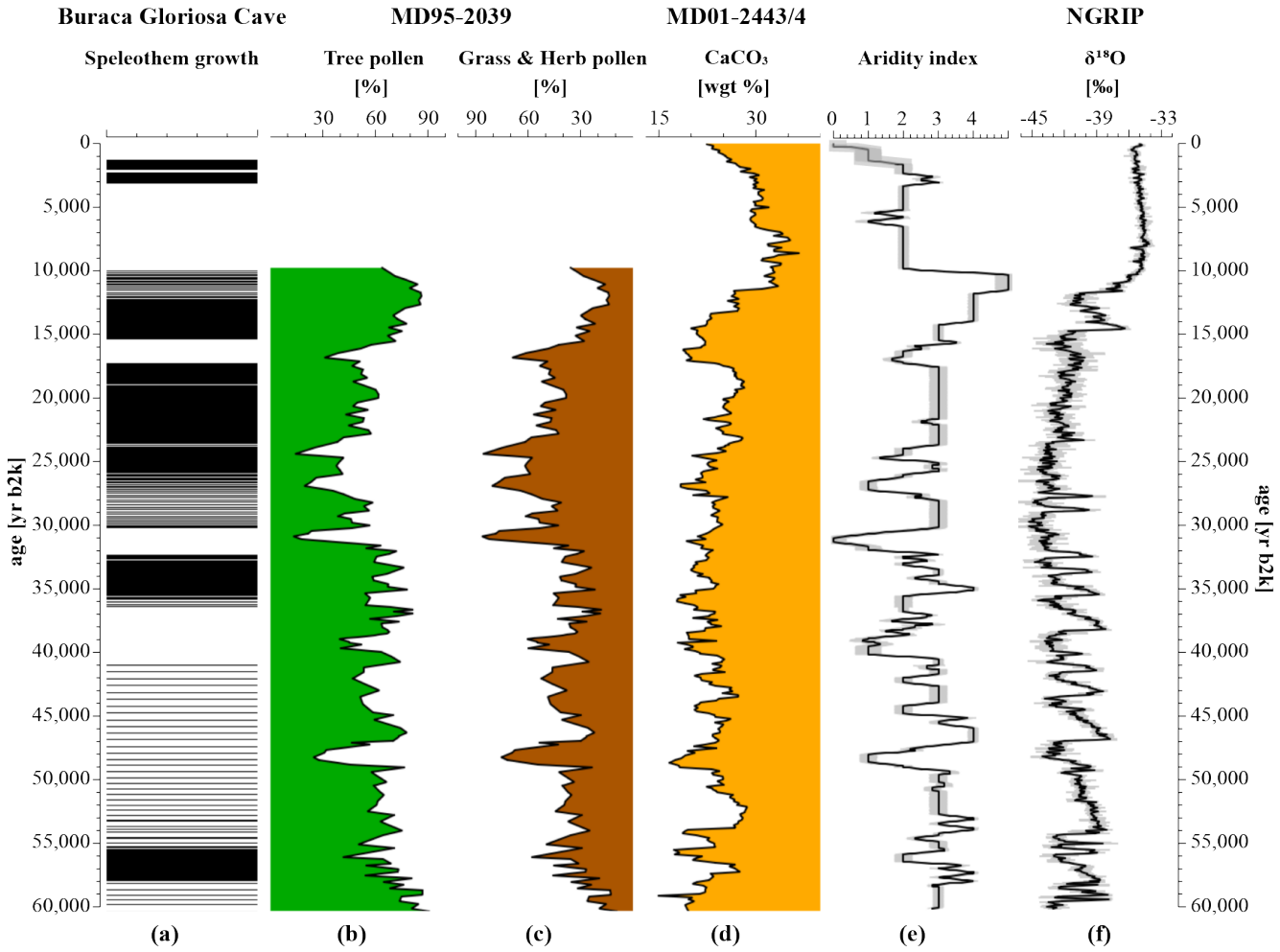

Figure S5: ~~Portuguese margin climate over the last 60 000 years: **(a)** Villars Cave (Genty et al., 2003a, 2006; Wainer et al., 2009) show speleothem growth phases, which require mobile water from frequent precipitation; **(b)** $\delta^{18}O$ data with few apparent GIs comparable to (g), more negative $\delta^{18}O$ values account for more humid conditions (Genty et al., 2003b); **(c, d):**~~ Portuguese margin climate over the last 60 000 years: **(a)** Buraca Gloriosa Cave (Denniston et al., 2018) show speleothem growth phases, which require mobile water from frequent precipitation; **(b, c)** MD95-2039 pollen data (Roucoux et al., 2005) are divided into tree- and herb & grass pollen. While trees require more precipitation, grasses are dominant for more arid conditions; **(ed)** MD01-2443/4 marine cores $CaCO_3$ (Hodell et al., 2013) indicates more arid conditions with lower values, higher values account for more humid conditions; ~~**(f)** Aridity index for Portuguese margin as result from **(a-e)**, for detailed information see method section; **(g)** SST from marine cores MD01-2443/4 (Martrat et al., 2007) resembling HE and most GIs; **(h)** Dol/Cal ration from IODP 306-U1313 (Naafs et al., 2013) show detailed HE structure; **(i**~~**e)** Aridity index for Portuguese margin as result from **(a-d)**, for detailed information see method section; **(f)** $\delta^{18}O$ data from NGRIP ice core (North Greenland Ice Core Project Members et al., 2004) in comparison.

S6 Mediterranean Sea:

Southern Europe and the Mediterranean Sea region are known for hot and dry summers and mild and wet winters. The temperature average is about 18.9 °C and the total precipitation about 1000 mm/year with more precipitation in the western

regions than in the eastern (Deutscher Wetterdienst, 2018). The archives for this synthesis are spread around the eastern Mediterranean region. The westernmost archive is the Lago Grande di Monticchio, a maar lake in Basilicata, ~~Southern~~southern Italy. The ~~core comprises~~cores comprise climate information for the last 140 000 years (Allen et al., 1999; Brauer et al., 1999; Watts, 1985 and others) and ~~is varvecounted fully, in addition, it is complemented~~completely varve counted, supplemented by a ~~Tephra~~tephra chronology. The pollen from Monticchio show similar behaviour to the NGRIP indicating a closely coupled system between North Atlantic and the Mediterranean region (Allen et al., 1999; see Fig.~~-~~ S6). Speleothem growth occurs at several sites. Dim Cave in south western Turkey shows continuous speleothem growth from 12 000 yr b2k until 90 000 yr b2k with significant lower growth rates during glacial times (40 000 – 18 000 yr b2k, Ünal-İmer et al., 2015). A second speleothem from Soreq Cave in Israel shows continuous growth for the last 140 000 years. Two distinct isotopic events can be separated within the record within the last 60 000 years (Bar-Matthews et al., 1997, 2000). ~~In addition, a comparison with the marine core LC21 from eastern Mediterranean Sea can be performed. Close accordance between Soreq Cave and LC21 $\delta^{18}O$ was found by Grant et al. (2012). The dust record in M40/4_SL71 from SE Ionian Sea shows increased K/C ratio during arid conditions due to deflation of Kaolinite bearing dust, which was sedimented~~The dust record in M40/4_SL71 from SE Ionian Sea shows increased K/C ratio during arid conditions due to deflation of Kaolinite bearing dust, which was sedimented into basins during more humid conditions (Ehrmann et al., 2017). Kaolinite is a common mineral in North African dust and hence a useful dust tracer. During Heinrich events, the Mediterranean region was heavily arid and minor maxima of Kaolinite appear. The timespan from 60 000 to 55 000 yr b2k comprises GIs 17 to 15. Speleothem growth occurs in Dim and Soreq Cave and $\delta^{18}O$ values are on relative highs around 57 000 yr b2k for both caves. The growth rates in Dim cave are lower than in younger parts of the speleothem. The amount of tree pollen is at intermediate values of 50 % and so is the K/C ratio, which shows H6 recorded in the sediment core at about 60 000 yr b2k. Overall, the aridity was at intermediate values.

GIs 14 to 9 are within the time of 55 000 to 40 000 yr b2k. The Dim Cave speleothem growth rate rises around 50 000 yr b2k, the $\delta^{18}O$ values sink, suggesting wetter climate. In addition, $\delta^{18}O$ ~~are~~was on ~~a maximum values supporting~~peak value, which confirms the ~~fast growth~~rapid. In Soreq Cave~~ and LC21 are the~~, $\delta^{18}O$ values ~~higher~~where between 55 000 and 52 000 yr b2k ~~showing~~higher and show similar conditions ~~to present day~~as today (Grant et al., 2012). Furthermore, Monticchio tree pollen are on a maximum during GI14 and GI12 (interpreted as pollen Assemblage Zones 13 and 11, see Allen et al., 1999). The core shows GI like appearance for this timespan. The dust record exhibits intermediate values with some minor peaks during stadial phases and H5 event. H4 is not visible due to a tephra layer within the event (Ehrmann et al., 2017). The precipitation was high during this time span considering fast speleothem growth, large amounts of tree pollen and intermediate dust values. The aridity index shows humid conditions, especially during interstadial times for this phase.

Glacial conditions are clearly visible between 40 000 and 17 200 yr b2k, with GIs 8 to 1. Speleothem growth is continuous through all time, but slowest during glacial at Dim Cave (Ünal-İmer et al., 2015). Soreq cave speleothem growth also continued showing variability in $\delta^{18}O$ on small scale with some minor peaks during GI3 and 4~~ which is also visible in LC21.~~. The Monticchio pollen are low to medium on tree content during this time span with some variability. Higher tree pollen amount

is present during interstadials and herbaceous taxa & steppe pollen increase in stadial times (Brauer et al., 2007). The K/C ratio shows H3 to H1 and is apart from that at intermediate values. The glacial time has frequent precipitation minima during Heinrich events and increased precipitation in times of interstadials. The aridity index remains on intermediate values during this time but showing climate ameliorations during interstadials.

Within the time span from 17 200 to 10 000 yr b2k are GI1 and the YD as well as the transition towards the Holocene. Speleothem growth at Dim and Soreq cave was fast and the $\delta^{18}O$ values increase in both speleothems ~~and the sediment core LC21.~~. Tree pollen ~~drastically~~rapidly increase from glacial values of about 30 % to nearly 90 % after Bølling / Allerød. The YD is clearly visible in the SL71 dust record with increased K/C ratio. The aridity index increases strongly towards humid conditions during the early Holocene.

During the Holocene (10 000 yr b2k to present) most of the records ~~stay~~remain constant. Dim Cave speleothem did not grow anymore but $\delta^{18}O$ values from Soreq cave ~~and LC21~~ show consistent values with a variation between 8 500 and 7 000 yr b2k, where low $\delta^{18}O$ values indicate doubled precipitation and present day temperatures (Bar-Matthews et al., 1997). The amount of tree pollen stays constantly high with a small decrease to 75 % at about 2 000 yr b2k. The largest variation can be seen in the dust content, where the dust deflation reaches maximum values after the early Holocene optimum (EHTO). The large dust deflation, mainly originating from Sahara (Ehrmann et al., 2017), is consistent with the northward extension of the Saharan desert in modern times compared to early Holocene conditions (Jolly et al., 1998). The precipitation and temperature for the Mediterranean region within the Holocene was nearly at present day conditions while the African continent underwent a huge change.

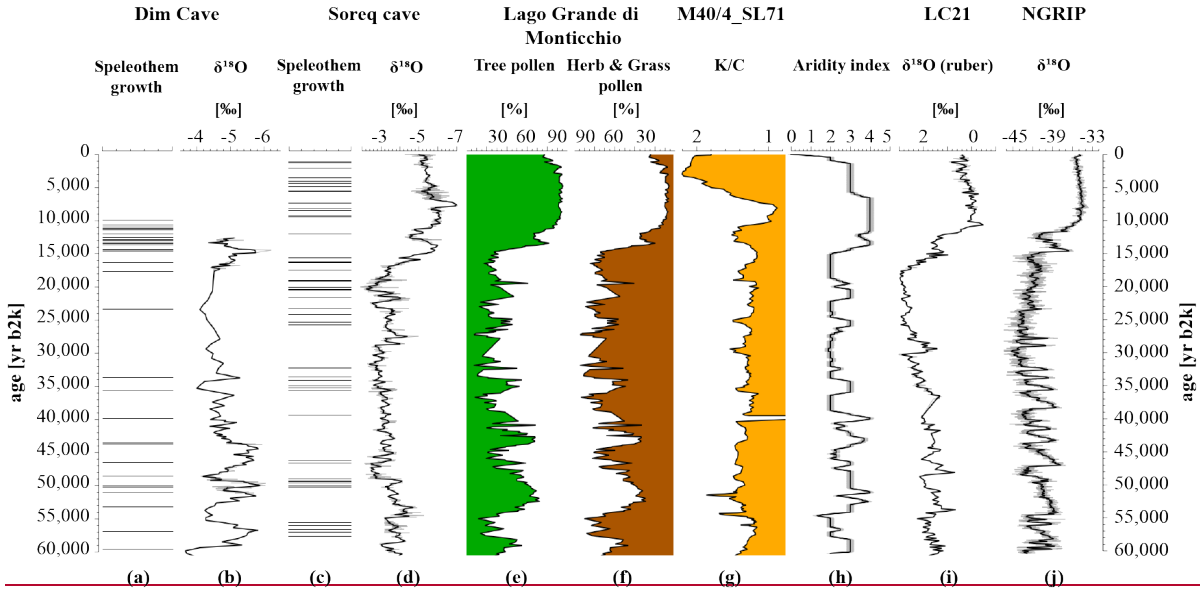

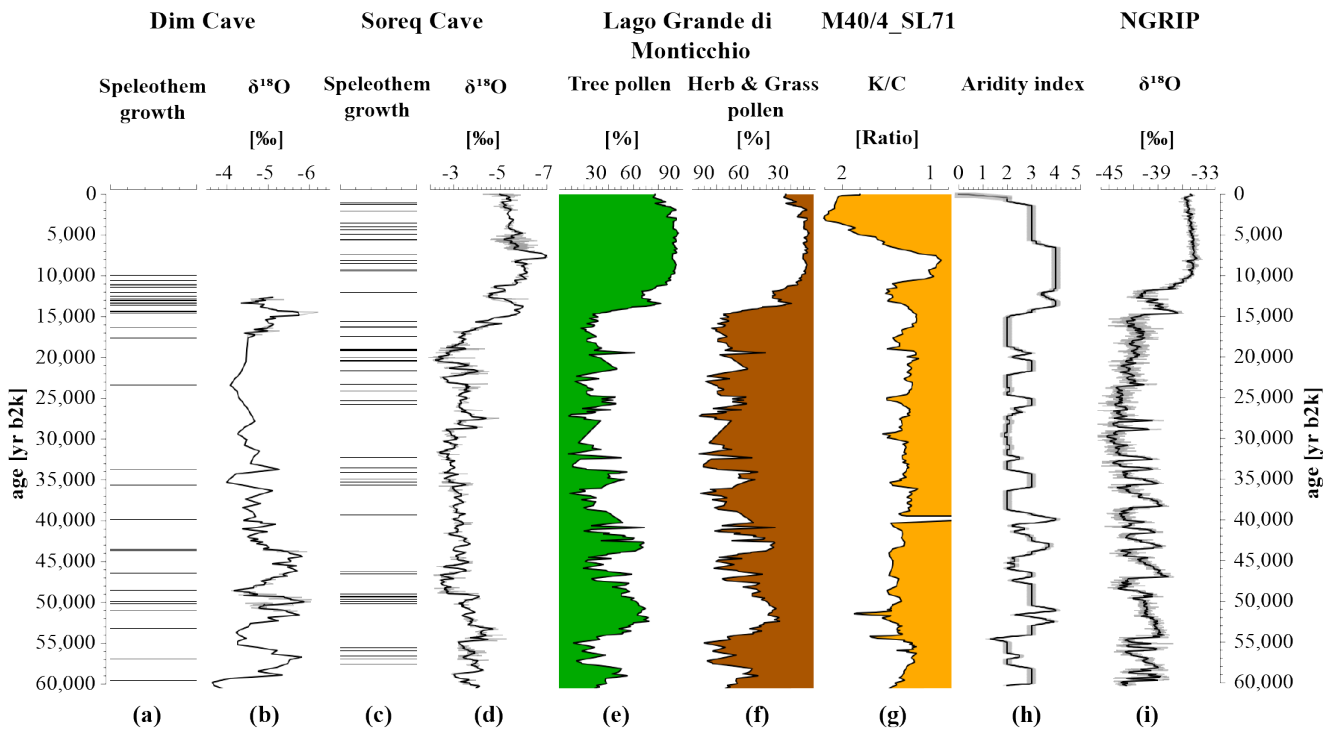

Figure S6: Mediterranean Sea climate over the last 60 000 years: Dim Cave (Ünal-İmer et al., 2015) **(a, b)** and Soreq Cave (Bar-Matthews et al., 2000; Grant et al., 2012) **(c, d)** show speleothem growth phases, which require mobile water from frequent precipitation; **(b, d)** $\delta^{18}O$ data with few apparent GIs comparable to **(j)**, more negative $\delta^{18}O$ values account for more humid conditions; **(e, f)** Lago Grande di Monticchio pollen data (Brauer et al., 2007) are divided into tree- and herb & grass pollen. While trees require more precipitation, grasses are dominant for more arid conditions; **(g)** Dust reconstruction from M40/4_SL71 marine core K/C ratio (Ehrmann et al., 2017) indicates more arid conditions with higher values, lower values account for more humid conditions; **(h)** Aridity index for Mediterranean Sea region as ~~result from **(a, c, e, f).** For detailed information see method section; **(i)** $\delta^{18}O$ data from marine core LC21 (Grant et al., 2012) in comparison to speleothem and NGRIP $\delta^{18}O$ data **(b, d, j); (j**~~reconstructed from **(a, c, e, g).** For detailed information see method section; **(i)** $\delta^{18}O$ data from NGRIP ice core (North Greenland Ice Core Project Members et al., 2004) in comparison.

S7 ~~Cariaco basin:~~

~~The Cariaco basin is located off the north central coast of Venezuela, directly south of the "Tortuga" island forming the Gulf of Cariaco. The basin is separated from the Caribbean Sea by a series of shallow sills. Below ~275 m water depth, anoxic conditions occur and lead to excellent preservation conditions (Gibson and Peterson, 2014). The sediment cores from the Cariaco basin are well known for their laminated sediments with darker layers from warmer interstadials in contrast to light colored, bioturbated sediments from stadials indicating deep water oxygenation (Deplazes et al., 2013; Hughen et al., 2004; Peterson et al., 2000). The lightness (L*) values as well as the molybdenum (Mo) content show good accordance with the NGRIP $\delta^{18}O$, all GIs are visible in the comparison (see Fig. S7). The cores which are used for that comparison are MD03-2661, MD03-2662 and the ODP 165-1002 site which were drilled close to each other and correlated in previous studies~~

(Deplazes et al., 2013; Gibson and Peterson, 2014; Peterson et al., 2000). The pollen were investigated for the timespan from 30 000 to 60 000 years b2k in core MD03-2622 by González and Dupont (2009). Speleothem growth at the Bahamas occurred between 24 000 and 44 000 yr b2k in the Sagittarius Blue Hole as well as between 9 800 and 15 000 yr b2k (Hoffmann et al., 2010). The speleothems were collected at a depth of 15 m below present sea level, a growth continuing during Holocene is impossible due to the rising sea level. Dust from the Sahara region is blown out during all times over the Atlantic and can be found in the Cariaco basin as well. Al/Ti ratios in the bulk sediment are higher during interglacials due to fluvial input (values of 27 represent pure fluvial input) and lower during stadials because of Saharan dust input (values of 14 represent pure Saharan dust input, Yarincik et al., 2000).

The Cariaco basin region is known for its high-resolution time series throughout the last glacial cycle. For the last 60 000 years, there are several variations within the archives. In the Reflectance and Mo data, all GIs are visible, except GI2. This indicates a closely coupled system of the Cariaco basin to the North Atlantic rapid climate changes. The dust values from Al/Ti ratio are in general at intermediate values, lower ratio representing higher Saharan dust contents during Heinrich events. The pollen record show tree pollen contents between 10 % and 50 %. Decreases in tree pollen contents during Heinrich events are related to an increase in salt marsh pollen (see Fig. S7: H5, 48 000 yr b2k). Extremely dry atmospheric conditions for the coastland of Cariaco basin combined with warm temperatures during Heinrich events and stadial times lead to hypersalinity and a drastic change in vegetation (González and Dupont, 2009). The aridity index stays at intermediate values during this time phase with inclines towards higher aridity during (Heinrich-) stadials. The speleothem growth started at 44 000 yr b2k during a phase of enhanced tree pollen content and relatively lower dust values indicating a general increase in precipitation. This increase followed shortly after GI 12, which is visible in the MD03-2622 core in the Mo content as well as in the Reflectance data of Core MD03-2621. Al/Ti ratio shows higher dust amount between 30 000 and 16 000 yr b2k with some variations, but still indicating less precipitation. The Sagittarius Blue Hole speleothem did not grow from 24 000 to 14 500 yr b2k (LGM), the same time as the highest dust values appear within the record. This suggests a relatively arid phase during LGM for the Cariaco region which is also visible within the aridity index. Precipitation seems to increase again together with higher temperatures between 14 500 and 9 300 yr b2k where speleothem growth occurs in the Sagittarius Blue Hole. The growth ends with rising sea level during Holocene. The Al/Ti ratio increases during Holocene towards more fluvial composition indicating more river discharge because of a higher precipitation. The aridity index rises with the onset of Bølling / Allerød but insufficient amount of data prevents an appropriate analysis during the Holocene.

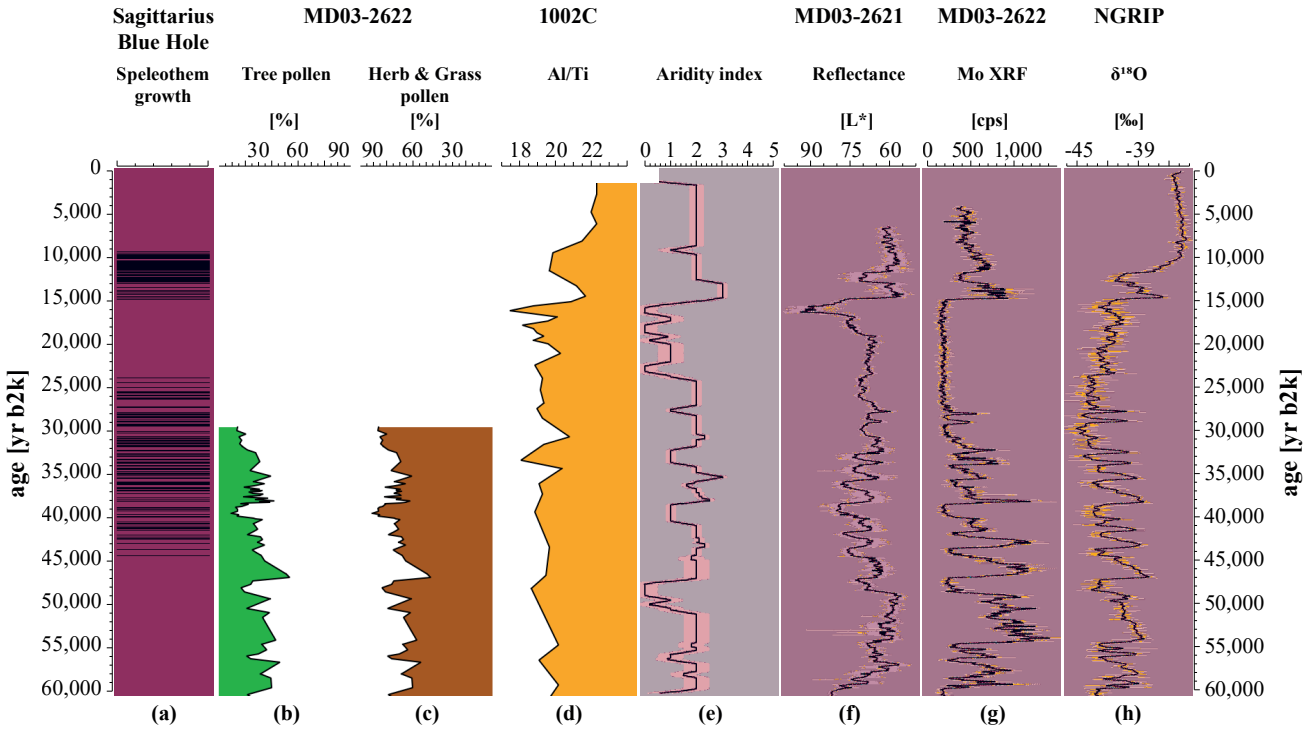

Figure S7: Cariaco Basin climate over the last 60 000 years: **(a)** Sagittarius Blue Hole (Hoffmann et al., 2010) show speleothem growth phases, which require mobile water from frequent precipitation; **(b, c)** MD03-2622 pollen data (González and Dupont, 2009) are divided into tree- and herb & grass pollen. While trees require more precipitation, grasses are dominant for more arid conditions; **(d)** Dust reconstruction from ODP-165-1002C marine core Al/Ti ratio (Yarincik et al., 2000) indicates more arid conditions with lower ratios, higher ratios account for more humid conditions; **(e)** Aridity index for Cariaco Basin region as result from **(a-d).** For detailed information see method section; **(f)** Reflectance data from marine core MD03-2621 (Deplazes et al., 2013) resembling GIs, lower L* values account for wetter and warmer climate; **(g)** Molybdenum data from marine core MD03-2622 higher counts show GIs (Gibson and Peterson, 2014); **(h)** $\delta^{18}O$ data from NGRIP ice core (North Greenland Ice Core Project Members et al., 2004) in comparison.

S8 Santa Barbara basin:

The region of the Santa Barbara basin is well known for its brief interstadial events of the past 60 000 years. The basin is located at the inner continental border of Southern California with a depth of about 600 m and contains oxygen-depleted water below 475 m (Behl, 1995; Behl and Kennett, 1996; Heusser, 1998). Due to this depletion zone, an excellent preservation of sediment material, pollen and warves occurs within the ODP-893A. In the benthic foraminifer record of ODP-893A (Cannariato et al., 1999) all GIs are visible as in the $\delta^{18}O$ record of the NGRIP ice core. About 800 km east of the Santa Barbara basin the "Cave of the Bells" speleothem in Arizona is located (Wagner et al., 2010). Aridity in the southwestern USA and climate information stored in the NGRIP show a similar pattern of fast interstadial / stadial changes. Cooler temperatures in high latitudes are connected to increased moisture in this region. Hence, higher $\delta^{18}O$ values were interpreted as warmer

temperatures corresponding to drier winters (Wagner et al., 2010). Also, a speleothem of the "Fort Stanton Cave" in New Mexico can help to understand variabilities within the region and shows the GIs 1-12 (Asmerom et al., 2010). No larger dust deflation is known for that region, hence no paleodust record can be used within the synthesis. The climate today is as in Mediterranean regions with temperatures between 9.9 °C and 18,6 °C and a precipitation of about 600 mm/year (NOAA-NCDC weather service, 2018).

Between 60 000 and 48 000 years b2k (early MIS3, GIs 17-13) a high amount of tree pollen of about 80 % indicates high temperatures and at least moderate precipitation (see Fig. ~~S8~~S7). The benthic foraminifers show high abundances, which is interpreted as an interstadial signal (Cannariato et al., 1999). Bells Cave speleothems show growth starting at about 54 000 years b2k. The $\delta^{18}O$ values of -9 ‰ indicate warm temperatures and moderate precipitation. Similarly, the Fort Stanton speleothem also shows high $\delta^{18}O$ values up to -5.5 ‰ during early MIS3 period. This time was characterized by warm temperatures and intermediate precipitation.

The timespan from 48 000 to 27 540 yr b2k comprises the GIs 12 to 3. All of them are visible in the foraminifer content as well as in the Fort Stanton speleothem. The Cave of the Bells speleothem comprises a hiatus between 24 000 and 29 000 yr b2k so that GI2 to 4 are missing within that record. The precipitation and temperature vary from interstadials to stadials, but the amount of tree pollen stays relatively constant at around 80 %. That indicates, the range of temperature and precipitation change did not pass a threshold on which an abrupt vegetational change would have occurred and temperatures and precipitation stayed close to early MIS3 conditions in respect to the stadial / interstadial changes.

From 27 540 to 14 700 yr b2k (onset of the Bølling / Allerød) the time is characterized by a drop of the Dysoxic benthic foraminifer content to low values between 0 and 15 % in contrast to the continuous high amount of tree pollen before. The Bells Cave speleothem's hiatus continues until 24 000 yr b2k and growth started again with the onset of GI-2 (23 340 yr b2k), also visible in the foraminifer content. Speleothem growth at the Fort Stanton speleothem was continuous during this time span. The combination of all proxies shows cooler temperatures and increased moisture for the Santa Barbara basin during this period.

The Holocene part from the onset of Bølling / Allerød (B/A, 14 700 yr b2k) until present shows the YD in all records~~.~~, but the records end around 10 000 yr b2k. Both speleothems show lower $\delta^{18}O$ values as well as ODP-893A low dysoxic foraminifer contents. The vegetational record shows a decrease in tree pollen and a corresponding increase in grass pollen. Most recently, the speleothems and the ODP-893A foraminifer records show the start of the Holocene at 11 700 yr b2k by increased values indicating warmer climate. The precipitation increases drastically with sinking tree pollen amount (Heusser, 1998) towards the Holocene.

Due to a lack of a dust record, continuous speleothem growth and insignificant changes in the amount of tree pollen, the aridity index for this region is inconclusive and constantly at intermediate values. Therefore, the Aridity index calculation for this region ends around 10 000 yr b2k.

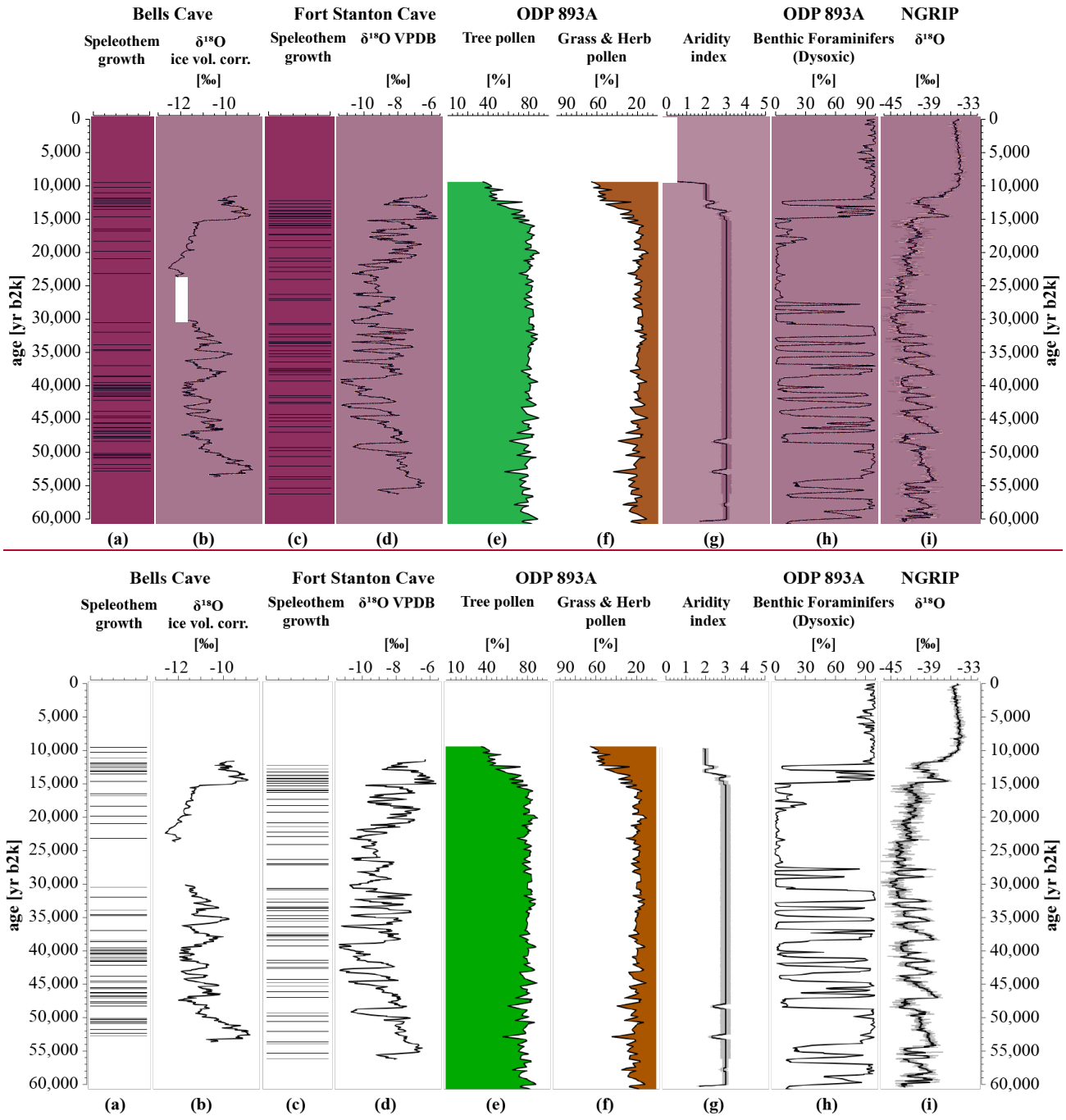

Figure ~~S8:~~S7: Santa Barbara Basin climate over the last 60 000 years: Bells Cave (Wagner et al., 2010) **(a, b)** and Fort Stanton (Asmerom et al., 2010) **(c, d)** show speleothem growth phases, which require mobile water from frequent precipitation; **(b, d)** $\delta^{18}O$ data with few apparent GIs comparable to **(h)** and **(j)**, more positive $\delta^{18}O$ values account for increased precipitation; **(e, f)** ODP893A marine core pollen data (Heusser, 1998) are divided into tree- and herb & grass pollen. While trees require more precipitation, grasses are dominant for more arid conditions; **(g)** Aridity index for St. Barbara Basin region as result from **(a, c, e).** For detailed information see method section; **(h)** Dysoxic Benthic Foraminifer data from marine core ODP893A (Cannariato et al., 1999) with distinguishable GIs in comparison to

speleothem and NGRIP $\delta^{18}O$ data **(b, d, ~~j~~), (~~j~~i)**; **(i)** $\delta^{18}O$ data from NGRIP ice core (North Greenland Ice Core Project Members et al., 2004) in comparison.

~~S9 Australia – Oceania:~~

~~Long, continuous and high resolution paleoclimate archives from southern hemisphere are scarce beside ice cores from Antarctica, so the processes behind climate observation and climate changes on SH are hard to distinguish. One of the important parts of the global climate system are the southern hemisphere westerlies. Together with the Antarctic circumpolar current, both processes regulate meridional heat flux and transport global climatic signals (Toggweiler et al., 2006). Present days mean annual precipitation is similar for the sites. About 2 500 mm/yr is typical for the speleothem sites in New Zealand as well as for the paleovegetation record in Australia, the mean annual temperature varies around 13 °C. This region is strongly imprinted by the southern westerlies, the Hollywood Cave in the north of the Southern New Zealand island is directly affected as the cave is below the flow current. These speleothems are the closest, long term and well dated ones to the Lynch Crater pollen profile. The speleothem HW3 shows continuous growth for the last 73 000 years (see Fig. S9). More negative isotopic values indicate wetter climate as well as stronger westerlies, accounting for North Atlantic cooling. This speleothem resembles Greenland Ice Core Isotopic profiles and Heinrich events although it is antipodean to Greenland and North Atlantic (Whittaker et al., 2011). Lynch Crater pollen profiles are known for their continuous records. The Crater is caused by a volcanic explosion and is filled with lake and swamp deposits. Inlets from surrounding springs feed the lake, which receives most rainfall between December and April nowadays. Only few dust archives are established for the Australia – Oceania region, high resolution records are missing entirely. The E26.1 marine sediment core from 'Lord Howard Rise' lies in the Tasmanian Sea between the pollen and speleothem record and comprises the dust history of the last 350 000 years, sadly on low resolution of about 5 000 years but with significantly higher dust rates during glacial times (Fitzsimmons et al., 2013; Hesse, 1994; Hesse and McTainsh, 2003).~~

~~The timespan from 60 000 to 52 000 yr b2k (GIs 17 to 14) is marked by very high amounts of tree pollen. According to Kershaw (1976), subtropical rainforest surrounded the Lynch Crater. This would support the lower $\delta^{18}O$ values of Hollywood Cave speleothem accounting for wetter climate conditions (Whittaker et al., 2011). Speleothem growth is apparent throughout the last 60 000 years with continuous growth but different growth rates, which were relatively high during this period. Dust record from E26.1 is relatively low but indicating an increase towards the end of that period. The aridity was low during this time, as indicated by high amounts of tree pollen, high speleothem growth rates and lower dust values.~~

~~From 52 000 to 39 000 yr b2k (GIs 13–9) the climate was fluctuating. While the speleothem growth rates were high at the beginning and the end of that period, the time between 44 000 and 48 000 yr b2k shows the lowest growth rates of the record. The amount of tree pollen decreases to about 40 % in average, also with major variations. The isotope values of the speleothem remain low, accounting for wetter conditions with a clearly visible H5 and 4 events around 48 000 and 30 000 yr b2k with lowest isotope values through that time (Whittaker et al., 2011). A dust peak comes along with a low tree pollen zone around~~

~~50 000 yr b2k and a decrease in dust afterwards according to H5 times with more precipitation related to less dust transport. The aridity index for this time shows variable, humid conditions and resemble the climate amelioration of southern hemisphere during H5 as well as the following intermediate conditions.~~

~~Between 39 000 and 29 000 yr b2k (GIs 8 – 5), climate getting unstable also visible in intermediate aridity. Although the speleothem continuously grows, the isotopes indicate drier conditions than before, beside an increase during H3 (~ 30 000 yr b2k) accounting for wetter conditions towards the end. The amount of tree pollen decreases to values around 20 % according for minimum of that time. The vegetation changed to sclerophylls, which needs less precipitation compared to rainforest vegetation before (Kershaw, 1976). Dust stays on intermediate values through that time. An increase in tree pollen going along with a decrease in isotopes $\delta^{18}O$ and $\delta^{13}C$ in Hollywood Cave mark the begin of the next time phase (LGM from 29 000 to 16 000 yr b2k, GIs 4 – 2 within) with climate amelioration for parts of this region. A drastic increase in tree pollen to about 55 %, increased speleothem growth and lower isotopes indicate higher precipitation and warmer climate, contrarily the dust content also increases during LGM, indicating arid conditions for Central Australia dust deflation regions with increased dune activity (Fitzsimmons et al., 2013). The dust peak in Tasmanian Sea is synchronous to the EDML dust maximum from Antarctica (Wegner et al., 2015). The aridity index displays variable precipitations at low to intermediate conditions at average. After LGM ends (16 000 yr b2k to present, GI1) the onset towards the Holocene took place. Younger Dryas (NH cold event) is clearly visible as a tree pollen spike within the otherwise intermediate values (around 30 %). Speleothem growth rates were high until 10 000 yr b2k, no further isotope data are publically available for this speleothem. Dust values decrease throughout the whole period, also showing the YD as warm / wet event, supporting the idea of a YD warm event for southern hemisphere (Carlson, 2013; Shakun and Carlson, 2010). Varying tree pollen amounts are apparent for the rest of the Holocene, dust decreases further and speleothems grow, indicating humid conditions until 5 000 yr b2k and a drastic decrease in climate conditions afterwards.~~

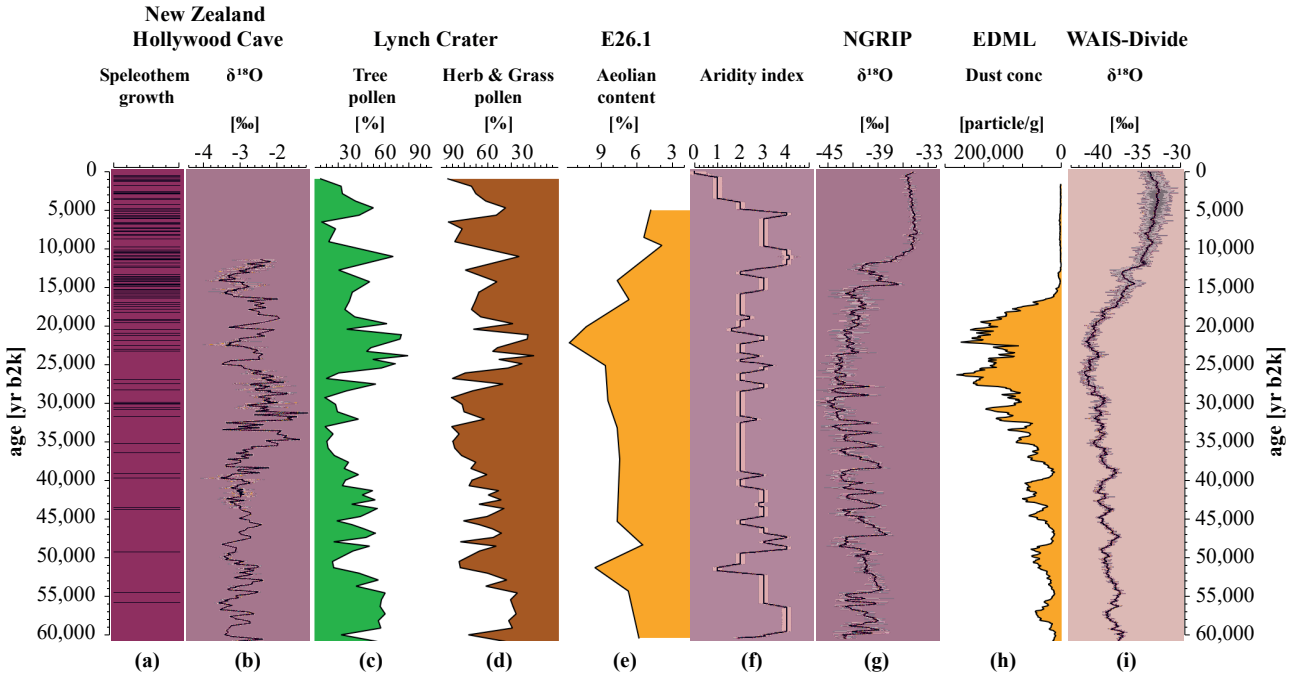

Figure S9: Australia – Oceania climate over the last 60 000 years: **(a)** Hollywood Cave New Zealand (Hellstrom et al., 1998; Whittaker et al., 2011; Williams, 1996; Williams et al., 2005) shows speleothem growth phases, which require mobile water from frequent precipitation; **(b)** $\delta^{18}O$ data with few apparent GIs comparable to **(g)**, more positive $\delta^{18}O$ values account for increased precipitation (Whittaker et al., 2011); **(c, d)** Lynch Crater pollen data from NE Australia (Kershaw, 1994) are divided into tree- and herb & grass pollen. While trees require more precipitation, grasses are dominant for more arid conditions; **(e)** Aeolian content from E26.1 marine core (Hesse, 1994) indicates more arid conditions with higher values, lower values account for more humid conditions; **(f)** Aridity index for Australia – Oceania region as result from **(a, c–e).** For detailed information see method section; **(g)** $\delta^{18}O$ data from NGRIP ice core (North Greenland Ice Core Project Members et al., 2004) in comparison. **(h)** Dust concentration from EDML (Wegner et al., 2015), higher particle concentrations indicate more arid conditions and vice versa; **(i)** $\delta^{18}O$ data from WAIS-Divide ice core (WAIS-Divide Project Members et al., 2015) in comparison to speleothem and NGRIP $\delta^{18}O$ data **(b, g)**.

~~S 10 Global tree pollen pattern~~

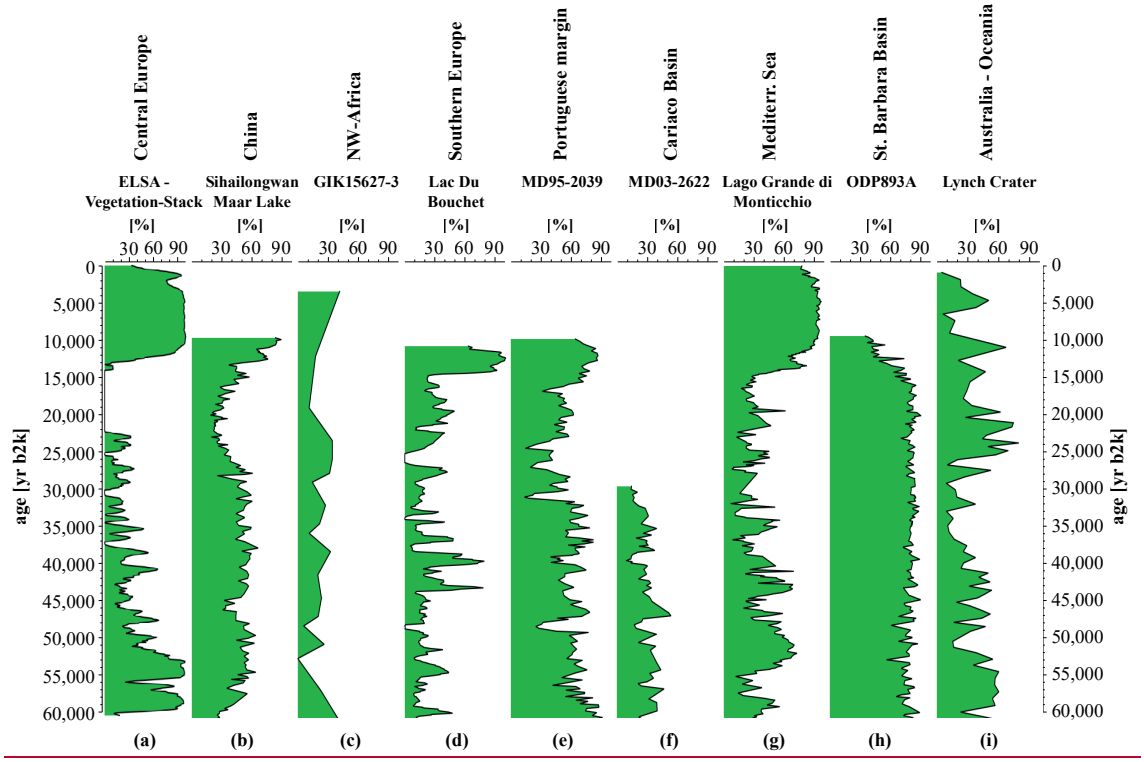

~~Figure S10:~~S 8 Global tree pollen pattern

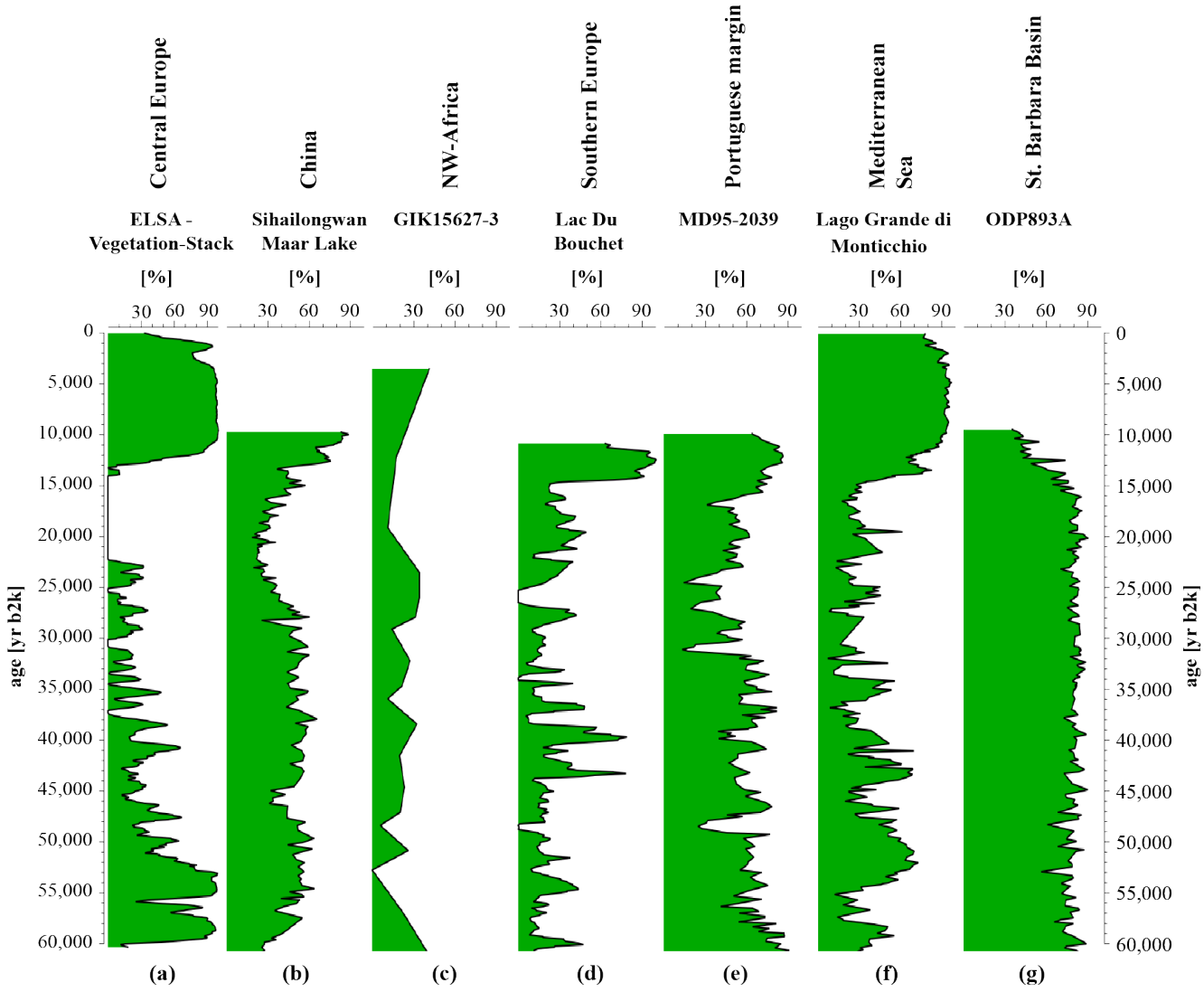

Figure S87: Global tree pollen records for the last 60 000 years. Higher amounts of tree pollen indicate increased humidity. **(a)** Central European ELSA-Vegetation-Stack ~~(Sirocko et al., 2016)~~(Sirocko et al., 2016); **(b)** Chinese Sihailongwan Maar Lake (Mingram et al., 2018); **(c)** North-West Africa marine core GIK15627-3 (Hooghiemstra et al., 1992); **(d)** Southern Europe Lac Du Bouchet (Reille and de Beaulieu, 1990); **(e)** Portuguese margin marine core MD95-2039 (Roucoux et al., 2005); **(f)** ~~Cariaco Basin marine core MD03-2622 (González and Dupont, 2009); (g)~~ Lago Grande di Monticchio for Mediterranean Sea region (Brauer et al., 2007); **(~~h~~g)** St. Barbara Basin marine core ODP893A (Heusser, 1998)~~; (i) Australian - Oceania Lynch Crater (Kershaw, 1994).~~

Figure ~~S10~~S8 shows all tree pollen of this synthesis. Only ~~four~~three regions worldwide ~~encompas~~encompass sediment cores with pollen data for the whole last 60 000 years. The ELSA-Vegetation-Stack for Central Europe ~~(Sirocko et al., 2016)~~(Sirocko et al., 2016) consists of the sediment cores from Holzmaar and Dehner Maar, which cover the last 60 000 years in total. The Mediterranean record from 'Lago Grande di Monticchio'~~, 'Lynch Crater' (Australia – Oceania)~~ also ~~cover~~covers this time as

well as pollen from the Sihailongwan Maar Lake (China). However, Sihailongwan Maar Lake pollen profiles of Mingram (Mingram et al., 2018) and Stebich (Stebich et al., 2015) diverge for Holocene and need to be adjusted. Pollen records for the Arabian Sea region are not available. The pollen assemblage of St. Barbara Basin is on very high values throughout the whole record due to sedimentation pattern in the marine basin as regional effects (Heusser, 1995, 1998).

Early MIS3 phase shows tree pollen maxima for the following regions: Central Europe, China, Portuguese margin~~, Mediterranean Sea, and Oceania. Although, the timings of the pollen maxima are not synchronous, enhanced precipitation and humidity for early MIS3 can be stated for these regions. The tree pollen show impairing climate conditions during late MIS3 towards LGM conditions. A well expressed LGM is visible in the pollen archives of Central Europe, China, Southern Europe, Portuguese margin and the Mediterranean Sea while the Oceania records shows increased tree pollen. This northern / southern hemisphere atmospheric teleconnection currently described by e.g. Shakun and Carlson (2010) and initially described by Sirocko et al. (1996b). Apart from Oceania, the LGM was mainly arid for all regions. The following transition towards the Holocene with the onset of Bølling / Allerød (14 700 yr b2k) is visible in all pollen records by massive changes in the tree pollen content. St. Barbara Basin and Oceania show decreasing pollen values (see S8 & S9).~~ and Mediterranean Sea. Although, the timings of the pollen maxima are not synchronous, enhanced precipitation and humidity for early MIS3 can be stated for these regions. The tree pollen show impairing climate conditions during late MIS3 towards LGM conditions. A well expressed LGM is visible in the pollen archives of Central Europe, China, Southern Europe, Portuguese margin and the Mediterranean. The LGM was mainly arid for all regions. The following transition towards the Holocene with the onset of Bølling / Allerød (14 700 yr b2k) is visible in all pollen records by massive changes in the tree pollen content. St. Barbara Basin shows decreasing pollen values (see S7). All other regions show increasing tree pollen amounts indicating more humid conditions and climate amelioration for the early Holocene.

~~S11~~S9 Stratigraphies and age / depths relations

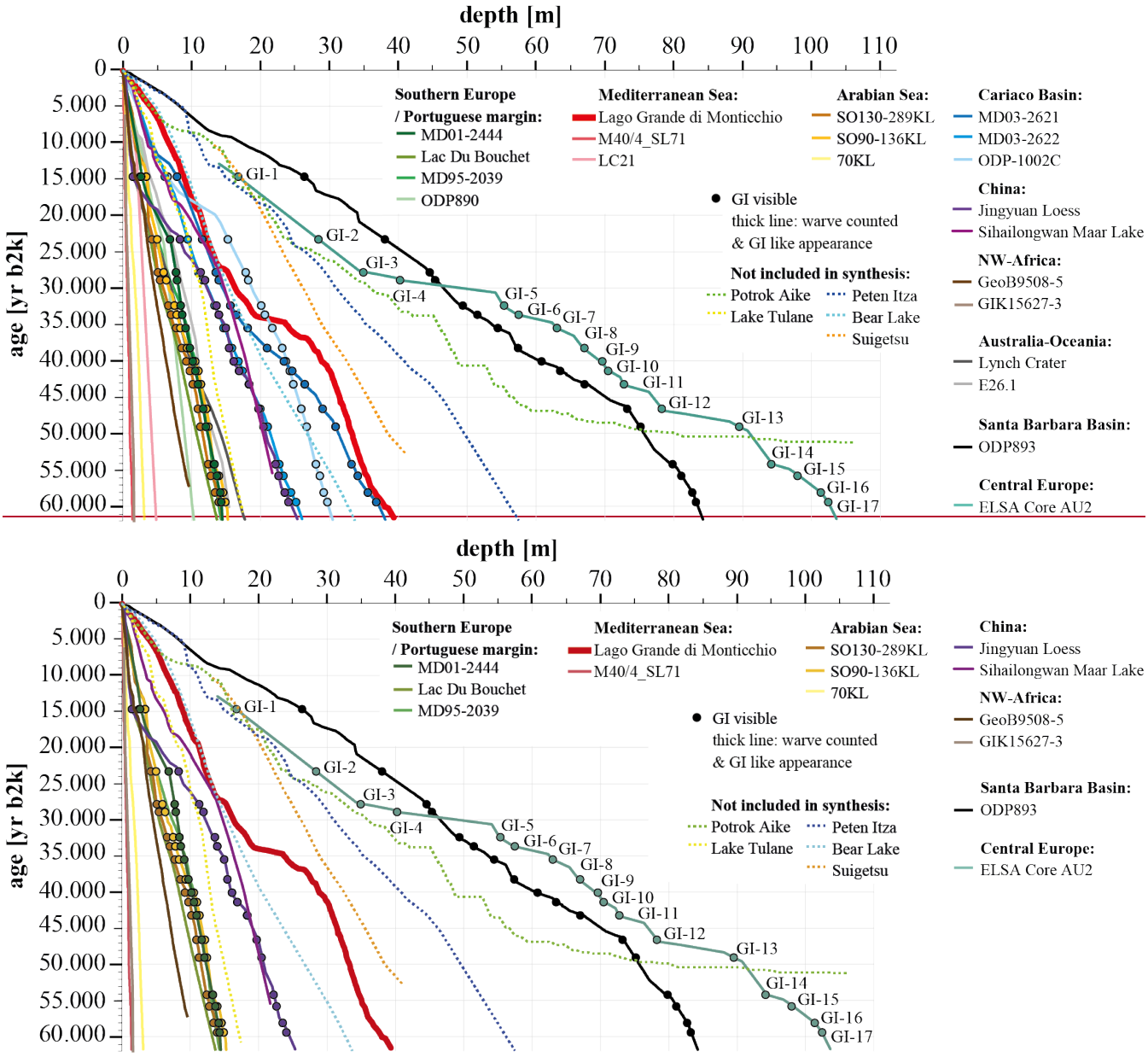

Figure ~~S11:~~S9: Global age / depths relations of various sediment cores. Solid lines show cores used for this synthesis. Thick red line shows Lago Grande di Monticchio, which is warve counted and shows GI like appearance. Points show apparent GIs. Dotted lines give other well-known high resolution records not included in this synthesis. For references of included cores see chapter 2 and S1-~~S9~~S7; Potrok Aike, Southern Patagonia, Argentina (Kliem et al., 2013); Lake Tulane, Florida, USA (Grimm et al., 2006); Petén-Itzá, Guatemala (Correa-Metrio et al., 2012); Bear Lake, Utah-Idaho, USA (Jiménez-Moreno et al., 2007); Lake Suigetsu, Japan (Bronk Ramsey et al., 2012).

Stratigraphical uncertainties are the major sources of error for this synthesis. All stratigraphies of original publications remained unchanged, apart from referring all records to years b2k (before the year 2000 CE). Different dating methods in

general have various uncertainties. Archives of this synthesis were dated by ^{14}C ages, optically stimulated luminescence (OSL), U/Th dating of speleothems, ~~warve~~varve counting~~ or by~~, tuning to NGRIP or marine isotope stack~~.~~, paleomagnetismus correlation, tephra chronology or cross correlating (see Tab. S1). Age uncertainties of speleothem U/Th dating range between 1 and 4 %, resulting in the most reliable ages for speleothems. ^{14}C calibrations were greatly improved and e.g. Hughen et al. (2006) has calibrated the ^{14}C curves with the absolutely dated Hulu speleothems. Nevertheless, ^{14}C ages of this synthesis bear maximum errors up to 12 % - or up to 7 000 years. Error values of OSL dating range up to 10 % or about 5 000 years for the last 60 000 years. Warve counting errors depend strongly on the sedimentation rate of the archive, but error values can stack up to 5 000 years as well. For NGRIP tuning, age uncertainties of the ice core are minimized by several dating approaches and stack up to 2 500 years for the last 60 000 years. To sum it up, no definitive ages for the previously described turning point can be determined from this work. Nevertheless, synchronous patterns occurred during climate history and the estimated ages give a good evaluation of the turning points of the precipitation.

The sampling resolution of the records is also extremely important. More samples and analyses result in a much more detailed explanations and interpretations for the records. High frequency sampling, especially in sediment cores is mainly depending on the sedimentation rate. Figure ~~S11~~S9 shows all sediment archives and records of this work with the age-depths relation. The thick, red line accounts for the warve-counted Lago Grande di Monticchio core. Points indicate GI appearance in the marine records of Santa Barbara Basin (ODP893), ~~Cariaco Basin (ODP-165-1002),~~ Chinese Loess (Jingyuan Loess sequence), Arabian Sea (SO-136KL) and Portuguese margin (MD01-2444) and Lake sediments of Central Europe (ELSA-Dust-Stack). The highest sedimentation rates during the last 60 000 years can be found in Santa Barbara Basin and ELSA-AU2 core with about 1-2 mm/year.

Several other high resolution records with extend into MIS3 (Fig. ~~S11~~S9, dotted lines) are published but not used for this synthesis. They are additionally shown for comparison and completeness. These cores were too far away from the chosen ten key regions to fit into a proper synthesis or do not extend until the begin of MIS3 (60 000 yr b2k). However, these cores are good climate archives with striking sedimentation rates of 0.26 mm/yr (Lake Tulane), 0.5 mm/yr (Bear Lake), 0.75 mm/yr (Lake Suigetsu) up to Petén-Itzá (~1 mm/yr) and Potrok Aike (~1.6 mm/yr) and should be mentioned within this synthesis.

Region	Archive	Proxy type	Location	Time covered [ka b2k]	Dating method	Reference
Central Europe	Speleothem	Speleothem	Bunker Cave	0 - 52	1, 2	Fohlmeister et al., 2012, 2013; Weber et al., 2018
	Speleothem	Speleothem	Spannagel Cave	0 - 275	1	Holzkämper et al. 2005; Spötl & Mangini, 2002, 2012
	Lake Sediment core	Pollen	Dehner Maar & Holzmaar	0 - 63	2, 3, 4, 5	Sirocko et al., 2016
	Lake Sediment core	Dust	Dehner Maar	0 - 130	2, 6, 5	Seelos et al., 2009
Arabian Sea	Speleothem	Speleothem	Socotra Cave	2 - 5; 40 - 54	1	Fleitmann et al., 2007 and refs. within; Burns et al., 2003
	Speleothem	Speleothem	Oman Caves	0 - 11	1	Fleitmann et al., 2007 and refs. within
	Marine Sediment core	Dust	Western Arabian Sea	0 - 135	2, 4, 7	Leuschner & Sirocko, 2003
	Marine Sediment core	TOC	Western Arabian Sea	0 - 65	2, 4, 8	Schulz et al., 1998
	Marine Sediment core	Reflectance	Western Arabian Sea	0 - 80	2, 5	Deplazes et al., 2014
NW-Africa	Speleothem	Speleothem	Susah Cave	30 - 66	1	Hoffmann et al., 2016
	Speleothem	Speleothem	Grotte Prison de Chien	3 - 97	1	Wassenburg et al., 2012
	Marine Sediment core	Pollen	West off Morocco	6 - 250	2, 8	Hooghiemstra et al., 1992
	Marine Sediment core	Dust	West off Senegal	0 - 57	2, 8	Collins et al., 2013 and refs. within
	Marine Sediment core	SST	West off Portugal	0 - 110	2, 8	Bard, 2002
China	Speleothem	Speleothem	Hulu Cave	11 - 75	1, 8	Wang et al., 2001; Liu et al., 2010
	Lake Sediment core	Pollen	Sihailongwan Maar Lake	0 - 65	2, 3, 4	Mingram et al., 2018
	Lake Sediment core	Pollen	Sihailongwan Maar Lake	0 - 12	2	Stebich et al., 2015
	Loess profile	Dust	Jingyuan Loess	0 - 80	5, 6, 9	Sun et al., 2010
Southern Europe	Speleothem	Speleothem	Villars Cave	32 - 83	1	Genty et al., 2003
	Speleothem	Speleothem	Villars Cave	5 - 15	1	Genty et al., 2006
	Speleothem	Speleothem	Villars Cave	28 - 51	1	Wainer et al., 2009
	Lake Sediment core	Pollen	Lac Du Bouchet	15 - 68	2, 10	Reille & Beaulieu, 1989;
	Marine Sediment core	Dust	MD01-2443/4	0 - 420	2, 5, 7, 8, 9	Hodell et al., 2013, Barker et al., 2011
	Marine Sediment core	IRD	IODP-306-U1313	0 - 70	2, 5, 9	Naafs et al., 2013
Portuguese margin	Speleothem	Speleothem	Villars Cave	32 - 83	1	Genty et al., 2003
	Speleothem	Speleothem	Villars Cave	5 - 15	1	Genty et al., 2006
	Speleothem	Speleothem	Villars Cave	28 - 51	1	Wainer et al., 2009
	Marine Sediment core	Pollen	MD95-2039	10 - 65	2, 5, 9	Roucoux et al., 2005
	Marine Sediment core	Dust	MD01-2443/4	0 - 420	2, 5, 7, 8, 9	Hodell et al., 2013, Barker et al., 2011
	Marine Sediment core	IRD	IODP-306-U1313	0 - 70	2, 5, 9	Naafs et al., 2013
Mediterranean Sea	Speleothem	Speleothem	Dim Cave	5 - 85	1	Ünal-Imer et al., 2015
	Speleothem	Speleothem	Soreq Cave	0 - 150	1	Grant et al., 2012
	Speleothem	Speleothem	Soreq Cave	0 - 140	1	Bar-Matthews et al., 2000
	Lake Sediment core	Pollen	Lago Grande di Monticchio	0 - 130	2, 3, 9	Brauer et al., 2007
	Marine Sediment core	Dust	MD40/4_SL71	0 - 180	2, 4, 8	Ehrmann et al., 2017
	Marine Sediment core	Foraminifers ð18O	LC21	0 - 156	2, 8, 9	Grant et al., 2012
Cariaco Basin	Speleothem	Speleothem	Sagittarius Blue Hole, Bahamas	9 - 45	1, 2	Hoffmann et al., 2010
	Marine Sediment core	Pollen	MD03-2622	28 - 75	2, 8, 9	González & Dupont, 2009
	Marine Sediment core	Dust	ODP 1002C	0 - 578	2, 7, 8, 9	Yarincik et al., 2000; Haug et al., 2000
	Marine Sediment core	Reflectance	MD03-2621	0 - 80	2, 9	Deplazes et al., 2013
St. Barbara Basin	Speleothem	Speleothem	Bells Cave	8 - 53	1	Wagner et al., 2010
	Speleothem	Speleothem	Fort Stanton	11 - 57	1	Asmerom et al., 2010
	Marine Sediment core	Pollen	ODP 893A	9 - 135	2, 8, 9	Heusser, 1998
	Marine Sediment core	Foraminifers ð18O	ODP 893A	0 - 60	2, 8, 9	Cannariato et al, 1999
Australia - Oceania	Speleothem	Speleothem	Hollywood Cave, NZ	0 - 140	1	Hellstrom et al., 1998; Whittaker et al., 2011; Williams, 1996; Williams et al., 2005
	Lake Sediment core	Pollen	Lynch Crater	0 - 192	2	Kershaw, 1994
	Marine Sediment core	Dust	E26.1	0 - 340	2, 7	Hesse, 1994
Greenland	Ice Core	$\delta^{18}O$	NGRIP	0 - 105	3	NGRIP Members et al., 2004
Antarctica	Ice Core	$\delta^{18}O$	WAIS Divide	0 - 68	3	WAIS Divide Project Members, 2015

S10 Matlab code for error calculation:

```
%Aridity Index simulation
%input here your estimated error as [%]:
fehlerSp=2;
fehlerPo=3;
fehlerDu=5;

%read the CSV data without headlines. "," separated
m = csvread('filename_template.csv');

%Separate on columns
%m3=m(:,3)
%m4=m(:,4)
%m5=m(:,5)

mat=zeros(3,1201,100);
%mat(:,1)=m3

for k=1:3

   for i=1:100
      mat(k,:,i)=m(:,k+2);
   end
end

% fill matrix with random numbers
for a=1:1201
   nSp=mod(mat(1,a,1)+1,2);
   for i=1:fehlerSp
     mat(1,a,i)= nSp;
   end

   nPo=mat(2,a,1);
   if nPo==1
      for i=1:fehlerPo/2
         mat(2,a,i)=0;
      end

      for j=i:fehlerPo
         mat(2,a,j)=2;
      end
   else
      for i=1:fehlerPo
         mat(2,a,i)=1;
      end
   end

   nDu=mat(3,a,1);
   if nDu==1
```

```
        for i=1:fehlerDu/2
            mat(3,a,i)=0;
        end

        for j=i:fehlerDu
            mat(3,a,j)=2;
        end
    else
        for i=1:fehlerDu
            mat(3,a,i)=1;
        end
    end

end

%simulation starts here-->
%number of simulations
noRuns = 100000;

%Std Matrix erstellen
sims=zeros(noRuns,1201);

for sIndex=1:noRuns
    %1201 Random Werte zwischen 0 und 2
    r1 = ceil(rand(1201,1)*100);

    %recalculate index from mat
    vec_speleothem=zeros(1,1201);
    vec_pollen=zeros(1,1201);
    vec_dust=zeros(1,1201);

    for i=1:1201
        vec_speleothem(i)=mat(1,i,r1(i));
        vec_pollen(i)=mat(2,i,r1(i));
        vec_dust(i)=mat(3,i,r1(i));
    end

    tmp =(vec_speleothem+vec_pollen+vec_dust);
    sims(sIndex,:) =tmp;
end

result=zeros(1201:1);

%stadtad deviation for each value individually
for k=1:1201
    result(k) = std(sims(:,k));
end
resultTransp=result.';
csvwrite('error_template_name.txt',resultTransp);
```

Region	Archive	Proxy type	Location	Time covered [ka b2k]	Dating method	Reference
Central Europe	Speleothem	Speleothem	Bunker Cave	0 - 52	1, 2	Fohlmeister et al., 2012, 2013; Weber et al., 2018
	Speleothem	Speleothem	Spannagel Cave	0 - 275	1	Holzkämper et al. 2005; Spötl & Mangini, 2002, 2012
	Lake Sediment core	Pollen	Dehner Maar & Holzmaar	0 - 63	2, 3, 4, 5	Sirocko et al., 2016
	Lake Sediment core	Dust	Dehner Maar	0 - 130	2, 6, 5	Seelos et al., 2009
Arabian Sea	Speleothem	Speleothem	Socotra Cave	2 - 5; 40 - 54	1	Fleitmann et al., 2007 and refs. within; Burns et al., 2003
	Speleothem	Speleothem	Oman Caves	0 - 11	1	Fleitmann et al., 2007 and refs. within
	Marine Sediment core	Dust	Western Arabian Sea	0 - 135	2, 4, 7	Leuschner & Sirocko, 2003
	Marine Sediment core	TOC	Western Arabian Sea	0 - 65	2, 4, 8	Schulz et al., 1998
	Marine Sediment core	Reflectance	Western Arabian Sea	0 - 80	2, 5	Deplazes et al., 2014
NW-Africa	Speleothem	Speleothem	Grotte de Piste	5 - 12	1	Wassenburg et al., 2012, 2016
	Speleothem	Speleothem	Grotte Prison de Chien	3 - 97	1	Wassenburg et al., 2012
	Marine Sediment core	Pollen	West off Morocco	6 - 250	2, 8	Hooghiemstra et al., 1992
	Marine Sediment core	Dust	West off Senegal	0 - 57	2, 8	Collins et al., 2013 and refs. within
China	Speleothem	Speleothem	Hulu Cave	11 - 75	1, 8	Wang et al., 2001; Liu et al., 2010
	Lake Sediment core	Pollen	Sihailongwan Maar Lake	0 - 65	2, 3, 4	Mingram et al., 2018
	Lake Sediment core	Pollen	Sihailongwan Maar Lake	0 - 12	2	Stebich et al., 2015
	Loess profile	Dust	Jingyuan Loess	0 - 80	5, 6, 9	Sun et al., 2010
Southern Europe	Speleothem	Speleothem	Villars Cave	5 - 15; 32 - 83	1	Genty et al., 2006; Genty et al., 2003
	Speleothem	Speleothem	Villars Cave	0 -3	1	Labuhn et al., 2015
	Speleothem	Speleothem	Villars Cave	28 - 51; 11 - 178	1	Wainer et al., 2009; 2011
	Lake Sediment core	Pollen	Lac Du Bouchet	15 - 68	2, 10	Reille & Beaulieu, 1989;
	Marine Sediment core	Dust	MD01-2443/4	0 - 420	2, 5, 7, 8, 9	Hodell et al., 2013, Barker et al., 2011
Portuguese margin	Speleothem	Speleothem	Buraca Gloriosa Cave	0 - 220	1	Denniston et al., 2018
	Marine Sediment core	Pollen	MD95-2039	0 - 65	2, 5, 9	Roucoux et al., 2005, Vogelsang, E., 2001
	Marine Sediment core	Dust	MD01-2443/4	0 - 420	2, 5, 7, 8, 9	Hodell et al., 2013, Barker et al., 2011
Mediterranean Sea	Speleothem	Speleothem	Dim Cave	5 - 85	1	Ünal-Imer et al., 2015
	Speleothem	Speleothem	Soreq Cave	0 - 150	1	Grant et al., 2012
	Speleothem	Speleothem	Soreq Cave	0 - 140	1	Bar-Matthews et al., 2000
	Lake Sediment core	Pollen	Lago Grande di Monticchio	0 - 130	2, 3, 9	Brauer et al., 2007
	Marine Sediment core	Dust	MD40/4_SL71	0 - 180	2, 4, 8	Ehrmann et al., 2017
St. Barbara Basin	Speleothem	Speleothem	Bells Cave	8 - 53	1	Wagner et al., 2010
	Speleothem	Speleothem	Fort Stanton	11 - 57	1	Asmerom et al., 2010
	Marine Sediment core	Pollen	ODP 893A	9 - 135	2, 8, 9	Heusser, 1998
	Marine Sediment core	Foraminifers ð18O	ODP 893A	0 - 60	2, 8, 9	Cannariato et al, 1999
Greenland	Ice Core	$\delta^{18}O$	NGRIP	0 - 105	3	NGRIP Members et al., 2004
Antarctica	Ice Core	$\delta^{18}O$	WAIS Divide	0 - 68	3	WAIS Divide Project Members, 2015

Table S1: Paleoclimatic records used in this synthesis. Records with grey background are not included into the generation of the aridity index. Dating methods: 1 Th/U-dating; 2 ^{14}C-Radiocarbon dating; 3 Varve counting; 4 Tephrachronology; 5 Ice core tuning; 6 OSL Luminescence dating; 7 Orbital tuning; 8 Oxygen isotope tuning; 9 Cross correlation; 10 Paleomagnetic correlation

References:

Allen, J. R. M., Brandt, U., Brauer, A., Hubberten, H. W., Huntley, B., Keller, J., Kraml, M., Mackensen, A., Mingram, J., Negendank, J. F. W., Nowaczyk, R., Oberhänsli, H., Watts, W. A., Wulf, S. and Zolitschka, B.: Rapid environmental changes in southern Europe during the last glacial period, Nature, 400, 740–743, 1999.

Asmerom, Y., Polyak, V. J. and Burns, S. J.: Variable winter moisture in the southwestern United States linked to rapid glacial climate shifts, Nature Geoscience, 3(2), 114–117, doi:10.1038/ngeo754, 2010.

Bard, E.: Climate Shock: Abrupt Changes over Millennial Time Scales, Physics Today, 55(12), 32–38, doi:10.1063/1.1537910, 2002.

Bar-Matthews, M., Ayalon, A. and Kaufman, A.: Late Quaternary Paleoclimate in the Eastern Mediterranean Region from Stable Isotope Analysis of Speleothems at Soreq Cave, Israel, Quaternary Research, 47(2), 155–168, doi:10.1006/qres.1997.1883, 1997.

Behl, R. J.: Sedimentary facies and sedimentology of the late quaternary Santa Barbara basin, site 893, , 146–2, doi:10.2973/odp.proc.sr.146-2.1995, 1995.

Behl, R. J. and Kennett, J. P.: Brief interstadial events in the Santa Barbara basin, NE Pacific, during the past 60 kyr, Nature, 379, 243, 1996.

Brauer, A., Endres, C. and Negendank, J. F. W.: Lateglacial calendar year chronology based on annually laminated sediments from Lake Meerfelder Maar, Germany, Quaternary International, 61(1), 17–25, doi:10.1016/S1040-6182(99)00014-2, 1999.

Brauer, A., Allen, J. R. M., Mingram, J., Dulski, P., Wulf, S. and Huntley, B.: Evidence for last interglacial chronology and environmental change from Southern Europe, Proceedings of the National Academy of Sciences, 104(2), 450–455, doi:10.1073/pnas.0603321104, 2007.

Burns, S. J., Fleitmann, D., Matter, A., Kramers, J. and Al-Subbary A. A: Indian Ocean Climate and a Absolute Chronology over Dansgaard/Oescher Events 9 to 13, Science, 301, 1365–1367, 2003.

Cannariato, K. G., Kennett, J. P. and Behl, R. J.: Biotic response to late Quaternary rapid climate switches in Santa Barbara Basin: Ecological and evolutionary implications, Geology, 27(1), 63, doi:10.1130/0091-7613(1999)027<0063:BRTLQR>2.3.CO;2, 1999.

Carlson, A. E.: PALEOCLIMATE | The Younger Dryas Climate Event, in Encyclopedia of Quaternary Science, pp. 126–134, Elsevier., 2013.

Collins, J. A., Govin, A., Mulitza, S., Heslop, D., Zabel, M., Hartmann, J., Röhl, U. and Wefer, G.: Abrupt shifts of the Sahara-Sahel boundary during Heinrich stadials, Climate of the Past, 9(3), 1181–1191, doi:10.5194/cp-9-1181-2013, 2013.

Deplazes, G., Lückge, A., Peterson, L. C., Timmermann, A., Hamann, Y., Hughen, K. A., Röhl, U., Laj, C., Cane, M. A., Sigman, D. M. and Haug, G. H.: Links between tropical rainfall and North Atlantic climate during the last glacial period,

Nature Geoscience, 6(3), 213–217, doi:10.1038/ngeo1712, 2013.

Deplazes, G., Lückge, A., Stuut, J.-B. W., Pätzold, J., Kuhlmann, H., Husson, D., Fant, M. and Haug, G. H.: Weakening and strengthening of the Indian monsoon during Heinrich events and Dansgaard-Oeschger oscillations: INDIAN MONSOON DURING HEINRICH EVENTS, Paleoceanography, 29(2), 99–114, doi:10.1002/2013PA002509, 2014.

Deutscher Wetterdienst: Wetter und Klima - Deutscher Wetterdienst - Klimadaten weltweit, [online] Available from: https://www.dwd.de/DE/leistungen/klimadatenwelt/klimadatenwelt_node.html (Accessed 17 July 2018), 2018.

Ehrmann, W., Schmiedl, G., Beuscher, S. and Krüger, S.: Intensity of African Humid Periods Estimated from Saharan Dust Fluxes, edited by S.-P. Xie, PLOS ONE, 12(1), e0170989, doi:10.1371/journal.pone.0170989, 2017.

Fitzsimmons, K. E., Cohen, T. J., Hesse, P. P., Jansen, J., Nanson, G. C., May, J.-H., Barrows, T. T., Haberlah, D., Hilgers, A., Kelly, T., Larsen, J., Lomax, J. and Treble, P.: Late Quaternary palaeoenvironmental change in the Australian drylands, Quaternary Science Reviews, 74, 78–96, doi:10.1016/j.quascirev.2012.09.007, 2013.

Fleitmann, D., Burns, S. J., Mangini, A., Mudelsee, M., Kramers, J., Villa, I., Neff, U., Al-Subbary, A. A., Buettner, A., Hippler, D. and Matter, A.: Holocene ITCZ and Indian monsoon dynamics recorded in stalagmites from Oman and Yemen (Socotra), Quaternary Science Reviews, 26(1–2), 170–188, doi:10.1016/j.quascirev.2006.04.012, 2007.

Gac, J.-Y. and Kane, A.: Le fleuve Sénégal : I. Bilan hydrologique et flux continentaux de matières particulaires à l'embouchure. Senegal river. Part I. Water budget and flux of carried load through the estuary, Sciences Géologiques, bulletins et mémoires, 39(1), 99–130, doi:10.3406/sgeol.1986.1721, 1986.

Genty, D., Blamart, D., Ouahdi, R., Gilmour, M., Baker, A., Jouzel, J. and Van-Exter, S.: Precise dating of Dansgaard-Oeschger climate oscillations in western Europe from stalagmite data, Nature, 421(6925), 833–837, doi:10.1038/nature01391, 2003.

Genty, D., Blamart, D., Ghaleb, B., Plagnes, V., Causse, Ch., Bakalowicz, M., Zouari, K., Chkir, N., Hellstrom, J. and Wainer, K.: Timing and dynamics of the last deglaciation from European and North African δ13C stalagmite profiles—comparison with Chinese and South Hemisphere stalagmites, Quaternary Science Reviews, 25(17–18), 2118–2142, doi:10.1016/j.quascirev.2006.01.030, 2006.

Gibson, K. A. and Peterson, L. C.: A 0.6 million year record of millennial-scale climate variability in the tropics, Geophysical Research Letters, 41(3), 969–975, doi:10.1002/2013GL058846, 2014.

González, C. and Dupont, L. M.: Tropical salt marsh succession as sea-level indicator during Heinrich events, Quaternary Science Reviews, 28(9–10), 939–946, doi:10.1016/j.quascirev.2008.12.023, 2009.

Grant, K. M., Rohling, E. J., Bar-Matthews, M., Ayalon, A., Medina-Elizalde, M., Ramsey, C. B., Satow, C. and Roberts, A. P.: Rapid coupling between ice volume and polar temperature over the past 150,000 years, Nature, 491(7426), 744–747, doi:10.1038/nature11593, 2012.

Hellstrom, J., McCulloch, M. and Stone, J.: A Detailed 31,000-Year Record of Climate and Vegetation Change, from the Isotope Geochemistry of Two New Zealand Speleothems, Quaternary Research, 50(2), 167–178, doi:10.1006/qres.1998.1991, 1998.

Hesse, P. P.: The record of continental dust from Australia in Tasman Sea Sediments, Quaternary Science Reviews, 13(3), 257–272, doi:10.1016/0277-3791(94)90029-9, 1994.

Hesse, P. P. and McTainsh, G. H.: Australian dust deposits: modern processes and the Quaternary record, Quaternary Science Reviews, 22(18), 2007–2035, doi:10.1016/S0277-3791(03)00164-1, 2003.

Heusser, L.: Direct correlation of millennial-scale changes in western North American vegetation and climate with changes in the California Current System over the past ~60 kyr, Paleoceanography, 13(3), 252–262, doi:10.1029/98PA00670, 1998.

Hodell, D., Crowhurst, S., Skinner, L., Tzedakis, P. C., Margari, V., Channell, J. E. T., Kamenov, G., Maclachlan, S. and Rothwell, G.: Response of Iberian Margin sediments to orbital and suborbital forcing over the past 420 ka, Paleoceanography, 28(1), 185–199, doi:10.1002/palo.20017, 2013.

Hoffmann, D. L., Beck, J. W., Richards, D. A., Smart, P. L., Singarayer, J. S., Ketchmark, T. and Hawkesworth, C. J.: Towards radiocarbon calibration beyond 28ka using speleothems from the Bahamas, Earth and Planetary Science Letters, 289(1–2), 1–10, doi:10.1016/j.epsl.2009.10.004, 2010.

Hoffmann, D. L., Rogerson, M., Spötl, C., Luetscher, M., Vance, D., Osborne, A. H., Fello, N. M. and Moseley, G. E.: Timing and causes of North African wet phases during the last glacial period and implications for modern human migration, Scientific Reports, 6, 36367, doi:10.1038/srep36367, 2016.

Hooghiemstra, H., Stalling, H., Agwu, C. O. C. and Dupont, L. M.: Vegetational and climatic changes at the northern fringe of the sahara 250,000–5000 years BP: evidence from 4 marine pollen records located between Portugal and the Canary Islands, Review of Palaeobotany and Palynology, 74(1), 1–53, doi:10.1016/0034-6667(92)90137-6, 1992.

Hughen, K. A., Eglinton, T. E., Xu, L. and Makou, M.: Abrupt Tropical Vegetation Response to Rapid Climate Change, Science, 304, 1955–1959, 2004.

Jolly, D., Harrison, S. P., Damnati, B. and Bonnefille, R.: Simulated Climate and Biomes of Africa During the Late Quaternary: Comparison with Pollen and Lake Status Data, Quaternary Science Reviews, 17, 29, 1998.

Kershaw, A. P.: A late pleistocene and holocene pollen diagram from Lynch's Crater, North Eastern Queensland, Australia, New Phytologist, 77, 469–498, 1976.

Kershaw, A. P.: Pleistocene vegetation of the humid tropics of northeastern Queensland, Australia, Palaeogeography, Palaeoclimatology, Palaeoecology, 109(2–4), 399–412, 1994.

Leuschner, D. C. and Sirocko, F.: The low-latitude monsoon climate during Dansgaard-Oeschger cycles and Heinrich Events, Quaternary Science Reviews, 19(1–5), 243–254, 2000.

Leuschner, D. C. and Sirocko, F.: Orbital insolation forcing of the Indian Monsoon – a motor for global climate changes?, Palaeogeography Palaeoclimatology Palaeoecology, 197(1–2), 83–95, 2003.

Liu, D., Wang, Y., Cheng, H., Lawrence Edwards, R., Kong, X., Wang, X., Hardt, B., Wu, J., Chen, S., Jiang, X., He, Y., Dong, J. and Zhao, K.: Sub-millennial variability of Asian monsoon intensity during the early MIS 3 and its analogue to the ice age terminations, Quaternary Science Reviews, 29(9), 1107–1115, doi:10.1016/j.quascirev.2010.01.008, 2010.

Lu, H.-Y., Wu, N.-Q., Liu, K.-B., Jiang, H. and Liu, T.-S.: Phytoliths as quantitative indicators for the reconstruction of past

environmental conditions in China II: palaeoenvironmental reconstruction in the Loess Plateau, Quaternary Science Reviews, 26(5), 759–772, doi:https://doi.org/10.1016/j.quascirev.2006.10.006, 2007.

Martrat, B., Grimalt, J. O., Shackleton, N. J., Abreu, L. de, Hutterli, M. A. and Stocker, T. F.: Four Climate Cycles of Recurring Deep and Surface Water Destabilizations on the Iberian Margin, Science, 317(5837), 502–507, doi:10.1126/science.1139994, 2007.

McManus, J. F., Oppo, D. W. and Cullen, J. L.: A 0.5-Million-Year Record of Millennial-Scale Climate Variability in the North Atlantic, Science, 283(5404), 971–975, doi:10.1126/science.283.5404.971, 1999.

Mingram, J., Stebich, M., Schettler, G., Hu, Y., Rioual, P., Nowaczyk, N., Dulski, P., You, H., Opitz, S., Liu, Q. and Liu, J.: Millennial-scale East Asian monsoon variability of the last glacial deduced from annually laminated sediments from Lake Sihailongwan, N.E. China, Quaternary Science Reviews, 201, 57–76, doi:10.1016/j.quascirev.2018.09.023, 2018.

Mulitza, S., Prange, M., Stuut, J.-B., Zabel, M., Dobeneck, T. von, Itambi, A. C., Nizou, J., Schulz, M. and Wefer, G.: Sahel megadroughts triggered by glacial slowdowns of Atlantic meridional overturning, Paleoceanography, 23(4), doi:10.1029/2008PA001637, 2008.

Naafs, B. D. A., Hefter, J., Grützner, J. and Stein, R.: Warming of surface waters in the mid-latitude North Atlantic during Heinrich events: HIGH SSTs DURING HEINRICH EVENTS, Paleoceanography, 28(1), 153–163, doi:10.1029/2012PA002354, 2013.

North Greenland Ice Core Project Members, Andersen, K. K., Azuma, N., Barnola, J.-M., Bigler, M., Biscaye, P., Caillon, N., Chappellaz, J., Clausen, H. B., Dahl-Jensen, D., Fischer, H., Flückiger, J., Fritzsche, D., Fujii, Y., Goto-Azuma, K., Grønvold, K., Gundestrup, N. S., Hansson, M., Huber, C., Hvidberg, C. S., Johnsen, S. J., Jonsell, U., Jouzel, J., Kipfstuhl, S., Landais, A., Leuenberger, M., Lorrain, R., Masson-Delmotte, V., Miller, H., Motoyama, H., Narita, H., Popp, T., Rasmussen, S. O., Raynaud, D., Rothlisberger, R., Ruth, U., Samyn, D., Schwander, J., Shoji, H., Siggard-Andersen, M. L., Steffensen, J. P., Stocker, T., Sveinbjörnsdóttir, A. E., Svensson, A., Takata, M., Tison, J.-L., Thorsteinsson, T., Watanabe, O., Wilhelms, F. and White, J. W. C.: High-resolution record of Northern Hemisphere climate extending into the last interglacial period, Nature, 431(7005), 147–151, doi:10.1038/nature02805, 2004.

Peterson, L. C., Haug, G. H., Hughen, K. A. and Röhl, U.: Rapid Changes in the Hydrologic Cycle of the Tropical Atlantic During the Last Glacial, Science, 290(5498), 1947–1951, doi:10.1126/science.290.5498.1947, 2000.

Reille, M. and de Beaulieu, J. L.: History of the Würm and Holocene vegetation in western velay (Massif Central, France): A comparison of pollen analysis from three corings at Lac du Bouchet, Review of Palaeobotany and Palynology, 54(3), 233–248, doi:10.1016/0034-6667(88)90016-4, 1988.

Reille, M. and de Beaulieu, J. L.: Pollen analysis of a long upper Pleistocene continental sequence in a Velay maar (Massif Central, France), Palaeogeography, Palaeoclimatology, Palaeoecology, 80(1), 35–48, doi:10.1016/0031-0182(90)90032-3, 1990.

Roucoux, K. H., de Abreu, L., Shackleton, N. J. and Tzedakis, P. C.: The response of NW Iberian vegetation to North Atlantic climate oscillations during the last 65kyr, Quaternary Science Reviews, 24(14), 1637–1653,

doi:10.1016/j.quascirev.2004.08.022, 2005.

Ruth, U., Bigler, M., Röthlisberger, R., Siggaard-Andersen, M.-L., Kipfstuhl, S., Goto-Azuma, K., Hansson, M. E., Johnsen, S. J., Lu, H. and Steffensen, J. P.: Ice core evidence for a very tight link between North Atlantic and east Asian glacial climate, Geophysical Research Letters, 34(3), doi:10.1029/2006GL027876, 2007.

Schettler, G., Liu, Q., Mingram, J., Stebich, M. and Dulski, P.: East-Asian monsoon variability between 15 000 and 2000 cal. yr BP recorded in varved sediments of Lake Sihailongwan (northeastern China, Long Gang volcanic field), The Holocene, 16(8), 1043–1057, doi:10.1177/0959683606069388, 2006.

Schulz, H., von Rad, U., Erlenkeuser, H. and von Rad, U.: Correlation between Arabian Sea and Greenland climate oscillations of the past 110,000 years, Nature, 393(6680), 54–57, doi:10.1038/31750, 1998.

Shakun, J. D. and Carlson, A. E.: A global perspective on Last Glacial Maximum to Holocene climate change, Quaternary Science Reviews, 29(15), 1801–1816, doi:10.1016/j.quascirev.2010.03.016, 2010.

Sirocko, F., Garbe-Schönberg, D., McIntyre, A. and Molfino, B.: Teleconnections between the subtropical monsoon and high latitude climates during the last deglaciation, Science, 272, 526–529, 1996.

Stebich, M., Rehfeld, K., Schlütz, F., Tarasov, P. E., Liu, J. and Mingram, J.: Holocene vegetation and climate dynamics of NE China based on the pollen record from Sihailongwan Maar Lake, Quaternary Science Reviews, 124, 275–289, doi:https://doi.org/10.1016/j.quascirev.2015.07.021, 2015.

Stuut, J.-B., Zabel, M., Ratmeyer, V., Helmke, P., Schefuß, E., Lavik, G. and Schneider, R.: Provenance of present-day eolian dust collected off NW Africa, Journal of Geophysical Research: Atmospheres, 110(D4), doi:10.1029/2004JD005161, 2005.

Sun, Y., Wang, X., Liu, Q. and Clemens, S. C.: Impacts of post-depositional processes on rapid monsoon signals recorded by the last glacial loess deposits of northern China, Earth and Planetary Science Letters, 289(1–2), 171–179, doi:10.1016/j.epsl.2009.10.038, 2010.

Toggweiler, J. R., Russell, J. L. and Carson, S. R.: Midlatitude westerlies, atmospheric CO2, and climate change during the ice ages, Paleoceanography, 21(2), doi:10.1029/2005PA001154, 2006.

Ünal-İmer, E., Shulmeister, J., Zhao, J.-X., Tonguç Uysal, I., Feng, Y.-X., Duc Nguyen, A. and Yüce, G.: An 80 kyr-long continuous speleothem record from Dim Cave, SW Turkey with paleoclimatic implications for the Eastern Mediterranean, Scientific Reports, 5(1), doi:10.1038/srep13560, 2015.

Wagner, J. D. M., Cole, J. E., Beck, J. W., Patchett, P. J., Henderson, G. M. and Barnett, H. R.: Moisture variability in the southwestern United States linked to abrupt glacial climate change, Nature Geoscience, 3(2), 110–113, doi:10.1038/ngeo707, 2010.

Wainer, K., Genty, D., Blamart, D., Hoffmann, D. and Couchoud, I.: A new stage 3 millennial climatic variability record from a SW France speleothem, Palaeogeography, Palaeoclimatology, Palaeoecology, 271(1–2), 130–139, doi:10.1016/j.palaeo.2008.10.009, 2009.

WAIS Divide Project Members, Buizert, C., Adrian, B., Ahn, J., Albert, M., Alley, R. B., Baggenstos, D., Bauska, T. K., Bay, R. C., Bencivengo, B. B., Bentley, C. R., Brook, E. J., Chellman, N. J., Clow, G. D., Cole-Dai, J., Conway, H., Cravens, E.,

Cuffey, K. M., Dunbar, N. W., Edwards, J. S., Fegyveresi, J. M., Ferris, D. G., Fitzpatrick, J. J., Fudge, T. J., Gibson, C. J., Gkinis, V., Goetz, J. J., Gregory, S., Hargreaves, G. M., Iverson, N., Johnson, J. A., Jones, T. R., Kalk, M. L., Kippenhan, M. J., Koffman, B. G., Kreutz, K., Kuhl, T. W., Lebar, D. A., Lee, J. E., Marcott, S. A., Markle, B. R., Maselli, O. J., McConnell, J. R., McGwire, K. C., Mitchell, L. E., Mortensen, N. B., Neff, P. D., Nishiizumi, K., Nunn, R. M., Orsi, A. J., Pasteris, D. R., Pedro, J. B., Pettit, E. C., Buford Price, P., Priscu, J. C., Rhodes, R. H., Rosen, J. L., Schauer, A. J., Schoenemann, S. W., Sendelbach, P. J., Severinghaus, J. P., Shturmakov, A. J., Sigl, M., Slawny, K. R., Souney, J. M., Sowers, T. A., Spencer, M. K., Steig, E. J., Taylor, K. C., Twickler, M. S., Vaughn, B. H., Voigt, D. E., Waddington, E. D., Welten, K. C., Wendricks, A. W., White, J. W. C., Winstrup, M., Wong, G. J. and Woodruff, T. E.: Precise interpolar phasing of abrupt climate change during the last ice age, Nature, 520(7549), 661–665, doi:10.1038/nature14401, 2015.

Wang, Y. J., Cheng, H., Edwards, R. L., An, Z. S., Wu, J. Y., Shen, C.-C. and Dorale, J. A.: A High-Resolution Absolute-Dated Late Pleistocene Monsoon Record from Hulu Cave, China, Science, 294(5550), 2345, doi:10.1126/science.1064618, 2001.

Wassenburg, J. A., Immenhauser, A., Richter, D. K., Jochum, K. P., Fietzke, J., Deininger, M., Goos, M., Scholz, D. and Sabaoui, A.: Climate and cave control on Pleistocene/Holocene calcite-to-aragonite transitions in speleothems from Morocco: Elemental and isotopic evidence, Geochimica et Cosmochimica Acta, 92, 23–47, doi:10.1016/j.gca.2012.06.002, 2012.

Watts, W. A.: A long pollen record from Laghi di Monticchio, southern Italy: a preiminary account, Journal of the Geological Society, 142(3), 491–499, doi:10.1144/gsjgs.142.3.0491, 1985.

Wegner, A., Fischer, H., Delmonte, B., Petit, J.-R., Erhardt, T., Ruth, U., Svensson, A., Vinther, B. and Miller, H.: The role of seasonality of mineral dust concentration and size on glacial/interglacial dust changes in the EPICA Dronning Maud Land ice core: EPICA DML DUST RECORD, Journal of Geophysical Research: Atmospheres, 120(19), 9916–9931, doi:10.1002/2015JD023608, 2015.

Whittaker, T. E., Hendy, C. H. and Hellstrom, J. C.: Abrupt millennial-scale changes in intensity of Southern Hemisphere westerly winds during marine isotope stages 2–4, Geology, 39(5), 455–458, doi:10.1130/G31827.1, 2011.

Williams, P. W.: A 230 ka record of glacial and interglacial events from Aurora Cave, Fiordland, New Zealand, New Zealand Journal of Geology and Geophysics, 39(2), 225–241, doi:10.1080/00288306.1996.9514707, 1996.

Williams, P. W., King, D. N. T., Zhao, J. X. and Collerson, K. D.: Late Pleistocene to Holocene composite speleothem 18O and 13C chronologies from South Island, New Zealand—did a global Younger Dryas really exist?, Earth and Planetary Science Letters, 230(3–4), 301–317, doi:10.1016/j.epsl.2004.10.024, 2005.

Yarincik, K. M., Murray, R. W. and Peterson, L. C.: Climatically sensitive eolian and hemipelagic deposition in the Cariaco Basin, Venezuela, over the past 578,000 years: Results from Al/Ti and K/Al, Paleoceanography, 15(2), 210–228, doi:10.1029/1999PA900048, 2000.

Allen, J. R. M., Brandt, U., Brauer, A., Hubberten, H.-W., Huntley, B., Keller, J., Kraml, M., Mackensen, A., Mingram, J., Negendank, J. F. W., Nowaczyk, R., Oberhänsli, H., Watts, W. A., Wulf, S. and Zolitschka, B.: Rapid environmental changes in southern Europe during the last glacial period, Nature, 400, 740–743, 1999.

Antoine, P., Rousseau, D.-D., Zöller, L., Lang, A., Munaut, A.-V., Hatté, C. and Fontugne, M.: High-resolution record of the last Interglacial–glacial cycle in the Nussloch loess–palaeosol sequences, Upper Rhine Area, Germany, Quaternary International, 76–77, 211–229, doi:10.1016/S1040-6182(00)00104-X, 2001.

Asmerom, Y., Polyak, V. J. and Burns, S. J.: Variable winter moisture in the southwestern United States linked to rapid glacial climate shifts, Nature Geoscience, 3(2), 114–117, doi:10.1038/ngeo754, 2010.

Bar-Matthews, M., Ayalon, A. and Kaufman, A.: Late Quaternary Paleoclimate in the Eastern Mediterranean Region from Stable Isotope Analysis of Speleothems at Soreq Cave, Israel, Quaternary Research, 47(2), 155–168, doi:10.1006/qres.1997.1883, 1997.

Bar-Matthews, M., Ayalon, A. and Kaufman, A.: Timing and hydrological conditions of Sapropel events in the Eastern Mediterranean, as evident from speleothems, Soreq cave, Israel, Chemical Geology, 169(1–2), 145–156, 2000.

Behl, R. J.: Sedimentary facies and sedimentology of the late quaternary Santa Barbara basin, site 893, , 146–2, doi:10.2973/odp.proc.sr.146-2.1995, 1995.

Behl, R. J. and Kennett, J. P.: Brief interstadial events in the Santa Barbara basin, NE Pacific, during the past 60 kyr, Nature, 379, 243, 1996.

Brauer, A., Endres, C. and Negendank, J. F. W.: Lateglacial calendar year chronology based on annually laminated sediments from Lake Meerfelder Maar, Germany, Quaternary International, 61(1), 17–25, doi:10.1016/S1040-6182(99)00014-2, 1999.

Brauer, A., Allen, J. R. M., Mingram, J., Dulski, P., Wulf, S. and Huntley, B.: Evidence for last interglacial chronology and environmental change from Southern Europe, Proceedings of the National Academy of Sciences, 104(2), 450–455, doi:10.1073/pnas.0603321104, 2007.

Bronk Ramsey, C., Staff, R. A., Bryant, C. L., Brock, F., Kitagawa, H., van der Plicht, J., Schlolaut, G., Marshall, M. H., Brauer, A., Lamb, H. F., Payne, R. L., Tarasov, P. E., Haraguchi, T., Gotanda, K., Yonenobu, H., Yokoyama, Y., Tada, R. and Nakagawa, T.: A Complete Terrestrial Radiocarbon Record for 11.2 to 52.8 kyr B.P., Science, 338(6105), 370–374, doi:10.1126/science.1226660, 2012.

Burns, S. J., Fleitmann, D., Matter, A., Kramers, J. and Al-Subbary A. A: Indian Ocean Climate and a Absolute Chronology over Dansgaard/Oescher Events 9 to 13, Science, 301, 1365–1367, 2003.

Cannariato, K. G., Kennett, J. P. and Behl, R. J.: Biotic response to late Quaternary rapid climate switches in Santa Barbara Basin: Ecological and evolutionary implications, Geology, 27(1), 63, doi:10.1130/0091-7613(1999)027<0063:BRTLQR>2.3.CO;2, 1999.

Collins, J. A., Govin, A., Mulitza, S., Heslop, D., Zabel, M., Hartmann, J., Röhl, U. and Wefer, G.: Abrupt shifts of the Sahara-Sahel boundary during Heinrich stadials, Climate of the Past, 9(3), 1181–1191, doi:10.5194/cp-9-1181-2013, 2013.

Correa-Metrio, A., Bush, M. B., Hodell, D. A., Brenner, M., Escobar, J. and Guilderson, T.: The influence of abrupt climate change on the ice-age vegetation of the Central American lowlands: Abrupt climate change in ice-age Central America, Journal of Biogeography, 39(3), 497–509, doi:10.1111/j.1365-2699.2011.02618.x, 2012.

Denniston, R. F., Houts, A. N., Asmerom, Y., Wanamaker Jr., A. D., Haws, J. A., Polyak, V. J., Thatcher, D. L., Altan-Ochir,

S., Borowske, A. C., Breitenbach, S. F. M., Ummenhofer, C. C., Regala, F. T., Benedetti, M. M. and Bicho, N. F.: A stalagmite test of North Atlantic SST and Iberian hydroclimate linkages over the last two glacial cycles, Climate of the Past, 14(12), 1893–1913, doi:https://doi.org/10.5194/cp-14-1893-2018, 2018.

Deplazes, G., Lückge, A., Stuut, J.-B. W., Pätzold, J., Kuhlmann, H., Husson, D., Fant, M. and Haug, G. H.: Weakening and strengthening of the Indian monsoon during Heinrich events and Dansgaard-Oeschger oscillations: INDIAN MONSOON DURING HEINRICH EVENTS, Paleoceanography, 29(2), 99–114, doi:10.1002/2013PA002509, 2014.

Deutscher Wetterdienst: Wetter und Klima - Deutscher Wetterdienst - Klimadaten weltweit, [online] Available from: https://www.dwd.de/DE/leistungen/klimadatenwelt/klimadatenwelt_node.html (Accessed 17 July 2018), 2018.

Ehrmann, W., Schmiedl, G., Beuscher, S. and Krüger, S.: Intensity of African Humid Periods Estimated from Saharan Dust Fluxes, edited by S.-P. Xie, PLOS ONE, 12(1), e0170989, doi:10.1371/journal.pone.0170989, 2017.

Fleitmann, D., Burns, S. J., Mangini, A., Mudelsee, M., Kramers, J., Villa, I., Neff, U., Al-Subbary, A. A., Buettner, A., Hippler, D. and Matter, A.: Holocene ITCZ and Indian monsoon dynamics recorded in stalagmites from Oman and Yemen (Socotra), Quaternary Science Reviews, 26(1–2), 170–188, doi:10.1016/j.quascirev.2006.04.012, 2007.

Genty, D., Blamart, D., Ouahdi, R., Gilmour, M., Baker, A., Jouzel, J. and Van-Exter, S.: Precise dating of Dansgaard–Oeschger climate oscillations in western Europe from stalagmite data, Nature, 421(6925), 833–837, doi:10.1038/nature01391, 2003.

Genty, D., Blamart, D., Ghaleb, B., Plagnes, V., Causse, Ch., Bakalowicz, M., Zouari, K., Chkir, N., Hellstrom, J. and Wainer, K.: Timing and dynamics of the last deglaciation from European and North African δ13C stalagmite profiles—comparison with Chinese and South Hemisphere stalagmites, Quaternary Science Reviews, 25(17–18), 2118–2142, doi:10.1016/j.quascirev.2006.01.030, 2006.

Grant, K. M., Rohling, E. J., Bar-Matthews, M., Ayalon, A., Medina-Elizalde, M., Ramsey, C. B., Satow, C. and Roberts, A. P.: Rapid coupling between ice volume and polar temperature over the past 150,000 years, Nature, 491(7426), 744–747, doi:10.1038/nature11593, 2012.

Grimm, E. C., Watts, W. A., Jacobson Jr., G. L., Hansen, B. C. S., Almquist, H. R. and Dieffenbacher-Krall, A. C.: Evidence for warm wet Heinrich events in Florida, Quaternary Science Reviews, 25(17–18), 2197–2211, doi:10.1016/j.quascirev.2006.04.008, 2006.

Heusser, L.: Pollen stratigraphy and paleoecologic interpretation of the last 160 kyr from Santa Barbara Basin, ODP Hole 893A, in Proc. Ocean Drill. Program Sci. Results, vol. 146, edited by J. Kennett, J. G. Baldauf, and M. Lyle, pp. 265–279., 1995.

Heusser, L.: Direct correlation of millennial-scale changes in western North American vegetation and climate with changes in the California Current System over the past ~60 kyr, Paleoceanography, 13(3), 252–262, doi:10.1029/98PA00670, 1998.

Hodell, D., Crowhurst, S., Skinner, L., Tzedakis, P. C., Margari, V., Channell, J. E. T., Kamenov, G., Maclachlan, S. and Rothwell, G.: Response of Iberian Margin sediments to orbital and suborbital forcing over the past 420 ka, Paleoceanography, 28(1), 185–199, doi:10.1002/palo.20017, 2013.

Hooghiemstra, H., Stalling, H., Agwu, C. O. C. and Dupont, L. M.: Vegetational and climatic changes at the northern fringe of the sahara 250,000–5000 years BP: evidence from 4 marine pollen records located between Portugal and the Canary Islands, Review of Palaeobotany and Palynology, 74(1), 1–53, doi:10.1016/0034-6667(92)90137-6, 1992.

Hughen, K., Southon, J., Lehman, S., Bertrand, C. and Turnbull, J.: Marine-derived 14C calibration and activity record for the past 50,000 years updated from the Cariaco Basin, Quaternary Science Reviews, 25(23–24), 3216–3227, doi:10.1016/j.quascirev.2006.03.014, 2006.

Jiménez-Moreno, G., Anderson, S. R. and Fawcett, P.: Orbital- and millennial-scale vegetation and climate changes of the past 225ka from Bear Lake, Utah–Idaho (USA), Quaternary Science Reviews, 26(13–14), 1713–1724, doi:10.1016/j.quascirev.2007.05.001, 2007.

Jolly, D., Harrison, S. P., Damnati, B. and Bonnefille, R.: Simulated Climate and Biomes of Africa During the Late Quaternary: Comparison with Pollen and Lake Status Data, Quaternary Science Reviews, 17, 29, 1998.

Kliem, P., Enters, D., Hahn, A., Ohlendorf, C., Lisé-Pronovost, A., St-Onge, G., Wastegård, S. and Zolitschka, B.: Lithology, radiocarbon chronology and sedimentological interpretation of the lacustrine record from Laguna Potrok Aike, southern Patagonia, Quaternary Science Reviews, 71, 54–69, doi:10.1016/j.quascirev.2012.07.019, 2013.

Labuhn, I., Genty, D., Vonhof, H., Bourdin, C., Blamart, D., Douville, E., Ruan, J., Cheng, H., Edwards, R. L., Pons-Branchu, E. and Pierre, M.: A high-resolution fluid inclusion δ18O record from a stalagmite in SW France: modern calibration and comparison with multiple proxies, Quaternary Science Reviews, 110, 152–165, doi:10.1016/j.quascirev.2014.12.021, 2015.

Leuschner, D. C. and Sirocko, F.: The low-latitude monsoon climate during Dansgaard-Oeschger cycles and Heinrich Events, Quaternary Science Reviews, 19(1–5), 243–254, 2000.

Leuschner, D. C. and Sirocko, F.: Orbital insolation forcing of the Indian Monsoon - a motor for global climate changes?, Palaeogeography Palaeoclimatology Palaeoecology, 197(1–2), 83–95, 2003.

Liu, D., Wang, Y., Cheng, H., Lawrence Edwards, R., Kong, X., Wang, X., Hardt, B., Wu, J., Chen, S., Jiang, X., He, Y., Dong, J. and Zhao, K.: Sub-millennial variability of Asian monsoon intensity during the early MIS 3 and its analogue to the ice age terminations, Quaternary Science Reviews, 29(9), 1107–1115, doi:10.1016/j.quascirev.2010.01.008, 2010.

Lu, H.-Y., Wu, N.-Q., Liu, K.-B., Jiang, H. and Liu, T.-S.: Phytoliths as quantitative indicators for the reconstruction of past environmental conditions in China II: palaeoenvironmental reconstruction in the Loess Plateau, Quaternary Science Reviews, 26(5), 759–772, doi:https://doi.org/10.1016/j.quascirev.2006.10.006, 2007.

Martrat, B., Grimalt, J. O., Shackleton, N. J., Abreu, L. de, Hutterli, M. A. and Stocker, T. F.: Four Climate Cycles of Recurring Deep and Surface Water Destabilizations on the Iberian Margin, Science, 317(5837), 502–507, doi:10.1126/science.1139994, 2007.

Mingram, J., Stebich, M., Schettler, G., Hu, Y., Rioual, P., Nowaczyk, N., Dulski, P., You, H., Opitz, S., Liu, Q. and Liu, J.: Millennial-scale East Asian monsoon variability of the last glacial deduced from annually laminated sediments from Lake Sihailongwan, N.E. China, Quaternary Science Reviews, 201, 57–76, doi:10.1016/j.quascirev.2018.09.023, 2018.

Mulitza, S., Prange, M., Stuut, J.-B., Zabel, M., Dobeneck, T. von, Itambi, A. C., Nizou, J., Schulz, M. and Wefer, G.: Sahel

megadroughts triggered by glacial slowdowns of Atlantic meridional overturning, Paleoceanography, 23(4), doi:10.1029/2008PA001637, 2008.

NOAA-NCDC weather service: NOAA-NCDC weather service, [online] Available from: https://www.ncdc.noaa.gov/ (Accessed 15 August 2018), 2018.

North Greenland Ice Core Project Members, Andersen, K. K., Azuma, N., Barnola, J.-M., Bigler, M., Biscaye, P., Caillon, N., Chappellaz, J., Clausen, H. B., Dahl-Jensen, D., Fischer, H., Flückiger, J., Fritzsche, D., Fujii, Y., Goto-Azuma, K., Grønvold, K., Gundestrup, N. S., Hansson, M., Huber, C., Hvidberg, C. S., Johnsen, S. J., Jonsell, U., Jouzel, J., Kipfstuhl, S., Landais, A., Leuenberger, M., Lorrain, R., Masson-Delmotte, V., Miller, H., Motoyama, H., Narita, H., Popp, T., Rasmussen, S. O., Raynaud, D., Rothlisberger, R., Ruth, U., Samyn, D., Schwander, J., Shoji, H., Siggard-Andersen, M.-L., Steffensen, J. P., Stocker, T., Sveinbjörnsdóttir, A. E., Svensson, A., Takata, M., Tison, J.-L., Thorsteinsson, T., Watanabe, O., Wilhelms, F. and White, J. W. C.: High-resolution record of Northern Hemisphere climate extending into the last interglacial period, Nature, 431(7005), 147–151, doi:10.1038/nature02805, 2004.

Reille, M. and de Beaulieu, J. L.: History of the Würm and Holocene vegetation in western velay (Massif Central, France): A comparison of pollen analysis from three corings at Lac du Bouchet, Review of Palaeobotany and Palynology, 54(3), 233–248, doi:10.1016/0034-6667(88)90016-4, 1988.

Reille, M. and de Beaulieu, J. L.: Pollen analysis of a long upper Pleistocene continental sequence in a Velay maar (Massif Central, France), Palaeogeography, Palaeoclimatology, Palaeoecology, 80(1), 35–48, doi:10.1016/0031-0182(90)90032-3, 1990.

Roucoux, K. H., de Abreu, L., Shackleton, N. J. and Tzedakis, P. C.: The response of NW Iberian vegetation to North Atlantic climate oscillations during the last 65kyr, Quaternary Science Reviews, 24(14), 1637–1653, doi:10.1016/j.quascirev.2004.08.022, 2005.

Ruth, U., Bigler, M., Röthlisberger, R., Siggaard-Andersen, M.-L., Kipfstuhl, S., Goto-Azuma, K., Hansson, M. E., Johnsen, S. J., Lu, H. and Steffensen, J. P.: Ice core evidence for a very tight link between North Atlantic and east Asian glacial climate, Geophysical Research Letters, 34(3), doi:10.1029/2006GL027876, 2007.

Schettler, G., Liu, Q., Mingram, J., Stebich, M. and Dulski, P.: East-Asian monsoon variability between 15 000 and 2000 cal. yr BP recorded in varved sediments of Lake Sihailongwan (northeastern China, Long Gang volcanic field), The Holocene, 16(8), 1043–1057, doi:10.1177/0959683606069388, 2006.

Schulz, H., von Rad, U., Erlenkeuser, H. and von Rad, U.: Correlation between Arabian Sea and Greenland climate oscillations of the past 110,000 years, Nature, 393(6680), 54–57, doi:10.1038/31750, 1998.

Sirocko, F., Garbe-Schönberg, D., McIntyre, A. and Molfino, B.: Teleconnections between the subtropical monsoon and high latitude climates during the last deglaciation, Science, 272, 526–529, 1996.

Sirocko, F., Knapp, H., Dreher, F., Förster, M. W., Albert, J., Brunck, H., Veres, D., Dietrich, S., Zech, M., Hambach, U., Röhner, M., Rudert, S., Schwibus, K., Adams, C. and Sigl, P.: The ELSA-Vegetation-Stack: Reconstruction of Landscape Evolution Zones (LEZ) from laminated Eifel maar sediments of the last 60,000years, Global and Planetary Change, 142, 108–

135, doi:10.1016/j.gloplacha.2016.03.005, 2016.

Stebich, M., Rehfeld, K., Schlütz, F., Tarasov, P. E., Liu, J. and Mingram, J.: Holocene vegetation and climate dynamics of NE China based on the pollen record from Sihailongwan Maar Lake, Quaternary Science Reviews, 124, 275–289, doi:https://doi.org/10.1016/j.quascirev.2015.07.021, 2015.

Sun, Y., Wang, X., Liu, Q. and Clemens, S. C.: Impacts of post-depositional processes on rapid monsoon signals recorded by the last glacial loess deposits of northern China, Earth and Planetary Science Letters, 289(1–2), 171–179, doi:10.1016/j.epsl.2009.10.038, 2010.

Ünal-İmer, E., Shulmeister, J., Zhao, J.-X., Tonguç Uysal, I., Feng, Y.-X., Duc Nguyen, A. and Yüce, G.: An 80 kyr-long continuous speleothem record from Dim Cave, SW Turkey with paleoclimatic implications for the Eastern Mediterranean, Scientific Reports, 5(1), doi:10.1038/srep13560, 2015.

Wagner, J. D. M., Cole, J. E., Beck, J. W., Patchett, P. J., Henderson, G. M. and Barnett, H. R.: Moisture variability in the southwestern United States linked to abrupt glacial climate change, Nature Geoscience, 3(2), 110–113, doi:10.1038/ngeo707, 2010.

Wainer, K., Genty, D., Blamart, D., Hoffmann, D. and Couchoud, I.: A new stage 3 millennial climatic variability record from a SW France speleothem, Palaeogeography, Palaeoclimatology, Palaeoecology, 271(1–2), 130–139, doi:10.1016/j.palaeo.2008.10.009, 2009.

Wang, Y. J., Cheng, H., Edwards, R. L., An, Z. S., Wu, J. Y., Shen, C.-C. and Dorale, J. A.: A High-Resolution Absolute-Dated Late Pleistocene Monsoon Record from Hulu Cave, China, Science, 294(5550), 2345, doi:10.1126/science.1064618, 2001.

Wassenburg, J. A., Immenhauser, A., Richter, D. K., Jochum, K. P., Fietzke, J., Deininger, M., Goos, M., Scholz, D. and Sabaoui, A.: Climate and cave control on Pleistocene/Holocene calcite-to-aragonite transitions in speleothems from Morocco: Elemental and isotopic evidence, Geochimica et Cosmochimica Acta, 92, 23–47, doi:10.1016/j.gca.2012.06.002, 2012.

Wassenburg, J. A., Dietrich, S., Fietzke, J., Fohlmeister, J., Jochum, K. P., Scholz, D., Richter, D. K., Sabaoui, A., Spötl, C., Lohmann, G., Andreae, M. O. and Immenhauser, A.: Reorganization of the North Atlantic Oscillation during early Holocene deglaciation, Nature Geoscience, 9(8), 602–605, doi:10.1038/ngeo2767, 2016.

Watts, W. A.: A long pollen record from Laghi di Monticchio, southern Italy: a preiminary account, Journal of the Geological Society, 142(3), 491–499, doi:10.1144/gsjgs.142.3.0491, 1985.

List of relevant changes:

- Linguistic revision of the entire manuscript
- Clarifications on methods and rephrasing the whole method section, including error estimations
- Deleted regions Oceania & Cariaco Basin as referees suggested
- Portuguese margin & NW-Africa: speleothem record changed, according to referees suggestions and mistakenly wrong cave selection by us
- Holocene section for villars cave speleothem added
- Unnecessary information throughout the manuscript were deleted
- Fig.2 (truncated before) changed
- Scripts and templates now available as supplementary material
- Discussion section on PalMod requirements impacting the site selection and results added